

X-TEX software

## Help and User Manual

version: 3.0

last updated: August 05, 2021

Bertalan Jóni

(Eötvös Loránd University, Budapest, Hungary)

contact: [xtexsoftware@gmail.com](mailto:xtexsoftware@gmail.com)

2021.

# Table of contents

1. Theory and Models.....	1
2. General Information.....	3
2.1 What is the X-TEX software? .....	3
2.2 Installing the X-TEX.....	3
2.3 About the control panel.....	4
2.4 System/program requirements.....	5
2.5 Subroutines.....	6
2.6 Necessary directories and files .....	6
2.6.1 Materials_Data.....	7
2.6.1.1 Atomic scattering factors file.....	7
2.6.1.2 Crystal data file .....	10
2.6.1.3 Material list file.....	12
2.6.2 Atomic positions/coordinates .....	12
2.6.3 Color code.....	15
2.7 Synchrotron and laboratory measurements .....	15
2.8 Basic diffraction concepts .....	15
3. Usage .....	18
3.1 Projects.....	18
3.2 Texture component parameters .....	20
3.2.1 Eulerian angles of the ideal orientation.....	21
3.2.2 Volume fraction of texture components.....	24
3.2.3 FWHM.....	24
3.2.4 Major, minor and random texture components.....	25
3.2.5 Creating the modeled texture.....	26
3.3 Pole figure .....	27
3.3.1 Simple textures .....	29
3.3.2 Complex textures, linking texture sub-components.....	31
3.3.3 Comparing modeled pole figures with measured ones .....	35
3.3.4 Pole figures with $\chi_0$ threshold value .....	35

3.4 Plot 2D detector image.....	38
3.4.1 Experimental parameters.....	38
3.4.1.1 Experimental geometry .....	38
3.4.1.2 Sample orientation .....	40
3.4.1.3 Lorentz-polarization factor .....	41
3.4.1.4 Detector parameters.....	41
3.4.1.5 hkl list .....	43
3.4.2 Detector images .....	44
3.5 Calculating $\chi_{hkl}$ values, plot 1D pattern.....	48
3.5.1 Specifying the integrated area .....	48
3.5.2 Plot 2D detector image with the integrated area.....	49
3.5.3 Plot 1D pattern.....	50
3.5.4 $\chi_{hkl}$ values of the peaks .....	53
3.6 Scanning function.....	54
3.6.1 Input parameters, initial sample orientation.....	55
3.6.2 Rotation map.....	57
3.7 Calculating Schmid factors .....	61
3.8 Fit/refine texture parameters .....	62
4. In the future.....	67
4.1 Neutron diffraction .....	67
4.2 Texture parameter refinement by measured pole figures .....	67
Appendix.....	68
A. Useful links .....	68
B. Atomic scattering factors .....	68
C. Atomic positions/coordinates .....	70
D. How to add gnuplot to the environmental variables.....	70
References.....	73



# 1. Theory and Models

The theory, the texture model, and the principles of the X-TEX method can be found in detail in [1] (in English) and [2] (in Hungarian).

The most important items:

Schematic figure of the experimental geometry and some notations:

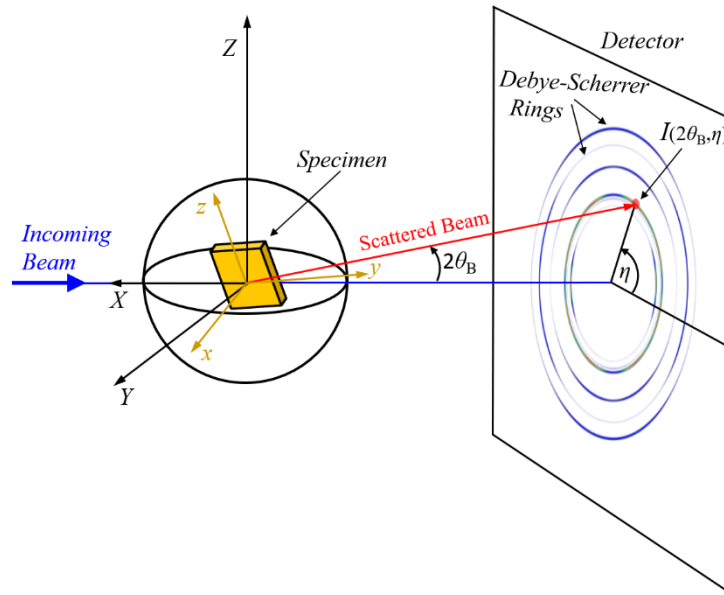


**Fig 1.1.** Schematic figure of the X-ray diffraction measurement geometry.  $\mathcal{K}_L = \{X, Y, Z\}$  is the laboratory coordinate system,  $\mathcal{K}_s = \{x, y, z\}$  is the specimen coordinate system,  $\theta_B$  is the Bragg and  $\eta$  is the azimuth angle of the scattered beam.

In the  $(2\theta_B, \eta)$  direction the diffracted X-ray intensity is proportional to the volume fraction of grains oriented in such a way that their  $hkl$  planes fulfil the Bragg's law, i.e. the  $\mathbf{e}_{hkl}$  normal vector of the  $hkl$  plane is pointing in the  $\mathbf{s}_{hkl}$  direction (**Fig.1.2**).

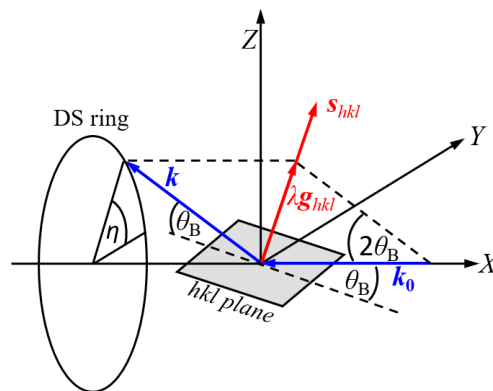


**Fig 1.2.** Illustration of the Bragg's law. DS is the Debye-Scherrer ring,  $\mathbf{k}_0$  and  $\mathbf{k}$  are unit vectors in direction of the incoming and the scattered beams,  $\mathbf{g}_{hkl}$  is the diffraction vector,  $\mathbf{s}_{hkl}$  is the unit vector in the direction of the diffraction vector.

Their relative volume fraction in the X-TEX method is obtained by assuming a Gaussian distribution of orientations around the ideal orientation of the  $i^{\text{th}}$  texture component:

$$\psi^i = A^i \cdot \exp\left(\frac{-(s_x - e_x^i)^2}{2\Delta^2}\right) \cdot \exp\left(\frac{-(s_y - e_y^i)^2}{2\Delta^2}\right) \cdot \exp\left(\frac{-(s_z - e_z^i)^2}{2\Delta^2}\right) = A^i G_x G_y G_z \quad (1.1)$$

where  $\Delta^2$  is the variance of the distribution and  $A^i$  is a normalization factor taking into account the  $f^i \in [0,1]$  volume fraction of grains belonging to the  $i^{\text{th}}$  texture component:

$$A^i = f^i / \int_{-\pi}^{\pi} \int_0^{\pi} G_x G_y G_z \sin \vartheta \, d\vartheta d\varphi \quad (1.2)$$

where  $\vartheta$  and  $\varphi$  are polar coordinates.

The  $\mathbf{s}_{hkl}$  vector is the unit vector in the direction of the diffraction vector of  $(2\theta_B, \eta)$ :

$$\mathbf{s}_{hkl} = \frac{1}{2 \sin(\theta_B)} (1 - \cos(2\theta_B), \sin(2\theta_B) \cos(\eta), \sin(2\theta_B) \sin(\eta)) \quad (1.3)$$

where  $\theta_B$  is the diffraction angle of  $hkl$  planes according to Bragg's law and  $\eta$  is the azimuth angle of the scattered beam. The  $\mathbf{e}_{hkl}$  vectors are the unit vectors normal to the crystallographic  $hkl$  planes. In the X-TEX method  $\mathbf{e}_{hkl}$  vectors for cubic (simple cubic, face-centered cubic, body-centered cubic, diamond), hexagonal and trigonal crystal systems are allowed currently.

The ideal orientation of a texture component,  $\hat{R}_{(\varphi_1, \Phi, \varphi_2)} \in SO(3)$  is interpreted as a three-dimensional rotation matrix with  $z$ - $x$ - $z$  convention:

$$\hat{R}_{(\varphi_1, \Phi, \varphi_2)} = \hat{R}_z(\varphi_1) \hat{R}_x(\Phi) \hat{R}_z(\varphi_2) \quad (1.4)$$

where the Eulerian angles  $\varphi_1$ ,  $\Phi$  and  $\varphi_2$  describe the rotation between the crystallographic and the sample coordinate system  $\mathcal{K}_S$ . The specimen orientation in  $\mathcal{K}_L$  is described by another rotation matrix with  $Z$ - $X$ - $Z$  convention:

$$\hat{R}_{(\alpha, \beta, \gamma)} = \hat{R}_Z(\alpha) \hat{R}_X(\beta) \hat{R}_Z(\gamma) \quad (1.5)$$

where  $\alpha$ ,  $\beta$  and  $\gamma$  are the Eulerian angles of the specimen rotation in  $\mathcal{K}_L$ . Rotating the specimen by  $\alpha$ ,  $\beta$  and  $\gamma$  angles, the normal vectors of the  $hkl$  planes for an ideal orientation of the  $i^{\text{th}}$  texture component will be

$$\mathbf{e}_{hkl}^i = \hat{R}_{(\alpha, \beta, \gamma)} \hat{R}_{(\varphi_1^i, \Phi^i, \varphi_2^i)} \mathbf{e}_{hkl} \quad (1.6)$$

The total intensity of the  $hkl$  reflection in the  $(2\theta_B, \eta)$  direction including the contribution of the random texture component is:

$$I_{(2\theta_B, \eta)}^{\text{tot}} = LP \left( \sum_i \sum_{\{hkl\}} |F_{hkl}|^2 \psi^i + \frac{f^r}{4\pi} \sum_{\{hkl\}} |F_{hkl}|^2 \right) = \sum_i I_{(2\theta_B, \eta)}^i + I_{(2\theta_B, \eta)}^r \quad (1.7)$$

where  $f^r$  is the volume fraction of the random texture component,  $LP$  is the Lorentz polarization factor,  $F_{hkl}$  is the structure factor and the  $\{hkl\}$  summation goes over permutations of the  $hkl$  indices.

The total intensity obtained by integrating the intensity distribution over an  $[\eta_{\min}, \eta_{\max}]$  interval:

$$I_{(2\theta_B)}^{\text{tot}} = \int_{\eta_{\min}}^{\eta_{\max}} I_{(2\theta_B, \eta)}^{\text{tot}} d\eta = \sum_i I_{(2\theta_B)}^i + I_{(2\theta_B)}^r. \quad (1.8)$$

The intensity contributions for  $hkl$  peaks provided by grains belonging to the  $i^{\text{th}}$  texture component are described with the

$$\chi_{hkl}^i = I_{(2\theta_B)}^i / I_{(2\theta_B)}^{\text{tot}} \quad (1.9)$$

intensity ratios. Peaks are considered to correspond to the investigated texture component, if their intensity ratio is larger than a chosen threshold value  $\chi_0$ .

In the X-TEX method, the goal is carrying out such diffraction measurements in that the measured diffraction peaks correspond to one texture component.

## 2. General Information

### 2.1 What is the X-TEX software?

Based on the principles and equations outlined above, a computer program called X-TEX has been developed for planning diffraction experiments in order to measure diffraction peaks mainly corresponding to one texture component with minimal intensity contribution of other alien texture components, i.e. we would like to measure peaks having as high  $\chi_{hkl}^i$  values as possible. The diffraction peaks measured in this way are characteristic of the examined texture component in question so that the microstructure of the examined texture component can be characterized separately from the other components by evaluating peaks with any standard X-ray line profile analysis technique. Using the X-TEX method, it is possible to characterize the microstructure of different texture components separately.

### 2.2 Installing the X-TEX

There is no need any special installing procedure, just download the latest version of the X-TEX software from the website (<http://metal.elte.hu/~berci/X-TEX.html>), extract the actual .rar file (X-TEX-2021-released.rar) and copy/replace the whole

extracted X-TEX directory to whatever the place you want to use it on your computer. The X-TEX directory and the whole content of it can be seen in Fig. 2.1.

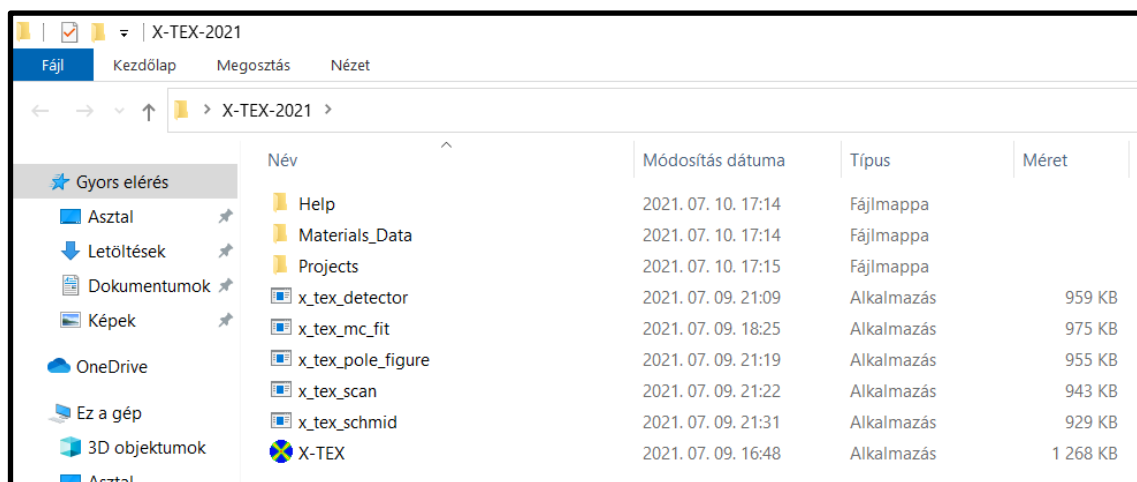


Fig 2.1. The content of the directory of the X-TEX software.

The application named X-TEX is the main software, it is the control panel which makes several subroutines work (more details later). Do not delete any content from this directory, otherwise the software won't work. You can create shortcuts for X-TEX application. For example, for desktop shortcut: right-click on the X-TEX application and select Send to > Desktop (create shortcut). Then there will be an X-TEX icon on your Desktop with which you can easily start the X-TEX control panel in the future.

## 2.3 About the control panel

The X-TEX software has multiple possible functions to carry out your aims and make your work easier. These functions are: pole figure plot, detector image plot, diffraction pattern plot, texture refinement, calculating Schmid factors and a scanning function for finding optimal sample orientations (more details later). On the control panel of the X-TEX (Fig. 2.2) all parameters are in one place, but also well separated corresponding to the different functions for the sake of the transparency. In the Usage section we will go through the usage and the specifications of all functions in detail. The control panel writes the corresponding parameters from the panel into some files, and the buttons on the control panel make subroutines work with those files (more details later). The control panel program is written in C# programming language and works in Windows operation system only. On the control panel helpful tooltips shows up when the cursor is on the labels of the parameters and buttons.



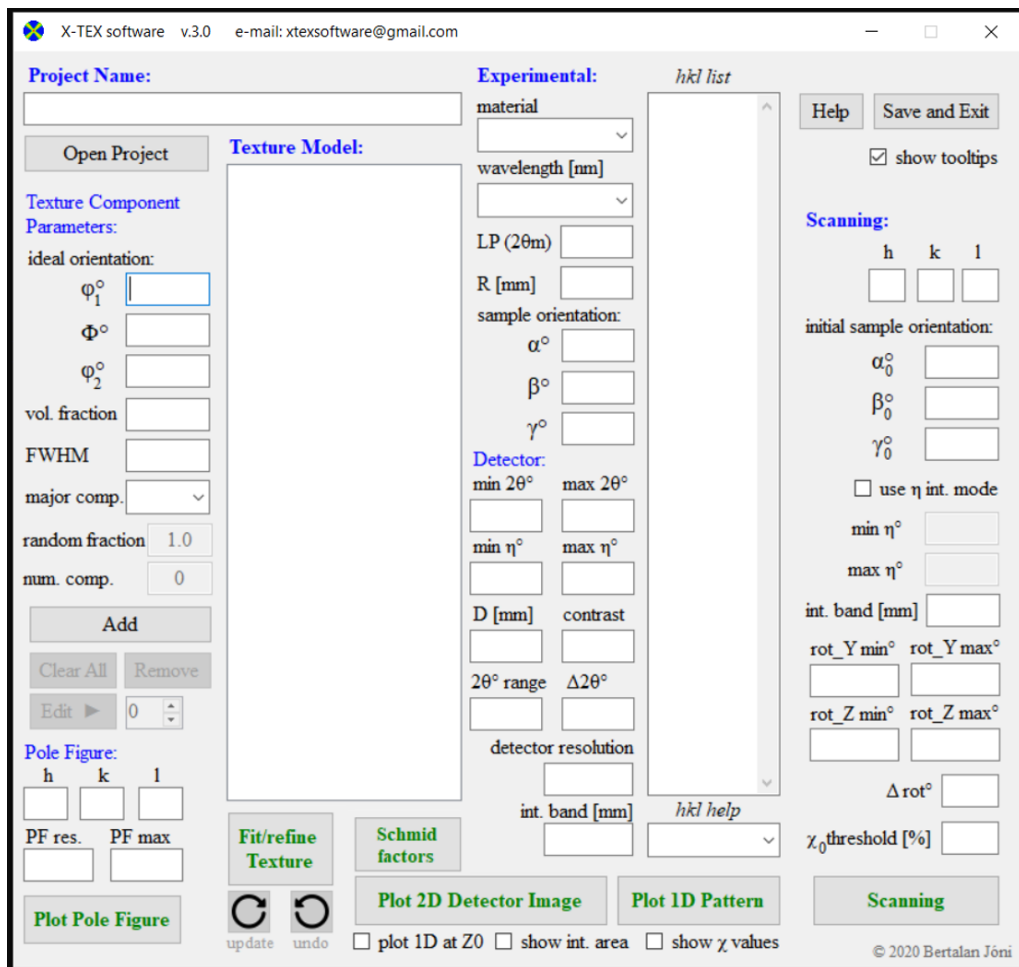
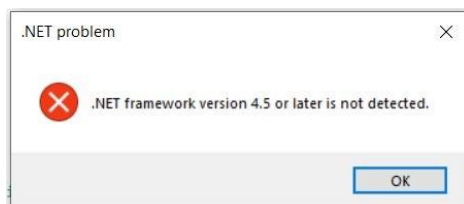


Fig 2.2. The control panel of the X-TEX software.

## 2.4 System/program requirements

- Windows operation system (Windows 7, Windows 8, Windows 10)
- .NET framework (version 4.6 or later)

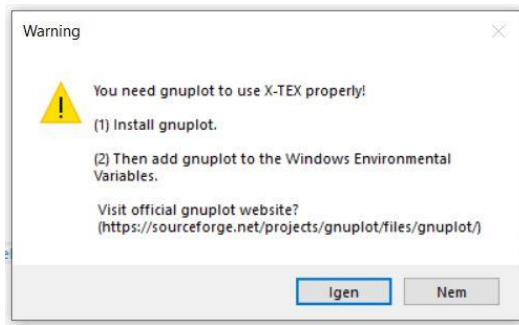
Error message if the framework is not sufficient:



- gnuplot software added to the Windows Environmental Variables

You can find in the **Appendix** how to add the gnuplot to the environmental variables.

Error message if the gnuplot is not added to the environmental variables:



- There are not particular constraints to the processor and RAM requirements. The X-TEX uses modeled texture which allows fast calculations, so there is no need serious hardware performance.

## 2.5 Subroutines

As mentioned above, the X-TEX control panel makes subroutines work. The subroutines were written in C++ programming language. The subroutines are:

x_tex_detector	2021. 07. 09. 21:09	Alkalmazás	959 KB
x_tex_mc_fit	2021. 07. 09. 18:25	Alkalmazás	975 KB
x_tex_pole_figure	2021. 07. 09. 21:19	Alkalmazás	955 KB
x_tex_scan	2021. 07. 09. 21:22	Alkalmazás	943 KB
x_tex_schmid	2021. 07. 09. 21:31	Alkalmazás	929 KB

**Fig 2.3.** Subroutines of the X-TEX software.

You cannot use these subroutines directly, you can only from the control panel make them work with the corresponding button on the panel, e.g. the **Plot Pole Figure** button starts the "x\_tex\_pole\_figure.exe" subroutine. The control panel also creates some files in your project directory containing the necessary parameters for the subroutines (more details later).

## 2.6 Necessary directories and files

There are two necessary directories for the X-TEX (as you can see in **Fig. 2.1**):

- 1) Projects
- 2) Materials\_Data

Do not delete these directories, otherwise the software won't work.

The Projects directory contains subdirectories and the files of your projects (more details later). These files are for the subroutines. The control panel writes the corresponding parameters from the panel into these files, and the buttons on the control panel make subroutines work with these files, so you don't have any business with these files.

## 2.6.1 Materials\_Data

The Materials\_Data directory contains three files which are necessary for the X-TEX:




Név	Módosítás dátuma	Típus	Méret
 x_tex_atomic_sc_f_data	2021. 07. 08. 21:44	DAT fájl	8 KB
 x_tex_crystal_data	2021. 07. 09. 12:52	DAT fájl	2 KB
 x_tex_material_list	2021. 07. 09. 12:53	DAT fájl	1 KB

Fig 2.4. Contents of the Materials\_Data directory.

These files basically form a material database containing the necessary information about the atomic scattering factors of elements, crystal systems and lattice parameters. These files are freely editable if you want to add a new element or material.

### 2.6.1.1 Atomic scattering factors file

The scattered X-ray intensity in the  $(2\theta_B, \eta)$  direction is calculated by Eq.1.7. This equation contains  $hkl$  dependent elements, such as the  $LP$  is the Lorentz polarization factor, or the  $F_{hkl}$  structure factor. Note that these elements do not play roll when you determine the  $\chi_{hkl}^i$  values in Eq (1.9), which is essentially the most important parameter of the X-TEX method. With  $\chi_{hkl}^i$  value you can basically divide the scattered intensity of the  $hkl$  peak according to the texture components, and the elements in question ( $LP$  and  $F_{hkl}$ ) are the same for the different intensity contributions of a  $hkl$  peak originated from different texture components. In other words,  $LP$  and  $F_{hkl}$  matters only when you want to compare peaks with different  $hkl$  indices (at different  $2\theta_B$  Bragg angles), e.g. in case of detector images and patterns containing different  $hkl$  peaks, or in case of texture parameter refinement procedure based on X-ray diffraction measurements with different  $hkl$  Debye-Scherrer (DS) rings (more details later). The  $LP$  factor can be calculated by a simple formula (see later), we are focusing on the  $F_{hkl}$  structure factor now. The structure factor depends on atomic positions:

$$F_{hkl} = \sum_n f_n \exp(2\pi i(hx_n + ky_n + lz_n)), \quad (2.1)$$

where sum is over all atoms in the unit cell,  $x, y, z$  are the coordinates on the  $n$ -th atom, and  $f_n$  is the atomic scattering factor of the  $n$ -th atom.

The 'x\_tex\_atomic\_sc\_f\_data.dat' file in the Materials\_Data directory contains atomic scattering factors for lots of atoms (Fig. 2.5). The X-TEX software uses this file for the structure factor calculations. This file is freely editable (even with a simple

notepad) if you want to add more scattering factors of materials. For this, just add another line to the end of the list (or insert the new line between two existing lines) in a proper form.

1	Atomic Scattering Factors vs. $\sin(\theta)/\lambda[\text{\AA}]$ :																	
2	material	0.00	0.10	0.20	0.30	0.40	0.50	0.60	0.70	0.80	0.90	1.00	1.10	1.20	1.30	1.40	1.50	
3																		
4	H	1.00	0.81	0.48	0.25	0.13	0.07	0.04	0.02	0.02	0.01	0.01	0.01	0.01	0.01	0.01	0.01	0.01
5	He	2.00	1.83	1.45	1.06	0.74	0.52	0.36	0.25	0.18	0.13	0.10	0.07	0.05	0.04	0.03	0.03	0.03
6	Li	3.00	2.22	1.74	1.51	1.27	1.03	0.82	0.65	0.51	0.40	0.32	0.26	0.21	0.16	0.16	0.16	0.16
7	Be	4.00	3.07	2.07	1.71	1.53	1.37	1.20	1.03	0.88	0.74	0.62	0.52	0.43	0.37	0.37	0.37	0.37
8	B	5.00	4.07	2.71	1.99	1.69	1.53	1.41	1.28	1.15	1.02	0.90	0.78	0.68	0.60	0.60	0.60	0.60
9	C	6.00	5.13	3.58	2.50	1.95	1.69	1.54	1.43	1.32	1.22	1.11	1.01	0.91	0.82	0.74	0.66	0.66
10	N	7.00	6.20	4.60	3.24	2.40	1.94	1.70	1.55	1.44	1.35	1.26	1.18	1.08	1.01	1.01	1.01	1.01
11	O	8.00	7.25	5.63	4.09	3.01	2.34	1.94	1.71	1.57	1.46	1.37	1.30	1.22	1.14	1.14	1.14	1.14
12	F	9.00	8.29	6.69	5.04	3.76	2.88	2.31	1.96	1.74	1.59	1.48	1.40	1.32	1.25	1.25	1.25	1.25
13	Ne	10.00	9.36	7.82	6.09	4.62	3.54	2.79	2.30	1.98	1.76	1.61	1.50	1.42	1.35	1.28	1.22	1.22
14	Na	11.00	9.76	8.34	6.89	5.47	4.29	3.40	2.76	2.31	2.00	1.78	1.63	1.52	1.44	1.37	1.31	1.31
15	Na+	10.00	9.55	8.39	6.93	5.51	4.33	3.42	2.77	2.31	2.00	1.79	1.63	1.52	1.44	1.37	1.30	1.30
16	Mg	12.00	10.50	8.75	7.46	6.20	5.01	4.06	3.30	2.72	2.30	2.01	1.82	1.65	1.54	1.54	1.54	1.54
17	Al	13.00	11.23	9.16	7.88	6.77	5.69	4.71	3.88	3.21	2.71	2.32	2.05	1.83	1.69	1.57	1.48	1.48
18	Si	14.00	12.16	9.67	8.22	7.20	6.24	5.31	4.47	3.75	3.16	2.69	2.35	2.07	1.87	1.71	1.60	1.60
19	P	15.00	13.17	10.34	8.59	7.54	6.67	5.83	5.02	4.28	3.64	3.11	2.69	2.35	2.10	1.89	1.75	1.75
20	S	16.00	14.33	11.21	8.99	7.83	7.05	6.31	5.56	4.82	4.15	3.56	3.07	2.66	2.34	2.34	2.34	2.34
21	Cl	17.00	15.33	12.00	9.44	8.07	7.29	6.64	5.96	5.27	4.60	4.00	3.47	3.02	2.65	2.65	2.65	2.65
22	Cl-	18.00	16.02	12.20	9.40	8.03	7.28	6.64	5.97	5.27	4.61	4.00	3.47	3.03	2.65	2.35	2.11	2.11
23	Ar	18.00	16.30	12.93	10.20	8.54	7.56	6.86	6.23	5.61	5.01	4.43	3.90	3.43	3.03	3.03	3.03	3.03
24	K	19.00	16.73	13.73	10.97	9.05	7.87	7.11	6.51	5.95	5.39	4.84	4.32	3.83	3.40	3.01	2.71	2.71
25	Ca	20.00	17.33	14.32	11.71	9.64	8.26	7.38	6.75	6.21	5.70	5.19	4.69	4.21	3.77	3.37	3.03	3.03
26	Sc	21.00	18.72	15.39	12.39	10.12	8.60	7.64	6.98	6.45	5.96	5.48	5.00	4.53	4.09	3.68	3.31	3.31
27	Ti	22.00	19.41	16.07	13.20	10.83	9.12	7.98	7.22	6.65	6.19	5.72	5.29	4.84	4.41	4.01	3.64	3.64
28	V	23.00	20.47	17.03	14.03	11.51	9.63	8.34	7.48	6.86	6.39	5.94	5.53	5.10	4.71	4.30	3.93	3.93
29	Cr	24.00	21.93	18.37	15.01	12.22	10.14	8.72	7.75	7.09	6.58	6.14	5.74	5.34	4.94	4.55	4.18	4.18
30	Mn	25.00	22.61	19.06	15.84	13.02	10.80	9.20	8.09	7.32	6.77	6.32	5.93	5.54	5.18	4.80	4.45	4.45
31	Fe	26.00	23.68	20.09	16.77	13.84	11.47	9.71	8.47	7.60	6.99	6.51	6.12	5.74	5.39	5.03	4.69	4.69
32	Fe-gamma	26.00	23.68	20.09	16.77	13.84	11.47	9.71	8.47	7.60	6.99	6.51	6.12	5.74	5.39	5.03	4.69	4.69
33	CoCrFeMnNi	26.00	23.75	20.17	16.82	13.86	11.50	9.75	8.50	7.63	7.01	6.51	6.11	5.72	5.37	5.00	4.66	4.66
34	CoCrFeMnNi-hcp	26.00	23.75	20.17	16.82	13.86	11.50	9.75	8.50	7.63	7.01	6.51	6.11	5.72	5.37	5.00	4.66	4.66
35	Co	27.00	24.74	21.13	17.74	14.68	12.17	10.26	8.88	7.91	7.22	6.70	6.29	5.91	5.58	5.23	4.90	4.90
36	Ni	28.00	25.80	22.19	18.73	15.56	12.91	10.85	9.33	8.25	7.48	6.90	6.47	6.08	5.75	5.41	5.09	5.09
37	Cu	29.00	27.19	23.63	19.90	16.48	13.65	11.44	9.80	8.61	7.76	7.13	6.65	6.25	5.90	5.57	5.25	5.25
38	Zn	30.00	27.92	24.33	20.77	17.42	14.51	12.16	10.37	9.04	8.08	7.37	6.84	6.42	6.07	5.73	5.43	5.43

Fig 2.5. Content of `x_tex_atomic_sc_f_data.dat` file (opened with Notepad++).

The first item in a line is the name of the atom/material, and the next 16 items (separated by Tab or Space from each other) are the atomic scattering factors at 0.0, 0.1, 0.2, ... 1.5 values of  $\sin \theta / \lambda [\text{\AA}]$ , where  $\lambda$  is the wavelength of the X-ray beam in Ångström. You can easily find atomic scattering factor values in different databases or even with a simple search on the internet. The current atomic scattering database in Fig 2.5 comes from [3].

The atomic scattering factors of X-ray diffraction depends on the  $\theta$  scattering angles, as it can be seen in Fig 2.5. In this file basically the atomic scattering factors are listed as a function of certain values of different  $\theta$  angles. However, for the measured  $hkl$  reflexions we need the atomic scattering factor values at values of  $\sin \theta_B / \lambda [\text{\AA}]$ . The X-TEX software uses a spline interpolation for this calculation (Fig.2.6), because the  $f(\theta)$  function is monotonous and smooth.

For the same material with different crystal structure you need to repeat the same line with the same atomic scattering values but with different material name, e.g. alpha iron with bcc crystal structure and gamma iron with fcc structure (line 31 and 32 in Fig 2.5). You cannot use "Fe" as name for both structures in the '`x_tex_atomic_sc_f_data.dat`'

file, since the software search the lattice parameters and crystal systems based on the name of the material (see later in the crystal data section).

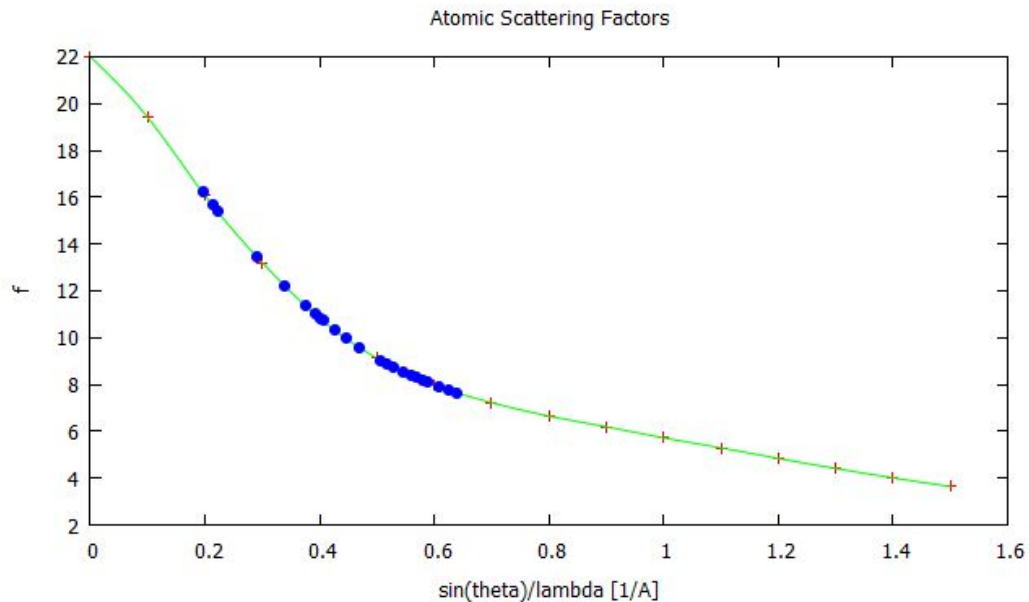


**Fig 2.6.** Illustration of the atomic scattering factor (asc) calculations of  $hkl$  reflexions. The red crosses are the asc values at certain  $\theta$  values given in the 'x\_tex\_atomic\_sc\_f\_data.dat' file, the green line is a spline for interpolation according to the red spots and the blue dots are the asc values at the  $\theta_B$  Bragg angles of the measured  $hkl$  peaks according to the applied X-ray wavelength.

In line 33 in **Fig.2.5**, you can see an example to a high entropy alloy (HEA) (CoCrFeMnNi). Since HEAs have (almost) equal proportions of elements, the average atomic scattering factor values of their elements can be used.

The structure factor in some simple cases can be expressed by simple formulas. For example [3,5]:

- fcc, face-centered cubic

$$F^2 = 16f^2 \text{ for } hkl \text{ unmixed}$$

$$F^2 = 0 \text{ for } hkl \text{ mixed} \tag{2.2.a}$$

- bcc, body-centered cubic

$$F^2 = 4f^2 \text{ for } h + k + l \text{ even}$$

$$F^2 = 0 \text{ for } h + k + l \text{ odd} \tag{2.2.b}$$

- sc, primitive cubic (simple cubic)

$$F^2 = f^2 \text{ for all } hkl \text{ values} \tag{2.2.c}$$

- dia, diamond cubic

$$\begin{aligned}
 F^2 &= 64f^2 \text{ for } h + k + l = 4N \\
 F^2 &= 32f^2 \text{ for } h + k + l \text{ odd} \\
 F^2 &= 0 \text{ for } hkl \text{ mixed} \\
 F^2 &= 0 \text{ for } h + k + l = 4N \pm 2
 \end{aligned}
 \tag{2.2.d}$$

- hcp, hexagonal close-packed

$$F_{hkl}^2 = 4f^2 \cos^2 \pi \left( \frac{h + 2k}{3} + \frac{l}{2} \right)
 \tag{2.2.e}$$

The X-TEX software uses these simple formulas only if the crystal structure (see next section) is fcc, bcc, sc, dia or hcp, and the name of the material can be found in the atomic scattering factor file (x\_tex\_atomic\_sc\_f\_data.dat).

However, in more complex cases, especially when the unit cell contains different type of atoms, e.g. NaCl, CaCO<sub>3</sub>, Fe<sub>2</sub>O<sub>3</sub>, ZnS, AlNi<sub>3</sub> and so on, X-TEX can use Eq.2.1 for calculating the structure factor if the correct atoms and their positions inside the unit cell are defined in an 'atomic\_positions.dat' file. See more details in chapter "Atomic positions/coordinates".

### 2.6.1.2 Crystal data file

The 'x\_tex\_crystal\_data.dat' file in the Materials\_Data directory contains the needed information about the crystal system and lattice parameters of materials (Fig. 2.7). This file is freely editable if you want to add more materials to the list. For this, just insert the new line of your material to the end of the list or between two existing line in a proper form.

The first item in a line is the name of the material (MN), which can be totally arbitrary (it is not necessary to be in the 'x\_tex\_atomic\_sc\_f\_data.dat' file).

The second item in a line is the name of the crystal system type of the material. X-TEX can handle cubic, hexagonal and trigonal crystal system types only.

The allowed names for crystal systems in the 'x\_tex\_crystal\_data.dat' file are:

**cubic, fcc, bcc, sc, dia, hcp, hexagonal, tri.**

As mentioned above, X-TEX uses simple formulas for calculating structure factor in case of fcc, bcc, sc, dia and hcp, so it is not necessary to specify the atomic positions. In these cases, the name of the material (MN) in 'x\_tex\_crystal\_data.dat' also has to be in 'x\_tex\_atomic\_sc\_f\_data.dat' file, since the atomic scattering factors of the MN has to be

known. In other cases (cubic, hexagonal, tri) X-TEX can use only the Eq.2.1 for calculating the structure factors and the atomic positions must be specified in an 'atomic\_positions.dat' file (more details in atomic positions/coordinates section).

The third and fourth items in a line are the  $a$  and  $c$  lattice parameters of the crystal system. Note that if there is no  $c$  lattice parameter (in case of cubic systems), zero  $c$  values must be used.

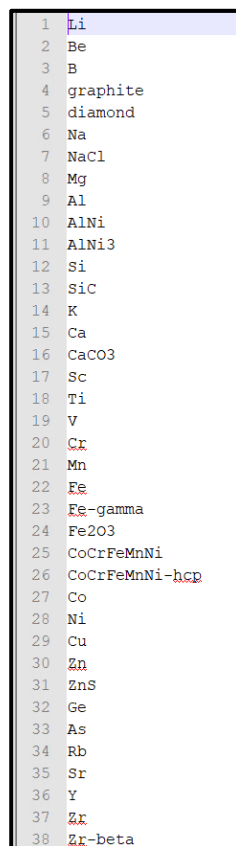
1		system	lat_a [nm]	lat_c [nm]
2				
3	Li	bcc	0.35100	0.00000
4	Be	hcp	0.22858	0.35843
5	B	tri	0.48999	1.25509
6	graphite	hexagonal	0.24600	0.67080
7	diamond	dia	0.35670	0.00000
8	Na	bcc	0.42906	0.00000
9	NaCl	fcc	0.56400	0.00000
10	Mg	hcp	0.32094	0.52112
11	Al	fcc	0.40495	0.00000
12	AlNi	cubic	0.28880	0.00000
13	AlNi3	cubic	0.35720	0.00000
14	Si	dia	0.54309	0.00000
15	SiC	fcc	0.43580	0.00000
16	K	bcc	0.53280	0.00000
17	Ca	fcc	0.55884	0.00000
18	CaCO3	tri	0.49890	1.70620
19	Sc	hcp	0.33090	0.52733
20	Ti	hcp	0.29505	0.46826
21	V	bcc	0.30274	0.00000
22	Cr	bcc	0.29100	0.00000
23	Mn	bcc	0.27994	0.00000
24	Fe	bcc	0.28664	0.00000
25	Fe-gamma	fcc	0.35911	0.00000
26	Fe2O3	tri	0.51048	1.39130
27	CoCrFeMnNi	fcc	0.35960	0.00000
28	CoCrFeMnNi-hcp	hcp	0.25350	0.41380
29	Co	hcp	0.25071	0.40695
30	Ni	fcc	0.35238	0.00000
31	Cu	fcc	0.36150	0.00000
32	Zn	hcp	0.26649	0.49468
33	ZnS	fcc	0.54200	0.00000
34	Ge	dia	0.56575	0.00000
35	As	tri	0.37598	1.05475
36	Rb	bcc	0.55850	0.00000
37	Sr	fcc	0.60849	0.00000
38	Y	hcp	0.36474	0.57306

Fig 2.7. Content of x\_tex\_crystal\_data.dat file (opened with Notepad++).

### 2.6.1.3 Material list file

The 'x\_tex\_material\_list.dat' file (Fig.2.8) in the Materials\_Data directory contains the names of the materials (MN). This file is simply a repetition of the first column of the 'x\_tex\_crystal\_data.dat' file. The control panel of the X-TEX loads this file to choose a material from the list.

If you create your proper database with 'x\_tex\_atomic\_sc\_f\_data.dat', 'x\_tex\_crystal\_data.dat' and 'x\_tex\_material\_list.dat' files (and 'atomic\_positions.dat' files when needed), then the only thing you have to do for your work in the future is choosing a material on the control panel.



```
1 Li
2 Be
3 B
4 graphite
5 diamond
6 Na
7 NaCl
8 Mg
9 Al
10 AlNi
11 AlNi3
12 Si
13 SiC
14 K
15 Ca
16 CaCO3
17 Sc
18 Ti
19 V
20 Cr
21 Mn
22 Fe
23 Fe-gamma
24 Fe2O3
25 CoCrFeMnNi
26 CoCrFeMnNi-hcp
27 Co
28 Ni
29 Cu
30 Zn
31 ZnS
32 Ge
33 As
34 Rb
35 Sr
36 Y
37 Zr
38 Zr-beta
```

Fig 2.8. Content of x\_tex\_material\_list.dat file.

### 2.6.2 Atomic positions/coordinates

For your all works you must choose a material name (MN) from the material listbox on the control panel. As mentioned above this list loads from the 'x\_tex\_material\_list.dat' file. The 'x\_tex\_crystal\_data.dat' file must contain MN as well with the corresponding crystal parameters. If the name of the crystal system is fcc, bcc, sc, dia or hcp, and the 'x\_tex\_atomic\_sc\_f\_data.dat' file also contains MN then the structure factor will be calculated by simple formulas (Eq.2.2a-e). For example, the



mentioned conditions for Ti can be seen in Fig. 2.9. In this case, the MN, i.e. Ti, is in both, the crystal data and the atomic scattering factor files and the name of the crystal system is hcp, so Eq.2.2e is used for  $F_{hkl}$ .

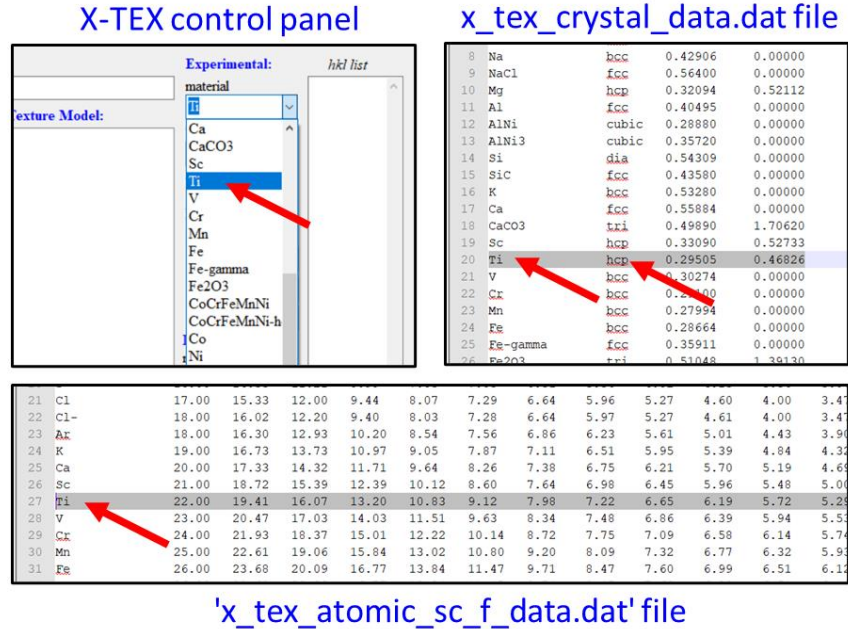
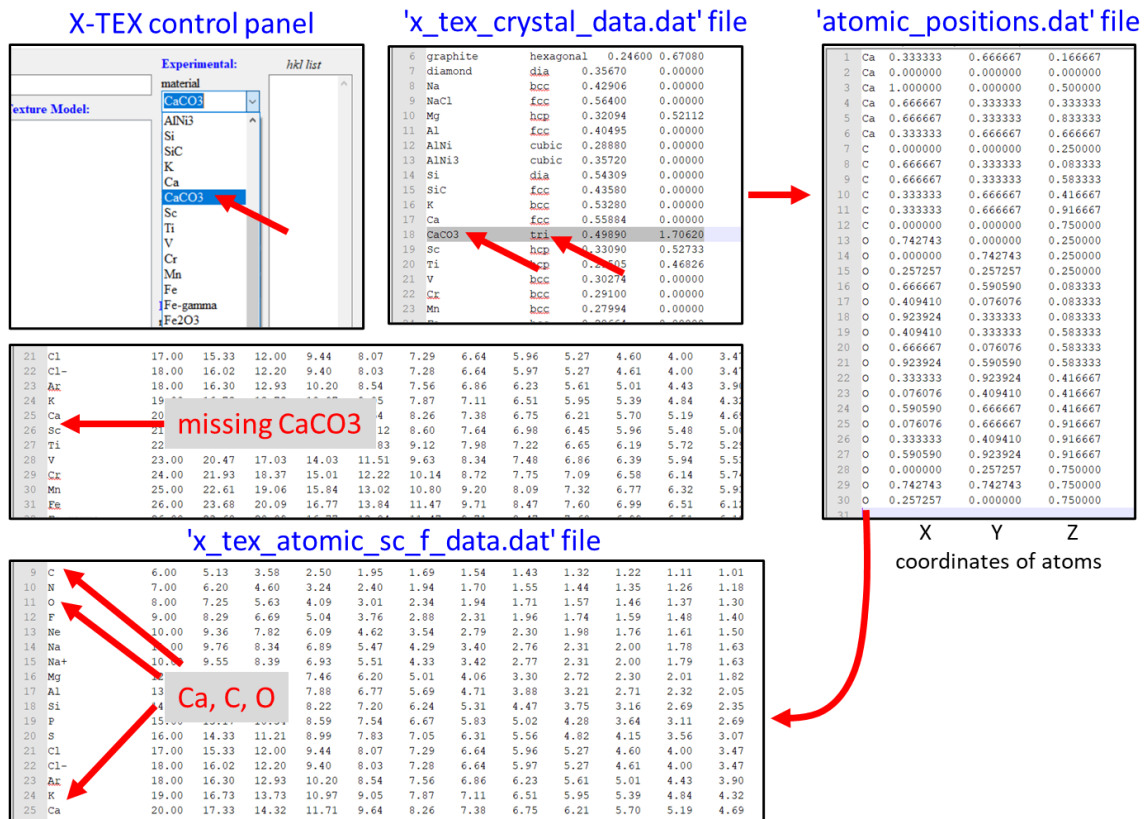


Fig 2.9. Illustration of the case when it is not necessary to specify the atomic positions. Ti from the list on the control panel is also in the crystal data file with hcp crystal system name, and Ti is also in the atomic scattering factor file. In this case Eq.2.2.e is used for  $F_{hkl}$  calculation.

However, if the name of the crystal system is cubic, hexagonal, tri, or the 'x\_tex\_atomic\_sc\_f\_data.dat' file does not contain MN then the structure factor will be calculated by Eq.2.1 therefore the atomic positions must be specified. An example for this case can be seen in Fig.2.10. for CaCO<sub>3</sub> (calcite). If the name CaCO<sub>3</sub> from the control panel list would not be in the 'x\_tex\_crystal\_data.dat' file, we would get fatal error (crystal system and lattice parameters are unknown). If the name CaCO<sub>3</sub> is in the 'x\_tex\_crystal\_data.dat' with the proper crystal parameters, then the software checks whether CaCO<sub>3</sub> is also in the 'x\_tex\_atomic\_sc\_f\_data.dat' file with the corresponding atomic scattering factor values. In our case, the name CaCO<sub>3</sub> cannot be found in the 'x\_tex\_atomic\_sc\_f\_data.dat' file. Then the program checks whether a file named 'atomic\_positions.dat' exist in your project directory (more details about the project directory in the Projects section). If the 'atomic\_positions.dat' file cannot be found, we get fatal error (structure factor calculation is not possible without atomic coordinates). If 'atomic\_positions.dat' file is found, the software check whether the atomic names in the

'atomic\_positions.dat' file is in the 'x\_tex\_atomic\_sc\_f\_data.dat' file. If not, we get fatal error (atomic scattering factors for Eq.2.1 must be known). If all atoms from the 'atomic\_positions.dat' file can also be found in 'x\_tex\_atomic\_sc\_f\_data.dat' file, the software can calculate the structure factor by using Eq.2.1.



**Fig 2.10.** Illustration of the case when the atomic positions must be specified in an 'atomic\_positions.dat' file (in the actual project directory). The name CaCO<sub>3</sub> in the list on the control panel is also in the crystal data file with 'tri' crystal system name. The CaCO<sub>3</sub> is not in the atomic scattering factor file. In this case Eq.2.1 is used for  $F_{hkl}$  calculation with the x,y,z atomic coordinates from the 'atomic\_positions.dat' file, if the atomic scattering factor file contains the atoms (Ca, C and O in this case). Atomic coordinates and lattice parameters for CaCO<sub>3</sub> from: <https://materialsproject.org>, from CaCO<sub>3</sub>\_mp-3953\_conventional\_standard.cif file.

The 'atomic\_positions.dat' file must contain lines with the name of atom and x and y and z coordinates separated by Tab or Space from each other, as it can be seen well in Fig 2.10.

Atomic positions for several materials/crystal system types and some helpful links can be found in Appendix A and C. In the Help subdirectory in the X-TEX directory you can also find cif files containing atomic coordinates downloaded from <https://materialsproject.org>.

### 2.6.3 Color code

You can set an arbitrary color palette for your 2D X-TEX figures (pole figure, 2D detector image, scan figure) by using a file named 'colorcode.dat' in your project directory. In this file only the first line matters, which must contain the palette code according to the gnuplot software. For more information visit the gnuplot website: [http://www.gnuplot.info/docs\\_4.2/node217.html](http://www.gnuplot.info/docs_4.2/node217.html)

This 'colorcode.dat' file is not required, if it does not exist, then a default color palette is used (Fig. 2.11).

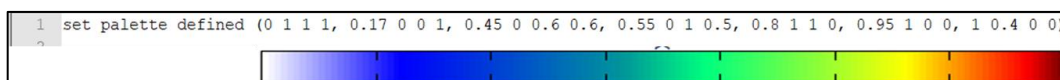


Fig 2.11. The first line of the 'colorcode.dat' file which is basically a gnuplot command line. The actual code on the figure shows the default color code for the X-TEX. The color bar corresponding to the color code also can be seen. If you use different color code in a file named 'colorcode.dat' located in the project directory, then you can change this default color bar.

## 2.7 Synchrotron and laboratory measurements

The X-TEX method can be applied for both, laboratory, and synchrotron measurements. The theory of the X-TEX method is valid for monochromatic, parallel incoming X-ray beam, when the intensity distribution of the diffracted beam produces a set of Debye-Scherrer rings on an area detector, i.e. the intensity distribution can be described as a function of the  $2\theta_B, \eta$  Bragg and azimuth angles. These conditions are usually given in synchrotron and laboratory measurements carried out for line profile analysis. Usually in synchrotron experiments transmission, and in laboratory measurements reflexion scheme is used. The X-TEX works with both schemes. The diffraction geometry can be found in the Experimental section in detail.

## 2.8 Basic diffraction concepts

In this section we summarize shortly the basic diffraction notations and concepts to clarify the meaning of expressions in the following.

In powder diffraction, when a parallel monochromatic beam hit a polycrystalline sample, the scattered radiation travels along cone surfaces according to the Bragg's law (Fig.2.12). The intensity distribution detected by a two-dimensional detector shows diffraction rings (called Debye-Scherrer rings) around the incoming beam axis. The scattering angle denoted as  $2\theta$ , and the azimuthal angle is denoted as  $\eta$ . The specific  $2\theta$

angles between the beam axis and the rings are called  $2\theta_B$  Bragg angles. In accordance with Bragg's law, each ring corresponds to a particular  $hkl$  Miller index. Note that for X-TEX software always need 3-index-notation of Miller indices, i.e. there is no need to give the fourth i-index in case of hexagonal or trigonal systems (of course the software also calculates with this index when permutes them).

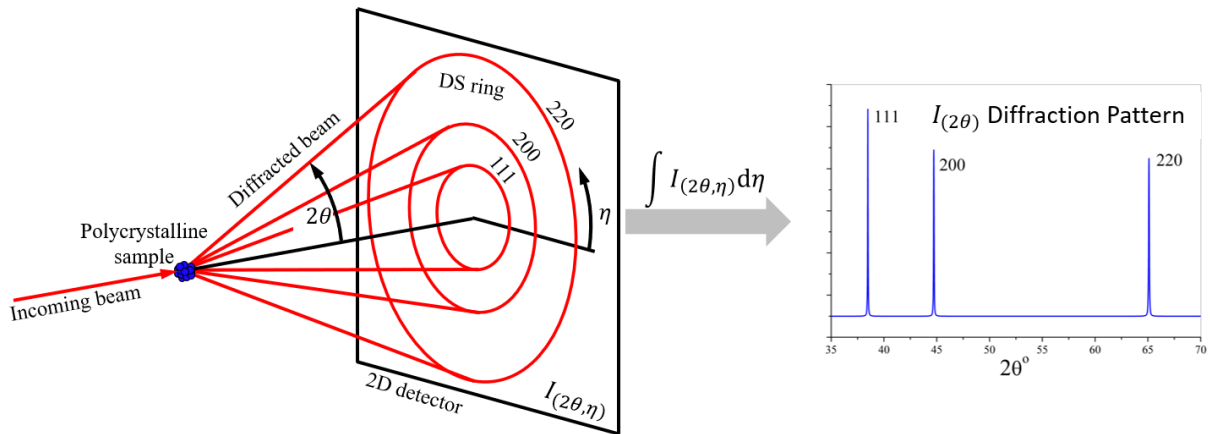


**Fig 2.12.** Basic diffraction concepts and notations of  $hkl$  diffraction rings, pattern and  $hkl$  peaks.

The integration of the  $I_{(2\theta, \eta)}$  two-dimensional intensity distribution alongside the azimuth angle leads to the  $I_{(2\theta)}$  one-dimensional diffraction pattern consisting of diffraction peaks (Fig.2.12, Fig.2.13). Note that each peak corresponds to a particular  $hkl$  Miller index as well.

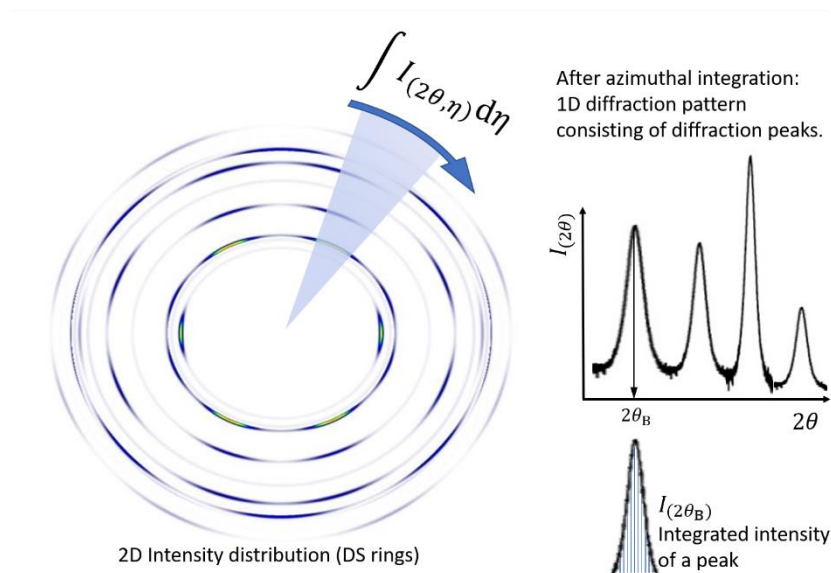


**Fig 2.13.** Illustration of the peak broadening and the integrated intensity of a peak.

In theory, narrow diffraction peaks appear at the Bragg angles. However, in the reality, the peaks are broadened (Fig.2.13) because of lattice defects and the finite size of the

crystal. Actually, this broadening and the shape of the peaks are the basis of line profile analysis techniques. In the X-TEX method, the calculated intensities of the peaks given by Eq.1.8,  $I_{(2\theta_B)}$ , are the functions of the Bragg angles. This  $I_{(2\theta_B)}$  calculated intensity represents the integrated intensity of the real measured peak (the whole area under the peaks). Since in the X-TEX plots (2D detector image and 1D pattern) infinitely narrow DS rings and peaks would not be illustrative, the rings and the peaks have constant, artificial Gaussian type broadening (this parameter can be set by the  $\Delta 2\theta^0$  parameter on the control panel). In these plots, the calculated  $I_{(2\theta_B)}$  values refer to the maximum intensities of the peaks correspond to the integrated intensity of the measured peaks.

## 3. Usage

### 3.1 Projects

When using the X-TEX software, you must always specify a project directory where the control panel saves the parameters (into some files) and from where the subroutines can access them. All project directories must be in the 'Projects' directory located in X-TEX main directory as it can be seen in Fig.2.1. For using any function of the X-TEX software you should specify the name of your project directory on the control panel (Fig.3.1) at 'Project Name' textbox.

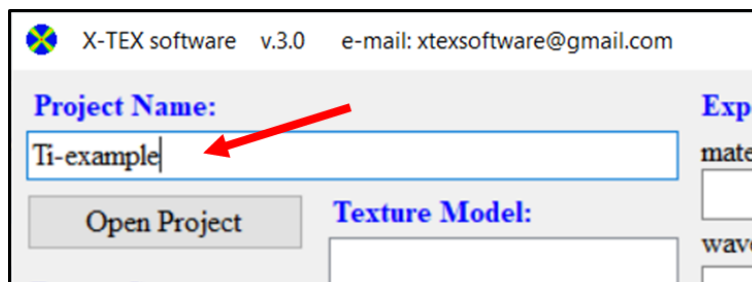


Fig 3.1. Specifying the name of your project directory (Ti-example) on the control panel. All necessary files will be saved into this directory. This directory must locate in 'Projects' directory in the X-TEX main directory.

The name of your project directory can be arbitrary, however you should avoid exotic characters. The space character in the name should also be avoided. The most recommended characters are English alphabetic characters, numbers and '-' or '\_' characters.

When you press any function button on the control panel or the 'Save and Exit' button, then a directory with name given in the 'Project Name' textbox will be created (created only if it did not exist already) in the 'Projects' directory, and all the files containing the parameters form the control panel will be saved into this project directory.

The names of these created files are:

- x\_tex\_experimental\_data.dat
- x\_tex\_hkl\_data.dat
- x\_tex\_plot\_data.dat
- x\_tex\_pole\_figure\_data.dat
- x\_tex\_scan\_data.dat
- x\_tex\_texture\_data.dat
- x\_tex\_temp.dat
- *materialname.xtex*

Note that you don't have to worry about these files, the control panel writes the corresponding parameters from the panel into these files, and the function buttons on the control panel make subroutines work with these files, so you don't have any business with these files.

Using subdirectories are also allowed, if the directories are separated by the '\ backslash symbol as it can be seen in **Fig.3.2**.

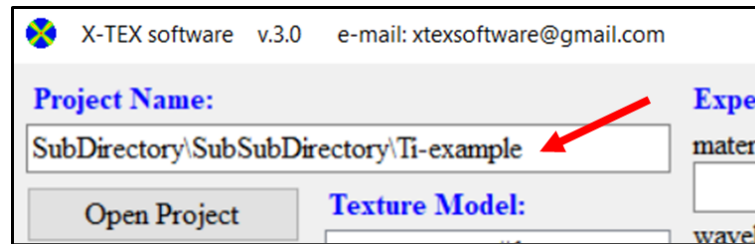


**Fig 3.2.** Using subdirectories are allowed this way. The subdirectories must be separated by backslash symbol.

With 'Open Project' button you can browse and open projects as it can be seen in **Fig.3.3**. With this function, you can continue your work where you left off last time.

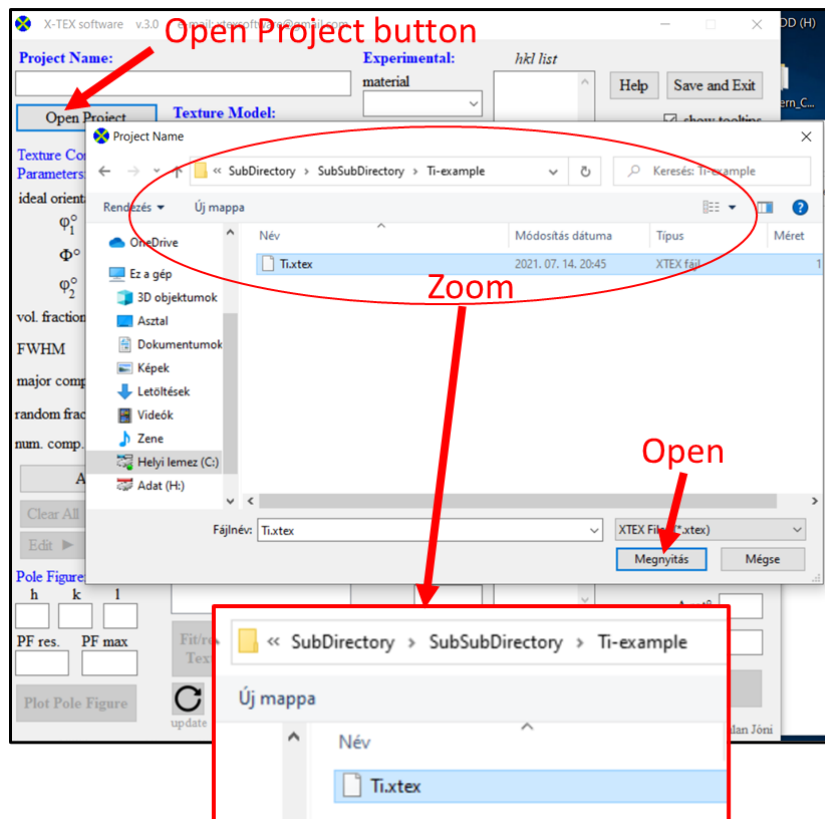


**Fig 3.3.** Opening a project. Browse in the 'Projects' directory, find your project directory and choose the .xtex file, then press Open.

## 3.2 Texture component parameters

In the X-TEX method the texture is modeled by Gaussian distributions of grain orientations around ideal orientations of texture components (Eq.1.1). The parameters of this model: Eulerian angles of the ideal orientation ( $\varphi_1$ ,  $\Phi$  and  $\varphi_2$ ), volume fraction of grains belonging to each texture component, FWHM of the Gaussian distribution and whether the component belongs to the major or to the minor component.

For better understanding of the Eq.1.1, let's see first the Fig 3.4. The normal vector of a  $hkl$  plane is denoted as  $e_{hkl}$ . Let's rotate this plane into the ideal orientation by applying Eq.1.4 rotation matrix. Let's denote the rotated normal vector as  $e'_{hkl}$  (Eq.1.6, but ignoring the sample rotation, we will come back to this later).

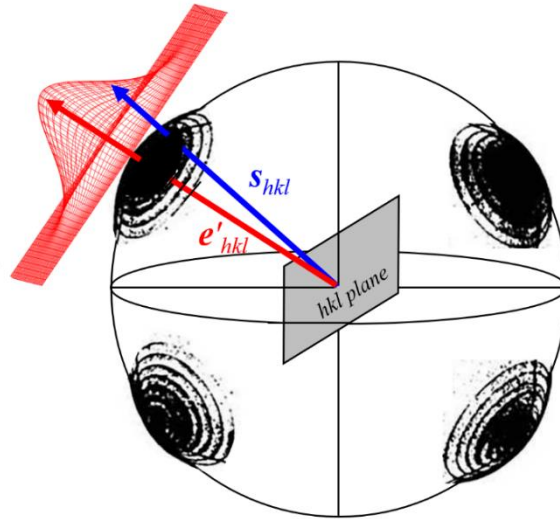


Fig 3.4. The illustration of the Gaussian distribution defined in Eq.1.1.

This  $hkl$  plane will only scatter the incoming beam into the  $(2\theta_B, \eta)$  direction, if the plane is oriented such a way that  $e'_{hkl} \parallel s_{hkl}$  condition is satisfied ( $s_{hkl}$  is defined in Eq.1.3, this is the unit vector in the direction of the diffraction vector of the  $(2\theta_B, \eta)$  direction, Fig.1.2). This condition is not fulfilled in Fig.3.4 for the ideal orientation of the texture component. However, for a real textured polycrystalline material, not all crystal grains are oriented exactly according to the preferred orientation, since the preferred orientation means that the grain orientations have some statistical tendency around this ideal orientation. In other words, the normal vector has a distribution around  $e'_{hkl}$  direction and this distribution is modeled by the Eq.1.1 Gaussian distribution, which can specify the relative volume fraction grains oriented as  $e'_{hkl} \parallel s_{hkl}$ . The diffracted X-ray intensity in the  $(2\theta_B, \eta)$  direction is proportional to this value.



### 3.2.1 Eulerian angles of the ideal orientation

In an orthogonal coordinate system, the unit vectors,  $\mathbf{e}_{hkl}$ , normal to the crystallographic  $hkl$  planes in cubic or hexagonal (and trigonal) crystals are:

$$\mathbf{e}_{hkl} = \frac{1}{\sqrt{h^2+k^2+l^2}}(h, k, l) \text{ or } \mathbf{e}_{hkl} = d_{hkl} \left( \frac{2h+k}{\sqrt{3}a}, \frac{k}{a}, \frac{l}{c} \right), \quad (3.1)$$

where  $d_{hkl}$  is the spacing of  $hkl$  planes and  $a$  and  $c$  are the lattice parameters. In the case of cubic crystals, the basis vectors of the cells are parallel to the axes of the orthogonal coordinate system (Fig.3.5). In the case of hexagonal (and trigonal) crystals, the unit cell is positioned in the following manner: the  $a_1$  basis vector has an angle of  $30^\circ$  with the  $x$ -axis and  $a_2$  and  $c$  are parallel to the  $y$ - and  $z$ -axis, respectively (Fig.3.5).

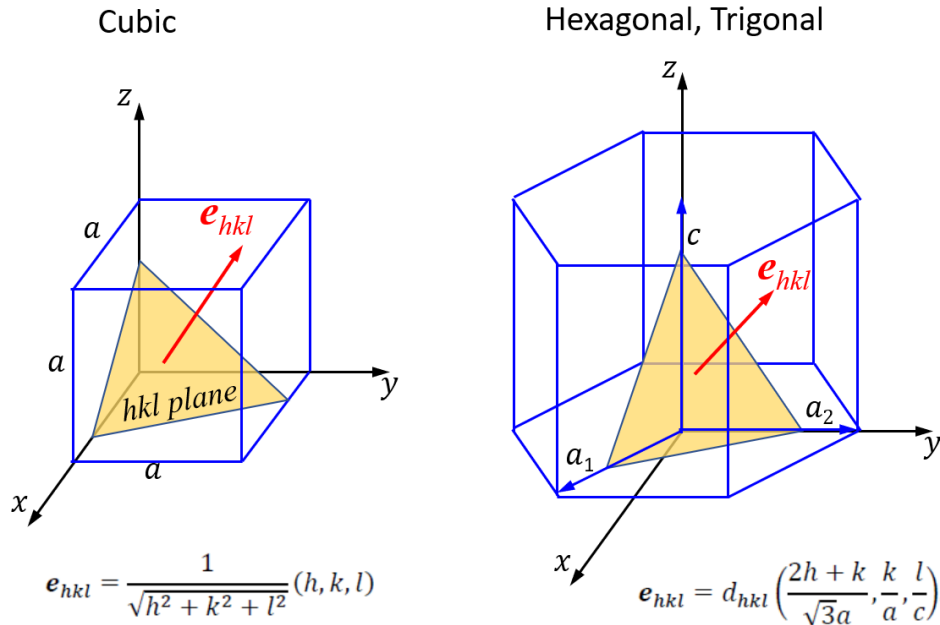
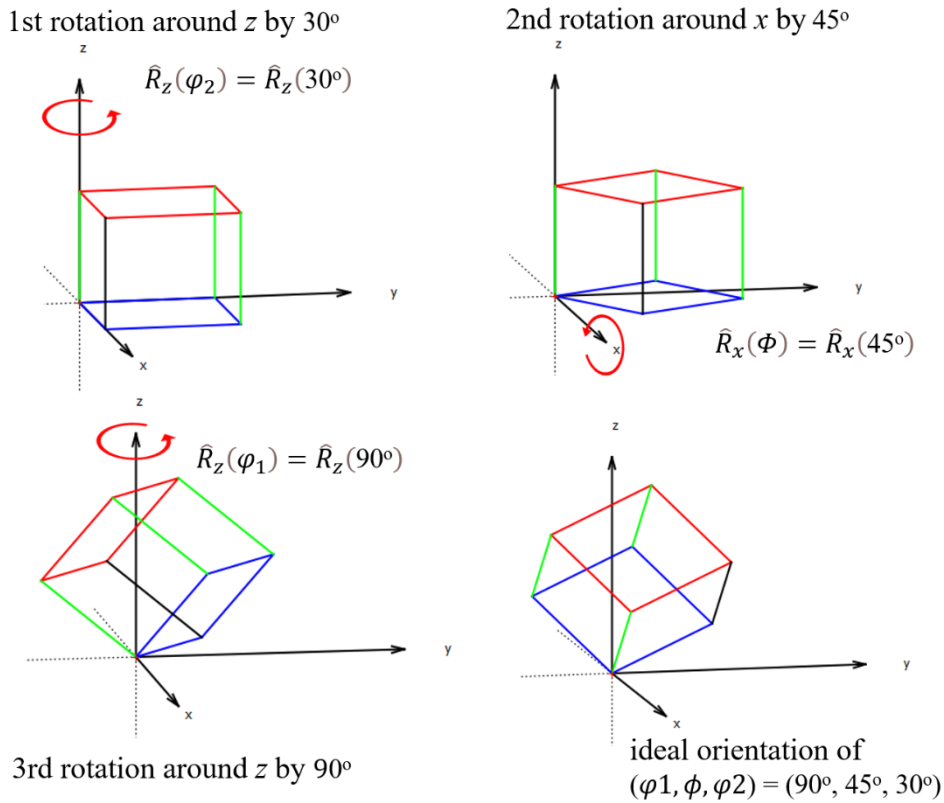


Fig 3.5. The crystallographic coordinate systems of cubic and hexagonal (trigonal) systems and the  $\mathbf{e}_{hkl}$  normal vectors of  $hkl$  planes expressed in an orthogonal coordinate system.

We can rotate the  $\mathbf{e}_{hkl}$  normal vectors from this initial orientation described by Eq.3.1 into the ideal orientation:

$$\mathbf{e}'_{hkl} = \hat{R}_{(\varphi_1, \Phi, \varphi_2)} \mathbf{e}_{hkl}, \quad (3.2)$$

where  $\hat{R}_{(\varphi_1, \Phi, \varphi_2)}$  is a three-dimensional rotation matrix with  $z$ - $x$ - $z$  convention defined in Eq.1.4 as  $\hat{R}_{(\varphi_1, \Phi, \varphi_2)} = \hat{R}_z(\varphi_1) \hat{R}_x(\Phi) \hat{R}_z(\varphi_2)$ . In other words, the Eulerian angles  $\varphi_1$ ,  $\Phi$  and  $\varphi_2$  describe the rotation between the crystallographic and the sample coordinate system  $\mathcal{K}_s$ .



**Fig 3.6.** The ideal orientation of  $(\varphi_1, \Phi, \varphi_2) = (90^\circ, 45^\circ, 30^\circ)$  divided into three basic rotations for cubic cell.

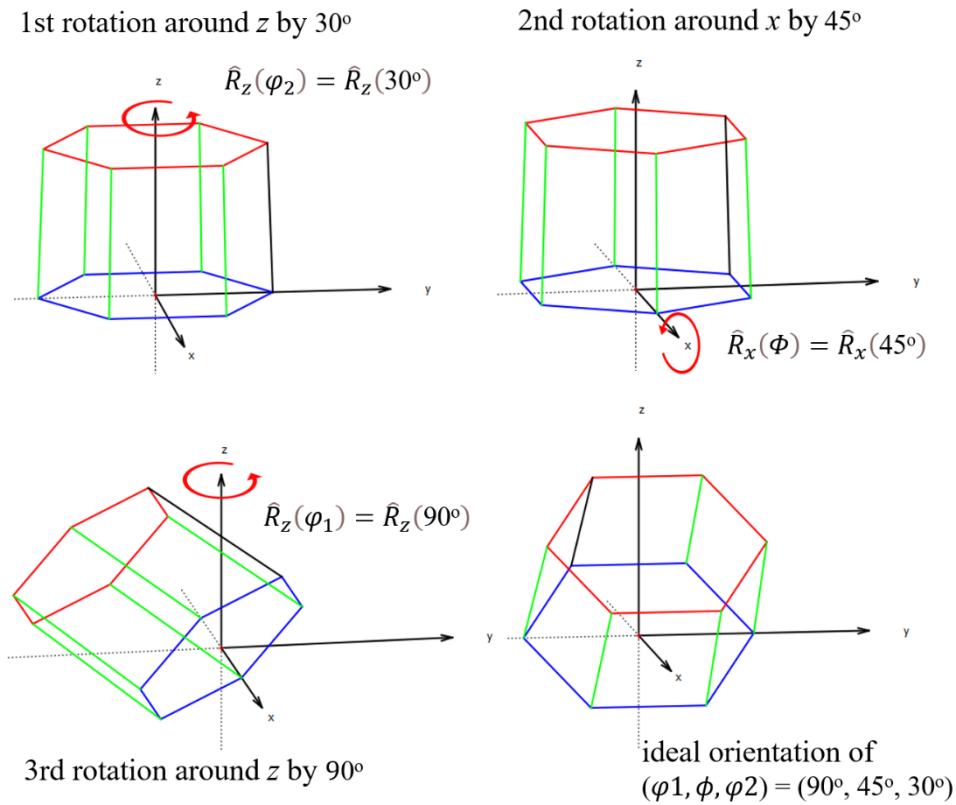


**Fig 3.7.** The ideal orientation of  $(\varphi_1, \Phi, \varphi_2) = (90^\circ, 45^\circ, 30^\circ)$  divided into three basic rotations for hexagonal (trigonal) cell.

The  $\hat{R}_{(\varphi_1, \Phi, \varphi_2)}$  rotation matrix describes three basic rotations of the Bravais cell one after the other in such a way that first rotates the cell (and normal vectors) around the z-axis by angle  $\varphi_2$ , then around the x-axis by angle  $\Phi$ , and finally again around the z-axis by angle  $\varphi_1$ , thus characterizing the ideal orientation of the cell in the  $\mathcal{K}_s$  system of the sample. For example, these basic rotations for the ideal orientation of  $(\varphi_1, \Phi, \varphi_2) = (90^\circ, 45^\circ, 30^\circ)$  can be seen for cubic Bravais cell in Fig.3.6 and for hexagonal (trigonal) cell in Fig.3.7.

The sign of the rotations is also important. The meaning of positive (+) and negative rotations can be seen in Fig.3.8.

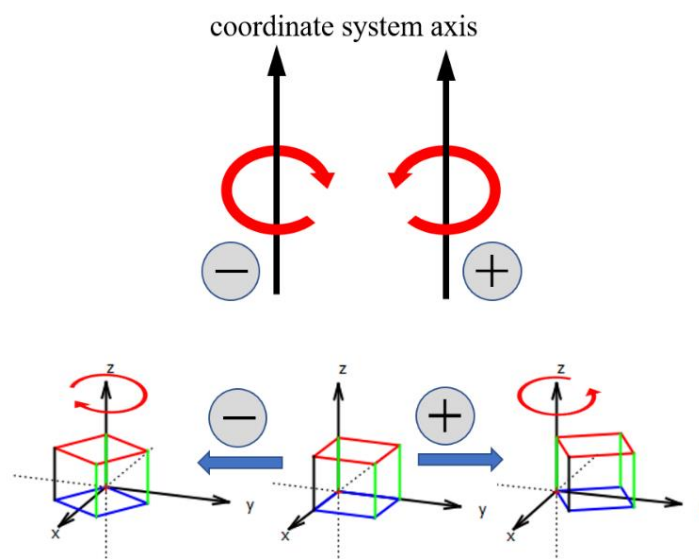


Fig 3.8. The definition of positive and negative signs of the rotations around a coordinate axis.

Note that though the trigonal crystal system has different symmetry from the hexagonal system, from the point of view of the normal vectors of the  $hkl$  planes it can be treated the same way, if its cell can be specify as  $a = b \neq c, \alpha = \beta = 90^\circ, \gamma = 120^\circ$ . Be careful when you give the lattice parameters and the atomic coordinates of a trigonal system.

### 3.2.2 Volume fraction of texture components

For the Gaussian distributions of grain orientations in Eq.1.1 the  $f^i \in [0,1]$  volume fraction of grains belonging to the  $i^{\text{th}}$  texture component, and  $f^r \in [0,1]$  the volume fraction of the random texture component need to be specified. The following criterion must be met:

$$1 = f^r + \sum_i f^i. \quad (3.3)$$

On the control panel only the  $f^i$  values of the different texture components need to be given and  $f^r$  is a calculated value from Eq.3.3.

### 3.2.3 FWHM

The full width at half maximum ( $\text{FWHM}=2\sqrt{2\ln 2}\Delta$ ) of the Gaussian distributions in Eq.1.1 for each texture component needs to be specified. Note that FWHM is not in degrees, it is a dimensionless parameter. However, a connection can be constructed if you prefer thinking in angles.

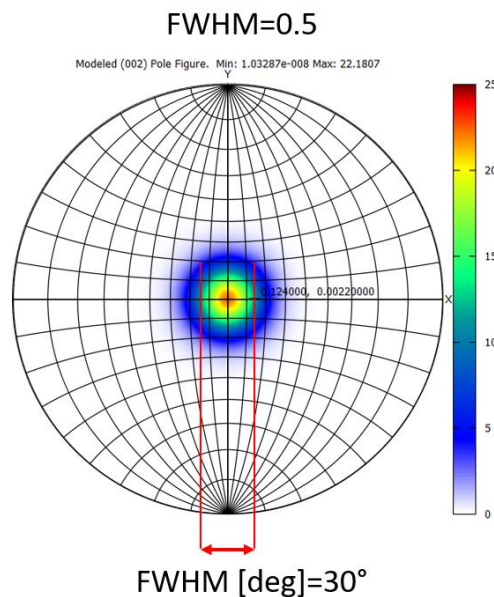


**Fig 3.9.** A modeled pole figure of  $hkl=002$  for Ti applying  $\text{FWHM}=0.5$  value on the control panel. The width of the pole at half-maximum can be read by using a Wulff net. It is found that  $\text{FWHM}=0.5$  corresponds to about 30 degree.

For example, in Fig.3.9 with a Wulff net on a modeled pole figure it can be seen, that  $\text{FWHM}=0.5$  corresponds to about 30 degree. Carrying out this analysis with several FWHM values, a linear correlation between the dimensionless values and the values expressed in degree can be found (Fig.3.10).

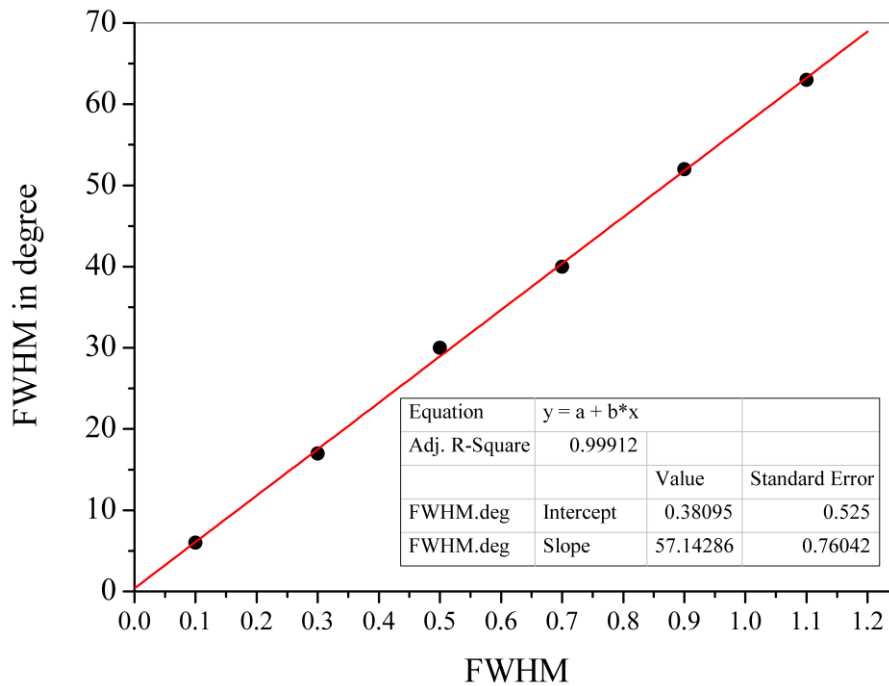


**Fig 3.10.** Connection between the dimensionless FWHM values and the FWHM values expressed in degree. The correlation is roughly a multiplication factor of 57.

It was found that there is roughly a multiplier factor of 57 between them, i.e. it is the same magnitude as between radian and degree. It means that if we know the FWHM value of the extension of a pole in degree (e.g. from texture measurement), we need to divide this value by 57 and this divided value should be used on the control panel. Or to put it another way, every tenth (0.1) means 5.7 degrees.

### 3.2.4 Major, minor and random texture components

In the X-TEX method the texture components are divided into three groups: major, minor (or other) and random.

You can set this on the control panel ('major comp.').

If this 'major comp.' parameter is:

'y', then the texture component belongs to the major texture component.

'n', then the texture component belongs to the minor (other) texture component.

(and the remaining fraction of grains belongs to the random component).

With this feature you can link several texture sub-components belonging to the same major texture component in order to be able to describe more complex textures, such as fibre texture.

### 3.2.5 Creating the modeled texture

The texture parameters listed above for each texture component must be specified in the corresponding textboxes on the control panel (Fig.3.11). After filling these textboxes, use the 'Add' button to add the texture parameters of one texture component to the 'Texture Model' listbox. X-TEX only takes into account texture components that are in the 'Texture Model' listbox. Create the needed texture model with several texture (sub-)components.

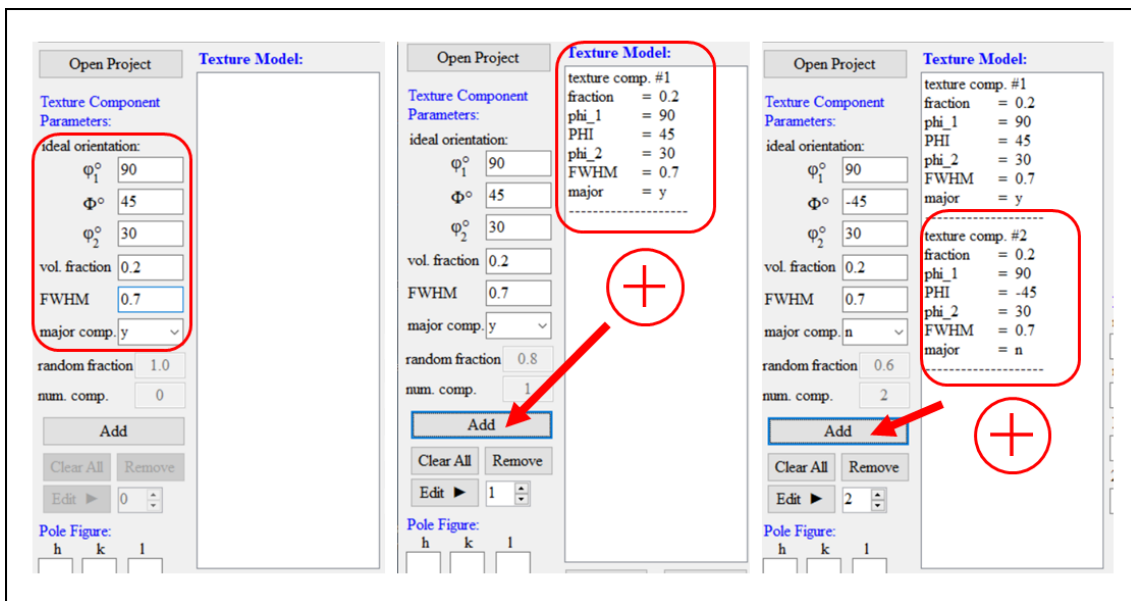


Fig 3.11. Creating the modeled texture. Fill the textboxes of the texture component parameters (at left) then press the 'Add' button to add these parameters to the 'Texture Model' listbox.

The 'Clear All' button clears the entire 'Texture Model' listbox. The 'Remove' button clears the last texture component from the 'Texture Model' listbox.

The texture components have a serial number (the number after the '#' character), this parameter is not relevant, only matters when editing the parameters with the 'Edit' button. You can modify the texture component parameters in the 'Texture Model' listbox with the 'Edit' button or with double click on the parameter in the listbox. When you use the 'Edit' button, you can edit the [#n]-th texture component of the 'Texture Model' listbox, where [#n] is the serial number and can be found next to the 'Edit' button. Set [#n] you want to modify, then change the parameter of the [#n]-th texture component in the corresponding textbox, then press the 'Edit' button.

### 3.3 Pole figure

After building the modeled texture, it is possible to plot a pole figure for any  $hkl$ . This feature is very useful because the theoretical pole figures calculated with the modelled texture is visually compared with measured pole figures. This also allows us to check the correctness of the specified texture parameters. The pole figures in the X-TEX method show stereographic projections and the intensity scale of the poles is in multiples of the uniform density (m.u.d).

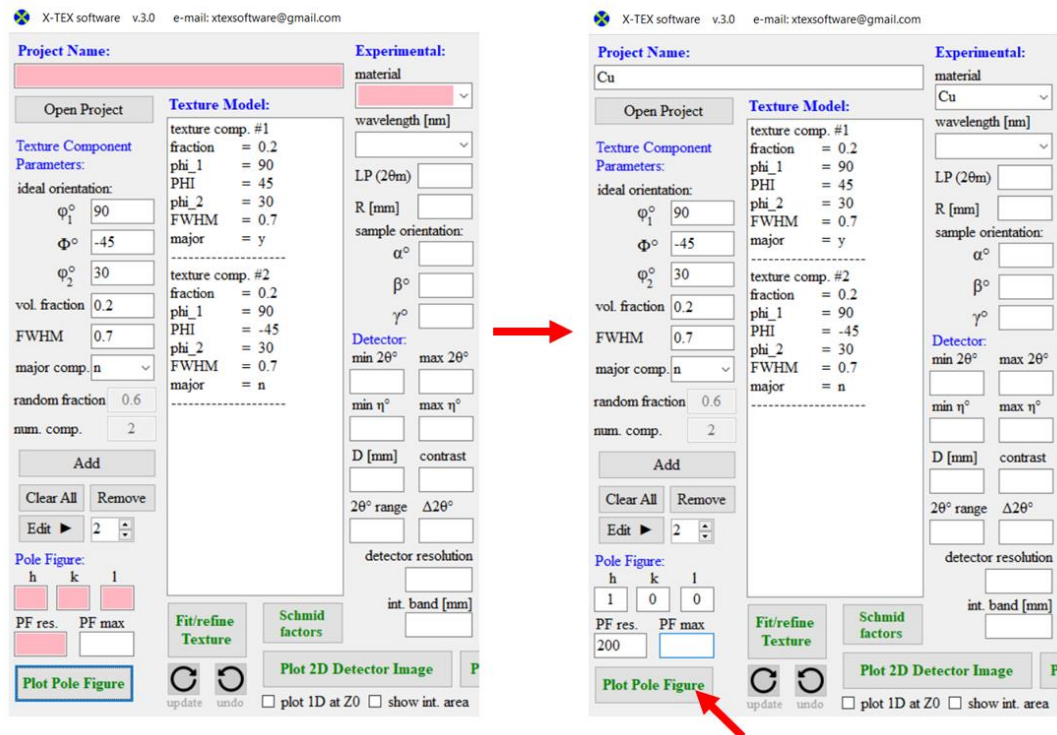


Fig 3.12. The necessary parameters for plotting a pole figure.

For pole figure plotting, first you need to specify the 'project name', the 'material', the  $h,k,l$  textboxes correspond to the pole figure and the 'PF res.' textbox (Fig.3.12). The 'PF res.' parameter is the resolution of the pole figure. This number is the number of pixels alongside horizontal and vertical directions of the plot.

Recommended value: 50 (low res.) - 500 (high res.)

Special values for 'PF res.':

- if last digit is 1, the pole figure will only show the area of the major texture component over  $\chi_0$  threshold value. (more details later)
- if last digit is 2, the pole figure will only show the area of the random texture component over  $\chi_0$  threshold value.

After specifying all needed parameters, press the 'Plot Pole Figure' button and a console application (x\_tex\_pole\_figure.exe subroutine) will show up to calculate and plot the figure with the gnuplot software (Fig.3.13).

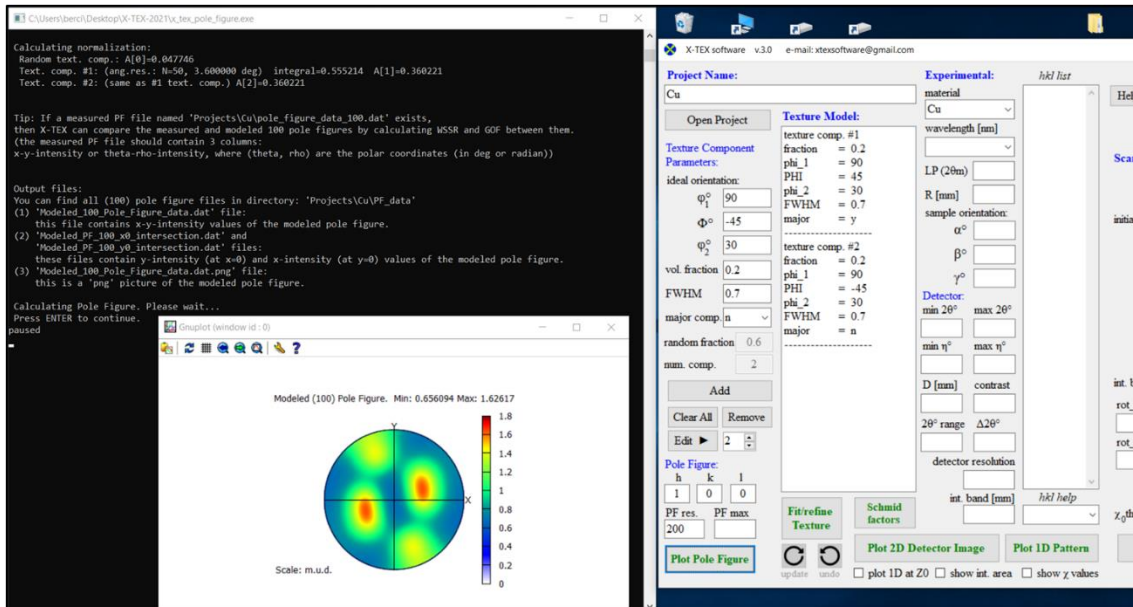


Fig 3.13. After clicking on the 'Plot Pole Figure' button, a console application and a gnuplot figure of the pole figure will show up.

On the pole figure, the *hkl* Miller indices of the plot, the minimum and maximum intensity values, the corresponding colorbar (can be modify with 'colorcode.dat' as mentioned above) and the *x* and *y* axis correspond to Fig.3.5 can be seen.

You can set the maximum intensity of the pole figure with the 'PF max' parameter on the control panel. If the maximum intensity of the pole figure is over this value, the intensities are limited to this value on the pole figure. If the maximum intensity of the pole figure is under this value, then the 'PF max' value will belong to the maximum of the color palette (default maximum color is red) instead of the maximum value of the pole figure (Fig.3.14). With this feature you can set the same intensity scale for different *hkl* pole figures. If 'PF max' is 0 or its field is empty, then there is no restriction for the intensities.

The output files created by the console application can be found in 'PF\_data' directory in the project directory. These are the data file of the *hkl* pole figure (this file contains the *x-y*-intensity values of the modeled pole figure), 1D intersections of *x* and *y* axes of the pole figure (these files contain *y*-intensity (at *x*=0) and *x*-intensity (at *y*=0) values of the modeled pole figure), and png pictures of the *hkl* pole figures.



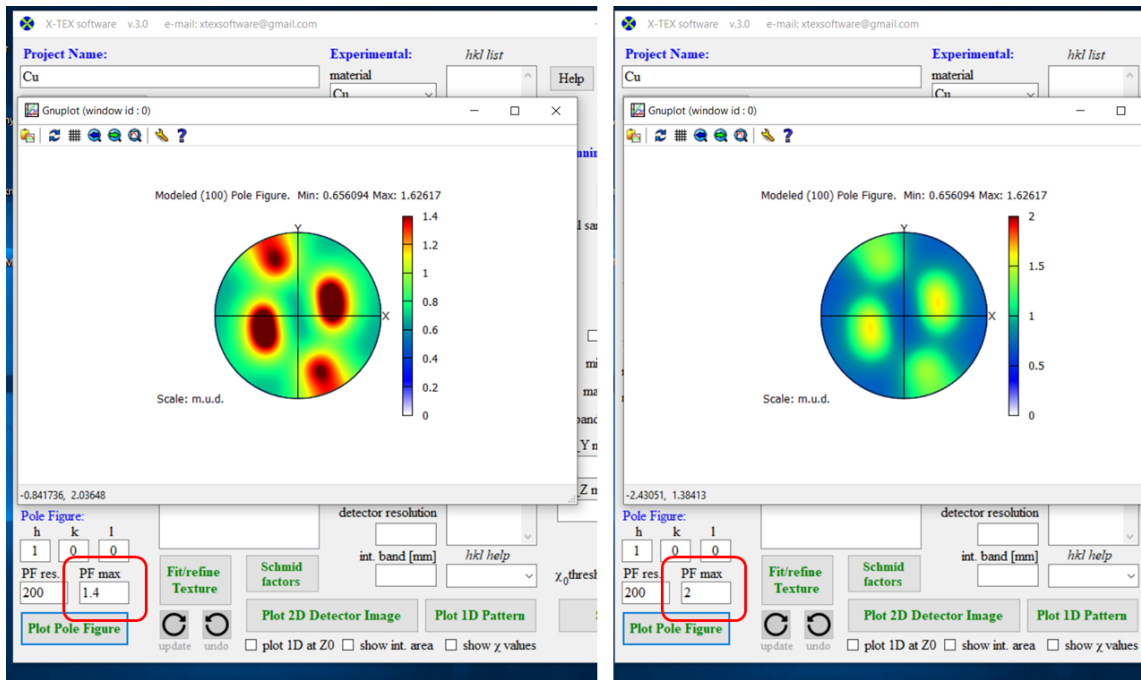


**Fig 3.14.** The illustration of the 'PF max' parameter. The intensity maximum of the (100) pole is 1.6. On the left side 'PF max' is 1.4, over this value the pole intensities are limited to this value. On the right side 'PF max' is 2, this value belongs to maximum of the color palette (red color).

### 3.3.1 Simple textures

In this section, we will look at an example of a simple texture. The material is Ti (hcp crystal system) with two texture components. The ideal orientations of the two components:  $(\varphi_1, \Phi, \varphi_2) = (90^\circ, \pm 45^\circ, 0^\circ)$  (one with positive  $\Phi$ , the other with negative  $\Phi$ ). The FWHM=0.5 and vol. fraction=0.4 are the same for both (vol. fraction for random component is 0.2), and the #1 component is considered as the major component, and #2 is the minor (other) component. The hexagonal Bravais cells of these two ideal orientations are shown in **Fig.3.15**.

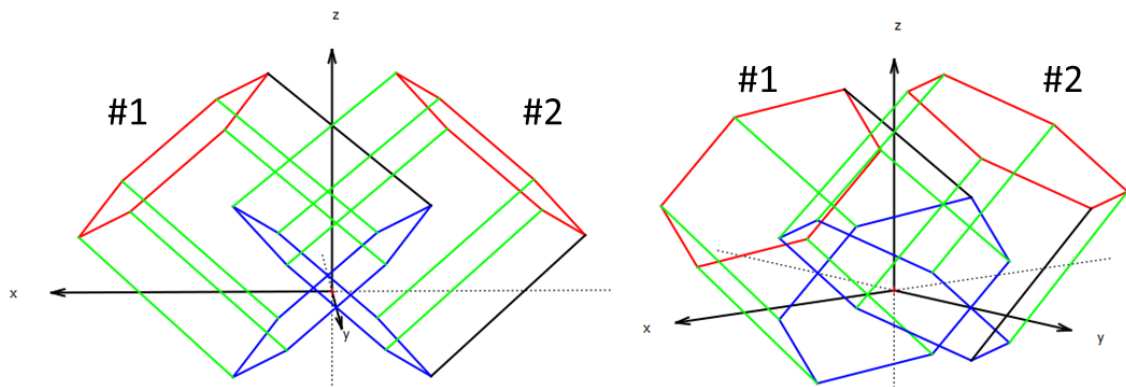


**Fig 3.15.** Two hcp cells with two different ideal orientations:  $(\varphi_1, \Phi, \varphi_2) = (90^\circ, \pm 45^\circ, 0^\circ)$ .

The modeled (100) and (002) pole figures of this textured Ti example and the control panel with the regarding texture parameters are shown in Fig.3.16. and Fig.3.17.

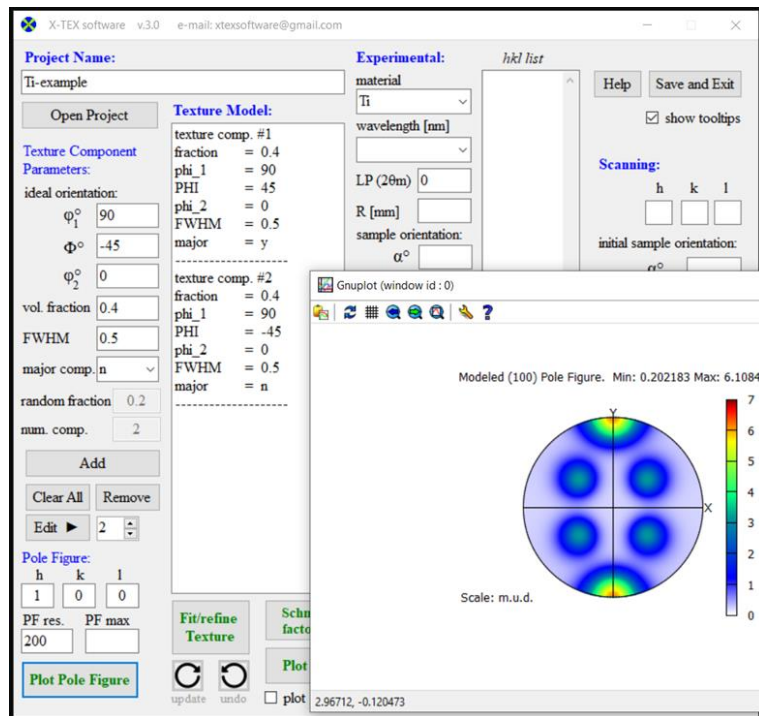


Fig 3.16. Modeled (100) pole figure of the Ti example.

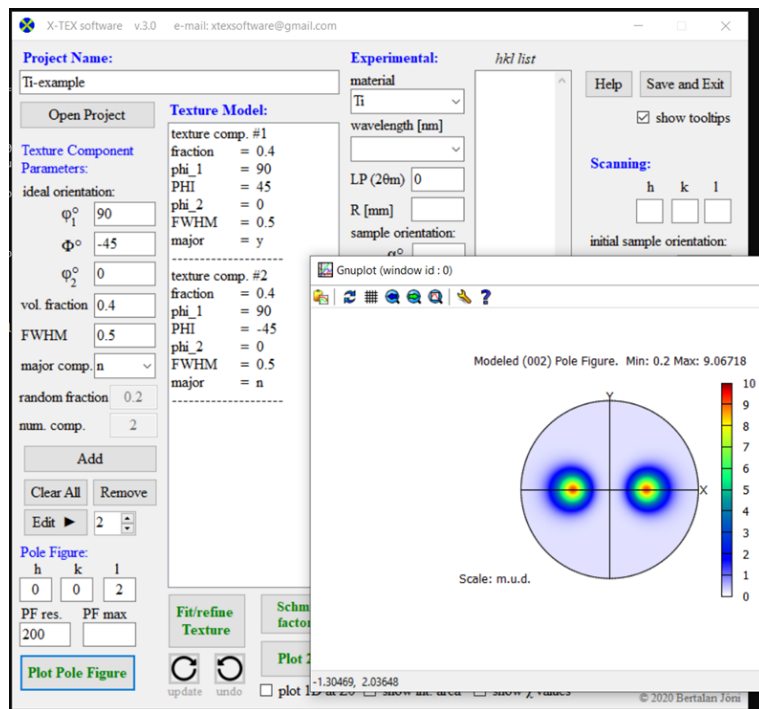
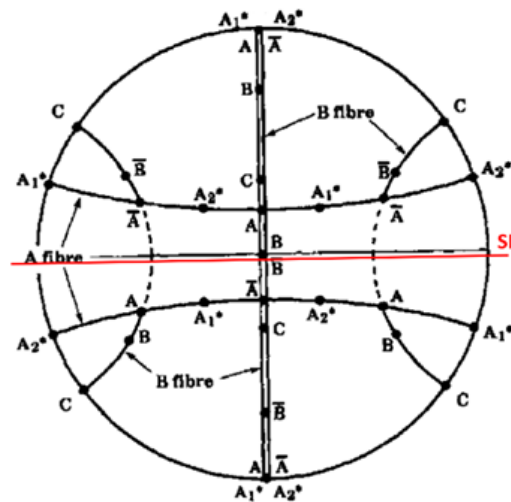


Fig 3.17. Modeled (002) pole figure of the Ti example.

### 3.3.2 Complex textures, linking texture sub-components

In the X-TEX method the texture components are divided into three groups: major, minor (or other) and random. The  $\chi_{hkl}$  values of diffraction peaks are calculated only for this three groups (more details later). This feature is useful because either you can calculate the  $\chi_{hkl}$  values only for one chosen texture component separated from the others, or you can link several texture sub-components belonging to the same major texture component (e.g. for modeling fiber textures or such texture components which cannot be described with symmetrical Gaussian distribution, but can be approximated as the sum of several Gaussian distributions). Let's see three examples.

As an example, let's look at the texture components formed in equal channel angular pressing (ECAP) deformed fcc metals and try to model the texture. ECAP deformation results in a strong, characteristic shear-plane (SP) -symmetric texture with seven possible main texture components in the material, the different orientations of which are shown in [Figure 3.19](#) [6]. The ideal orientations depend on the  $\Phi$  angle of the die, however, the transformation simply involves an additional  $\Phi/2$  rotation to  $\varphi_1$ .



[Fig 3.19](#). The ideal orientations (black dots) and their notations ( $A, \bar{A}, A_1^*, A_2^*, B, \bar{B}, C$ ) of texture components formed during simple shear deformation for fcc metals in the pole figure (111) [6]. The shear plane (SP) is indicated by a red line.

The literature values of the Eulerian angles of the ideal orientations of these seven texture components with and without the die angle (in our case  $\Phi=110^\circ$ ) are shown in [Table 3.1](#) [6]. The measured (111), (100) and (110) pole figures of an ECAP deformed Cu sample with  $\Phi=110^\circ$  are shown in [Fig.3.20a](#).

Texture component name	Eulerian angles of ideal orientation				FWHM	$f^i$	major comp.
	$\varphi_1+\Phi/2$	$\varphi_1$	$\Phi$	$\varphi_2$			
$A_1^*$	90.26	35.26	45	0	0.33	0.1	n
$A_2^*$	19.74	-35.26	45	0	0.33	0.1	n
$A$	55	0	35.26	45	0.33	0.2	n
$\bar{A}$	235	180	35.26	45	0.33	0.2	n
$B$	55	0	54.74	45	0.33	0.05	n
$\bar{B}$	115	60	54.74	45	0.33	0.05	n
$C$	145	90	45	0	0.33	0.25	y

**Table 3.1.** Texture parameters of an ECAP deformed Cu specimen with  $\Phi=110^\circ$  die angle. The Eulerian angles of the ideal orientations are values from the literature for simple shear in fcc metals [6]. The FWHM and  $f^i$  volume fraction values are determined from measured pole figures of this specimen. In this case the C component is considered as the major texture component and all the rest components are the minor (other).

Using the literature values of the ideal orientation (and FWHM and vol. fraction values listed in **Table 3.1**), the same  $hkl$  modelled pole figures are shown in **Fig.3.20b**. In the X-TEX method the 'major comp.' parameter determines whether a texture component is considered to belong to the major component or to the minor (other) component(s). In the case shown in **Table 3.1**, only the 'C' component is considered as major texture component (this can be change easily on the control panel). This way the  $\chi_{hkl}$  values of the  $hkl$  diffraction peaks can be determined only for 'C' separated from the other components, i.e.  $\chi_{hkl}^{\text{major}} = \chi_{hkl}^C$ , and  $\chi_{hkl}^{\text{other}} = \chi_{hkl}^{A+\bar{A}+A_1^*+A_2^*+B+\bar{B}}$  (and of course  $\chi_{hkl}^{\text{random}}$  for the random texture component is also calculated).

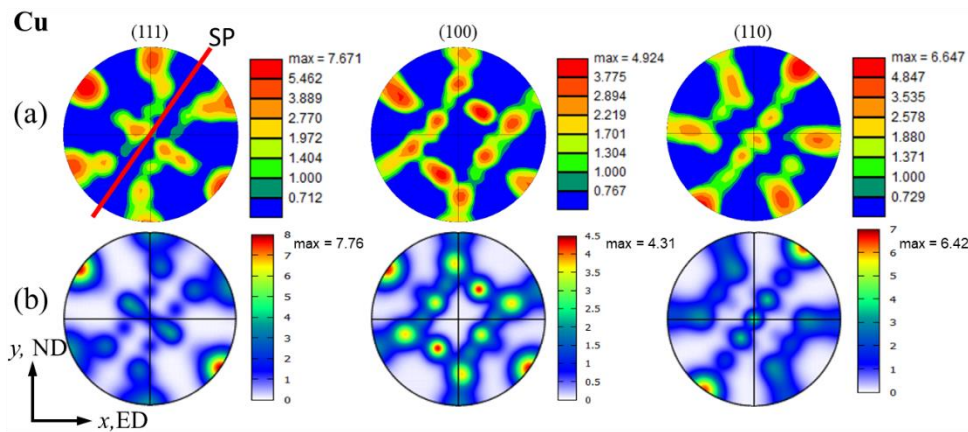


**Fig 3.20.** (a) Pole figures of (111), (100) and (110) obtained from orientation data acquired by EBSD on ECAP deformed Cu specimen. The shear plane (SP) is at  $\Phi/2=55^\circ$  to the  $x$ -axis. (b) Same pole figures modelled with X-TEX software considering the seven main texture components. Note that despite the measured and modelled figures have different color palette, the similarity is clear.

Another example is an extension of the titanium example from section 3.3.1 (Simple textures). Some measured  $hkl$  pole figures of a rolled and then 10% tensile deformed Ti specimen are shown in Fig.3.21 [1]. The (001) pole figure is very similar to the modeled pole figure in (Fig.3.17), however the (100) is quite different from the modeled one (Fig.3.16). While pole (002) has two maxima, pole (100) is more or less evenly distributed along great circles around the basal poles. These major texture components cannot be described by only one symmetrical Gaussian distribution (Eq.1.1), however each of the two major texture components can be well approximated by sum of two Gaussian distributions as subcomponents. The Eulerian angles of these four subcomponents:

$$\#1 \text{ major: } (\varphi_1, \Phi, \varphi_2) = (90^\circ, +36^\circ, 0^\circ)$$

$$\#2 \text{ major: } (\varphi_1, \Phi, \varphi_2) = (90^\circ, +36^\circ, 30^\circ)$$

$$\#3 \text{ minor: } (\varphi_1, \Phi, \varphi_2) = (90^\circ, -36^\circ, 0^\circ)$$

$$\#4 \text{ minor: } (\varphi_1, \Phi, \varphi_2) = (90^\circ, -36^\circ, 30^\circ)$$

The same modelled  $hkl$  pole figures using the Eulerian angles of these subcomponents are also shown in Fig.3.21 (all texture parameters including FWHM and vol. fractions are determined by texture parameter refinement, more details in [1]). The difference between the subcomponents of the same major component is in  $\varphi_2$ , a difference that ensures a slight rotation of the cell around the basal pole.

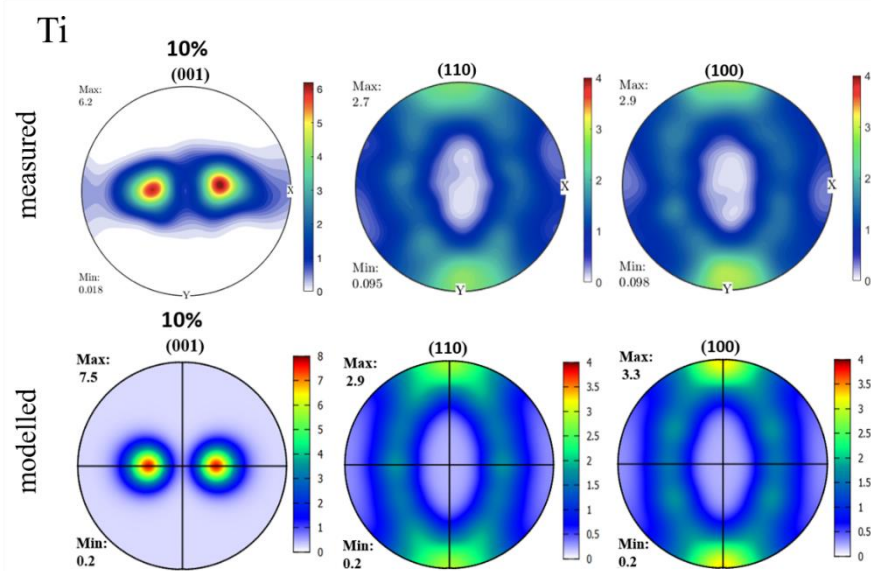


Fig 3.21. Measured and modelled pole figures of a rolled then 10% tensile deformed Ti specimen [1]. The two major texture components are produced by two subcomponent which ensures the more or less even distribution of (100).

The third example is a fiber texture. The fiber texture cannot be described by the Eq.1.1, because it is a symmetrical Gaussian distribution. However, even a fiber texture can also be approximated well by linking many texture sub-components. In Fig.3.22, some measured [7] and modelled pole figures for a Mg alloy are shown. These figures show typical basal fiber texture. Metals and alloys with  $c/a$  ratios approximately equal to the ideal  $c/a$  ratio of 1.633, such as Mg, tend to form basal fiber textures (as in Fig.3.22). The (002) basal pole has a well-defined maximum, however the other  $hkl$  poles are evenly distributed around this (002) pole. It means that there is no ideal orientation of cell in this texture, only there is an ideal direction. We can imagine the situation as if the hcp cells were randomly positioned, except for the axes of  $c$ , which is in the direction of the normal of the sheet ( $z$ -axis).

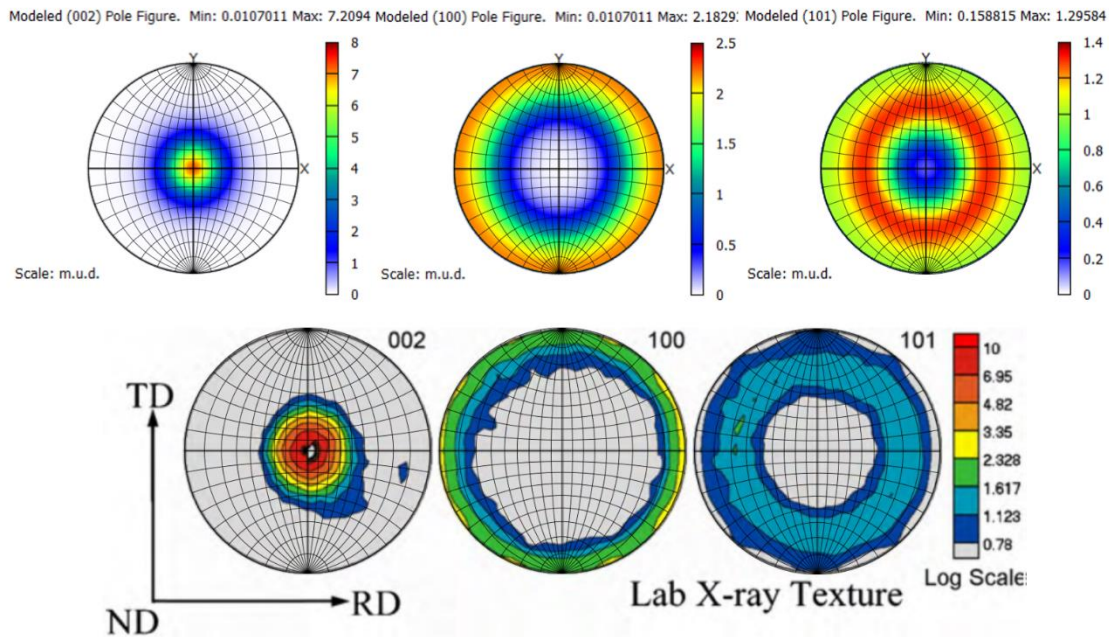


Fig 3.22. Measured [7] and modelled pole figures of Mg with basal fiber texture. The modeled texture is produced by sum of 12 subcomponents. Note that it is just an illustration, i.e. the correct FWHM and vol. fraction values are not known, the goal of this figure is just to show the creation of a fiber texture.

In this case the fiber texture component is approximated by sum of 12 Gaussian distributions:  $(\varphi_1, \Phi, \varphi_2) = (0^\circ, 0^\circ, [0^\circ - 55^\circ])$ , i.e. the  $\varphi_2$  values of the subcomponents vary from 0 to 55 in steps of 5 degrees (all 'major comp.' parameter of the subcomponents are 'y').

### 3.3.3 Comparing modeled pole figures with measured ones

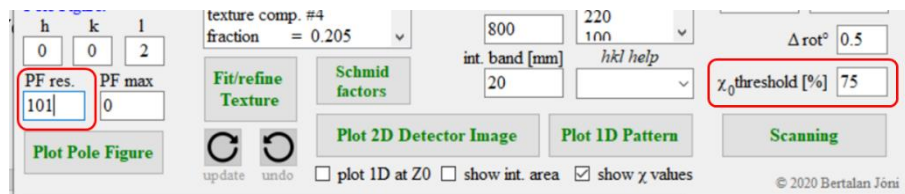
You have the opportunity to compare measured pole figures with the modelled ones quantitatively. For this, the measured pole figure data file has to be in the project directory and its name has to be "pole\_figure\_data\_hkl.dat" for the *hkl* pole figure (in the filename *hkl* is a number). The measured file must contain three columns: x-y-intensity or theta-rho-intensity, where (theta, rho) are the polar coordinates (in deg or radian). The x-y-intensity or theta-rho-intensity values must be separated by Tab or Space from each other. If a "pole\_figure\_data\_hkl.dat" file is detected (in the project directory) when pressing 'Plot Pole Figure' button, first the modelled *hkl* pole figure shows up, then after pressing Enter in the console application, a question appears about whether the measured pole figure data are given in polar coordinates (if yes, then a second question about whether they are in radian). After answering this question, the measured *hkl* pole figure shows up and the Weighted Sum of Squared Residuals (WSSR) and the Goodness of Fit (GOF) values are calculated between the measured and modeled figures. Additionally, a figure of the differences between the measured and modelled pole figures shows up too.

This feature is useful, because it gives an opportunity to check whether the input texture data are correct.

### 3.3.4 Pole figures with $\chi_0$ threshold value

It was mentioned above, that if the 'PF res.' parameter has special values, then on the pole figure we can see the area belonging to the major or the random component over a given  $\chi_0$  threshold value. It means, that the intensities of the pole figure on this area the intensity contribution of the major/random texture component is over this threshold value.

The  $\chi_0$  value can be set on the control panel:



The special values for 'PF res.':

- if last digit is 1, the pole figure will only show the area of the major texture component over  $\chi_0$  threshold value.
- if last digit is 2, the pole figure will only show the area of the random texture component over  $\chi_0$  threshold value.

If you choose this option, you can also choose whether you want to plot the area or just the boundary line of this area (a question shows up in the console application about this).

In **Fig.3.23** these types of pole figure plots are shown for 23% tensile deformed Ti specimen from [1]. The left side of the figure shows the area belonging to the major texture component over  $\chi_0=75\%$ , or only the boundary line of this area. The right side of the figure shows these for the random component over  $\chi_0=65\%$ .

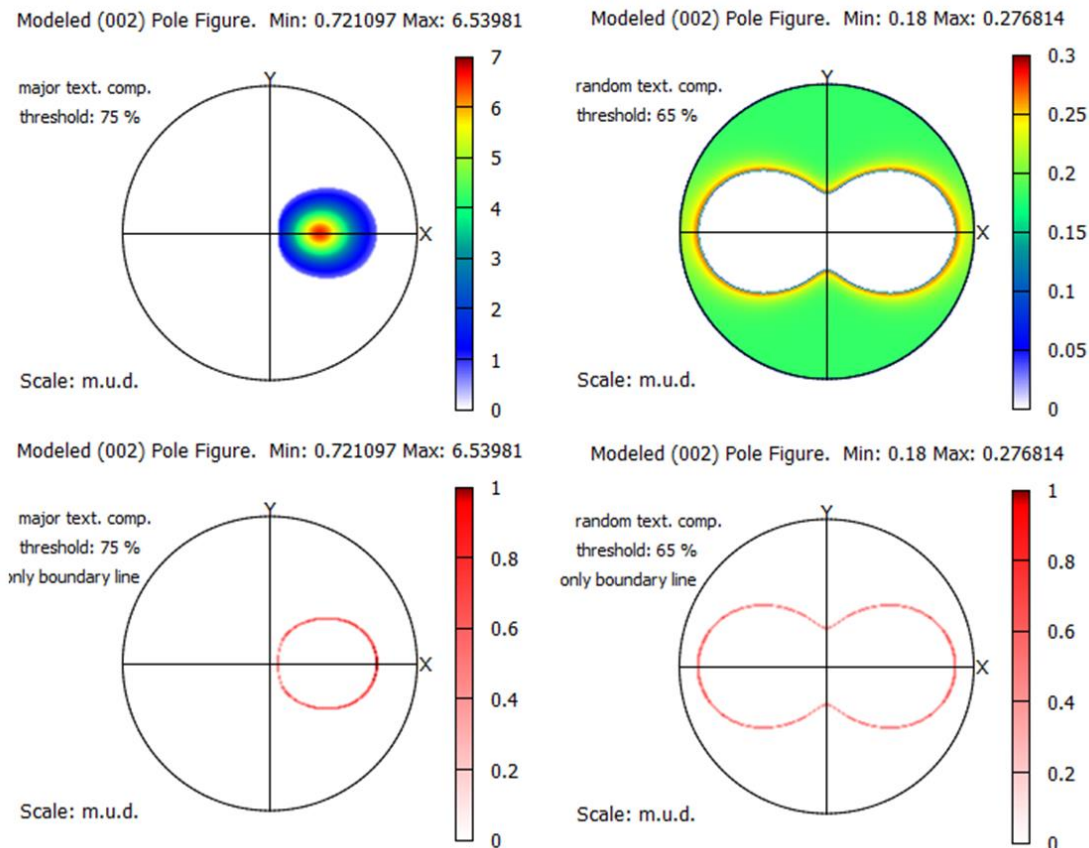


**Fig 3.23.** Modeled (002) pole figures only show the area of the major/random texture component over a given  $\chi_0$  threshold value. Note that in this case there are two texture components, but only one of them is considered as major, and the other one is considered as the minor component, that's why there is only one pole for the major component instead of two poles.

Why is this function useful? Let's see the **Fig.3.24**, in which an intersection of the (002) pole figure (along  $x$ , i.e. TD axis) and the (002), (110) and (100) pole figures with boundary lines for the two major and the random component with  $\chi_0^{\text{major}} = 60\%$  and  $\chi_0^{\text{random}} = 40\%$  threshold values are shown. The limit of 40% intensity contribution for the random texture component may appear to be a low value, however, as we can see on the pole figures, for this 40% limit the scattered intensity stems from grains tilted at least  $30^\circ$  from the ideal orientation of the major texture components, which is significant. In



the case of this Ti specimen, if we measure a  $hkl$  diffraction peak with  $\chi_{hkl}^{\text{random}} > 40\%$ , then considering this peak belongs to the random component is correct despite the apparently low threshold value. This example shows that chasing the highest  $\chi_{hkl}$  values is not always necessary; though choosing  $\chi_0$  is arbitrary, you should always consider what this threshold value physically means for each texture component.

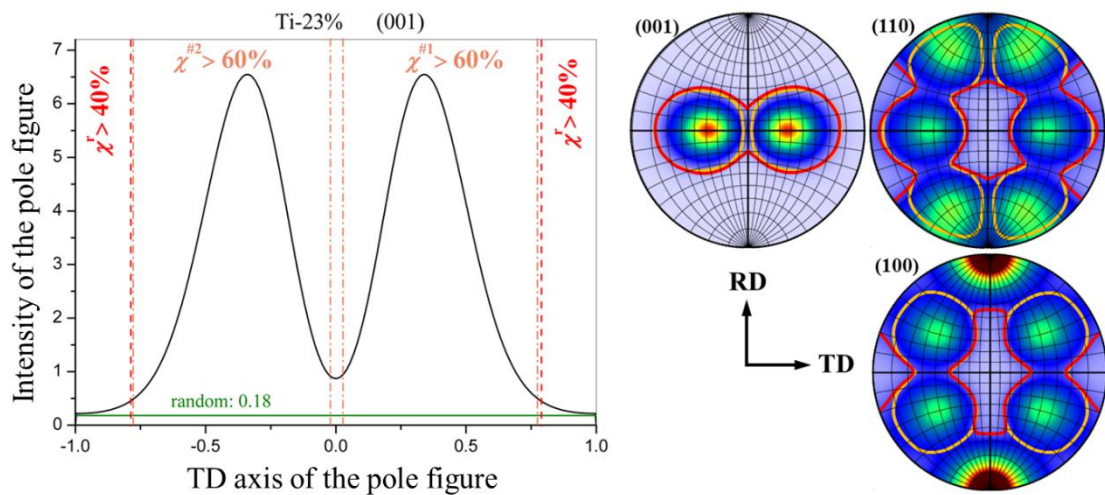


**Fig 3.24.** Illustration of the  $\chi_0$  threshold value for the major and the random texture components with  $\chi_0^r = 40\%$  and  $\chi_0^{\#1, \#2} = 60\%$ . In the (001), (110) and (100) pole figures, the orange line indicates the threshold for the major (#1 or #2), and the red line indicates the threshold for the random texture component. These boundaries can also be seen in the cross-section figure of the (001) pole figure alongside the TD axis. The pole figures show that for  $\chi_0^r = 40\%$ , grains are considered to belong to the random texture component if they are more than  $30^\circ$  inclined from the pole maxima of the major texture components.

## 3.4 Plot 2D detector image

### 3.4.1 Experimental parameters

The experimental parameters on the control panel are shown in Fig.3.25. The 'material' was discussed above in detail, select the investigated material from the drop-down list. The 'wavelength' parameter is the wavelength of the X-ray beam in [nm]. There are some built-in typical values to help, but any value can be entered. The other parameters are explained in more detail below. To do this, let's first look at a figure of the experimental geometry (Fig.3.26).

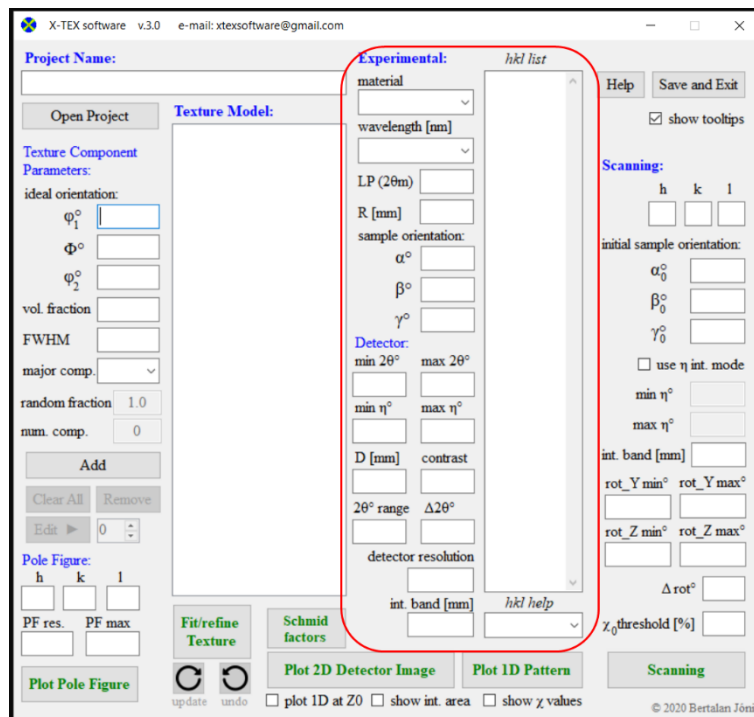


Fig 3.25. Experimental parameters on the control panel.

#### 3.4.1.1 Experimental geometry

The schematic figure of the X-ray diffraction measurement geometry was shown in Fig.1.1. Fig.3.26 shows the same with more details. The definition of the  $\mathcal{K}_L = \{X, Y, Z\}$  laboratory coordinate system, the  $2\theta$  scattering angle and the  $\eta$  azimuth angle of the scattered beam are also shown in this figure. The scattered radiation is detected by two-dimensional (2D) detector(s). In Fig.1.1, the detector appears to be flat, but in fact a curved detector is assumed around the sample, as shown in Fig.3.26. The height of the detector (in  $Z$  dimension with  $[+D/2, -D/2]$  size) is denoted by  $D$  and the radius of the detector (the distance between the origin of the laboratory coordinate system and the detector surface) is denoted by  $R$ . This geometry works for both laboratory and

synchrotron measurements. The X-ray tubes used in laboratories can produce the wavelength of the radiation of the order of 0.1 nm, while in the case of synchrotrons the wavelength is usually much smaller. Since the Bragg angle of the DS rings depend on the wavelength, therefore in laboratories the useful angle range is basically the full angle range [0-180 deg], but in the case of the synchrotrons it is much smaller, it can be even only a few degrees. Because of this, in the case of synchrotrons, usually flat detectors are used, like Fig.1.1 shows. However, the large sample-to-detector distance usually used in synchrotrons makes the curved detector a good approximation to a flat detector. In this case  $R$  is basically the sample-detector distance. In summary: geometry in Fig.3.26 is valid for curved detector and a good approximation for flat detector with large sample-to-detector distances.

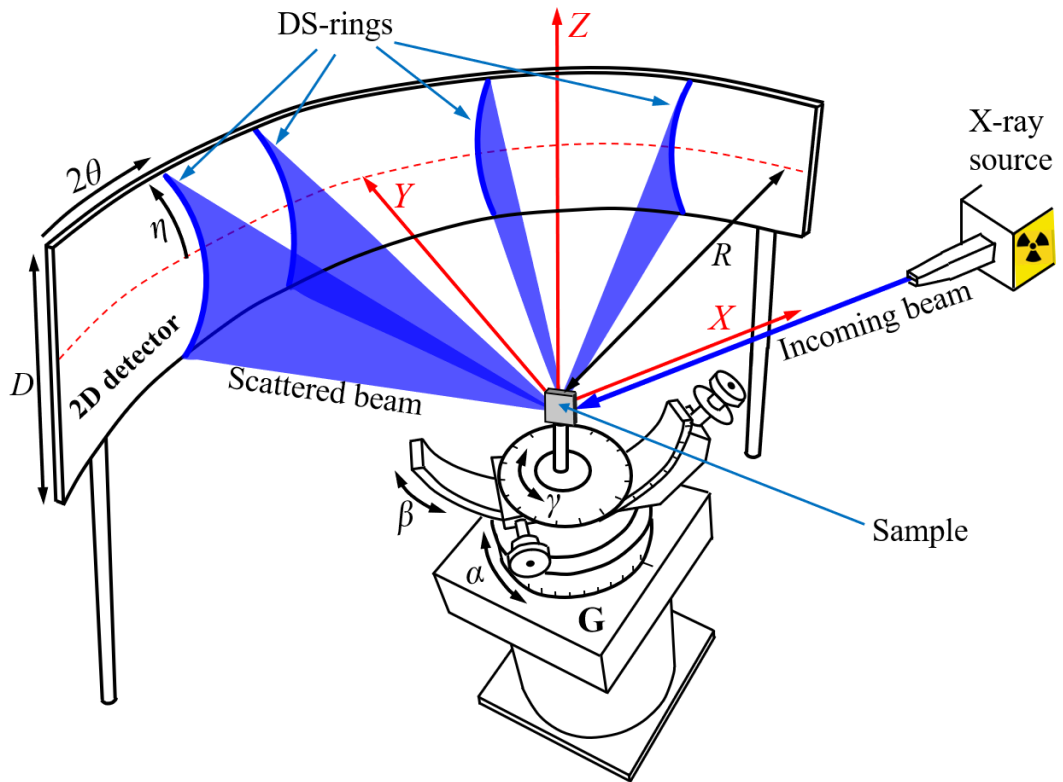


Fig 3.26. Experimental geometry.  $\mathcal{K}_L = \{X, Y, Z\}$  is the laboratory coordinate system,  $2\theta$  is the scattering angle and  $\eta$  is the azimuth angle of the scattered beam. The scattered radiation is detected by two-dimensional (2D) detectors with  $D$  height and  $R$  radius. The  $(\alpha, \beta, \gamma)$  orientation of the sample can be adjusted using a sample holder goniometer (G). The red dashed line marks the  $X$ - $Y$  plane at  $Z=0$ .

Note that whether the detector is curved or flat is only relevant 1) for the 2D detector image, 2) for DS integration using a band area, and 3) for the determination of the  $\chi$  values using a band area (more details about integration on a band area later). For

synchrotrons the integration of the DS rings and the determination of the  $\chi$  values usually are done according to the  $2\theta$  and  $\eta$  variables, and the curvature of the detector does not matter at all in these cases. In other words, there is a problem only if you want to 1) determine  $\chi$  values using a flat detector with a small sample-detector distance and the integration area is a "band", or 2) make 2D detector image using a flat detector with a small sample-detector distance. In all other cases, the geometry shown in Fig.3.26 works.

### 3.4.1.2 Sample orientation

The sample orientation in  $\mathcal{K}_L$  laboratory coordinate system is described the same way as the ideal orientation of a texture component in  $\mathcal{K}_S$  detailed in section 3.2.1 (Eulerian angles of the ideal orientation). Initially  $\mathcal{K}_L = \{X, Y, Z\}$  laboratory coordinate system and  $\mathcal{K}_S = \{x, y, z\}$  the sample coordinate system coincide, i.e.,  $x \parallel X$ ,  $y \parallel Y$  and  $z \parallel Z$  (Fig.3.27a). The sample (and its  $\mathcal{K}_S$  system) from this initial orientation is rotated in the laboratory  $\mathcal{K}_L$  system according to the sample orientation used in the X-ray diffraction measurement. This rotation is described by a three-dimensional rotation matrix with Z-X-Z convention defined in Eq.1.5 as  $\hat{R}_{(\alpha, \beta, \gamma)} = \hat{R}_Z(\alpha)\hat{R}_X(\beta)\hat{R}_Z(\gamma)$ , where  $\alpha$ ,  $\beta$  and  $\gamma$  are the Eulerian angles of the sample rotation in  $\mathcal{K}_L$ .

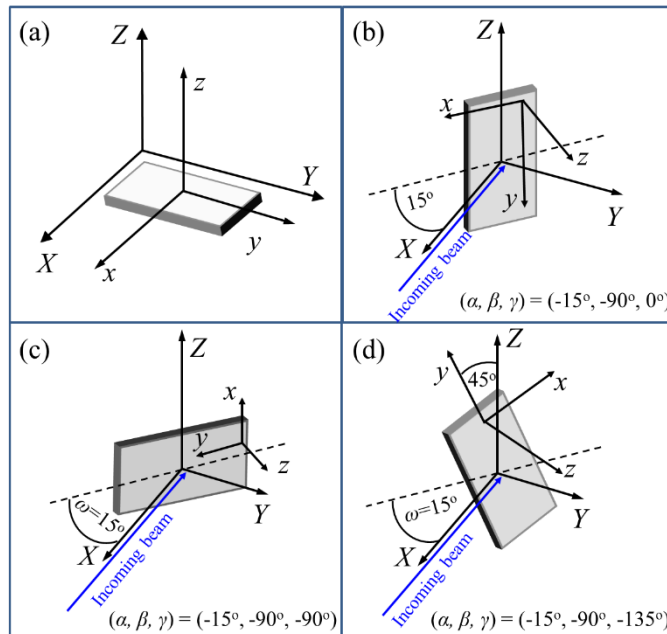


Fig 3.27. (a) The initial sample orientation and (b-d) some examples for the  $(\alpha, \beta, \gamma)$  sample orientations.

The  $\hat{R}_{(\alpha, \beta, \gamma)}$  rotation matrix describes three basic rotations of the sample one after the other in such a way that first rotates the sample around the Z-axis by angle  $\gamma$ , then

around the X-axis by angle  $\beta$ , and finally again around the Z-axis by angle  $\alpha$ , thus characterizing the sample orientation in the  $\mathcal{K}_L$ . The initial sample orientation and three examples for sample orientations are shown in Fig.3.27.

### 3.4.1.3 Lorentz-polarization factor

The  $LP$  Lorentz-polarization factor in Eq.1.7 can be set by the parameter 'LP(2 $\theta$ m)' on the control panel.  $LP = L \cdot P$  is the combination of the  $L$  Lorentz part and the  $P$  polarization part.

- The polarization part is:

$$P = \begin{cases} \frac{1 + \cos^2(2\theta_M)\cos^2(2\theta)}{1 + \cos^2(2\theta_M)}, & \text{if } LP \text{ parameter is } 2\theta_M \\ 1, & \text{if } LP \text{ parameter is } 0. \end{cases} \quad (3.4)$$

In Eq.3.4  $P = \frac{1 + \cos^2(2\theta_M)\cos^2(2\theta)}{1 + \cos^2(2\theta_M)}$  is the polarization factor when monochromator is used in the case of unpolarized X-ray beam [4,8], where  $2\theta_M$  is the Bragg angle of the monochromator crystal (in degrees). In Eq.3.4  $P = 1$  means a polarized beam.

If you want to model a synchrotron measurement with polarized beam, then leave the 'LP(2 $\theta$ m)' empty or use 0 value. In other case 'LP(2 $\theta$ m)' is the  $2\theta_M$  value.

- The Lorentz part is:

$$L = \frac{1}{\sin(\theta)} \quad (3.5)$$

The Lorentz correction factor includes three different terms [4]:

$$L = L_1 L_2 L_3 = \left(\frac{1}{\sin(2\theta)}\right) (\cos \theta) \left(\frac{1}{\sin(2\theta)}\right),$$

but the last term is considered by the integration of the DS rings, so in this case it is  $L = L_1 L_2 = \frac{\cos \theta}{2 \sin \theta \cos \theta} \sim \frac{1}{\sin(\theta)}$ . Note that

$LP$  does not play roll when you determine the  $\chi_{hkl}^i$  values in Eq (1.9), because for the same  $hkl$   $LP$  is also the same.  $LP$  only matters when different  $hkl$  peaks or rings are compared, e.g. texture refinement based on many  $hkl$  rings.

### 3.4.1.4 Detector parameters

First, we need to define the horizontal and vertical dimensions of the detector image. The vertical limits of the 2D detector image are given by the detector height ( $D$ ) parameter (in  $Z$  dimension with  $[+D/2, -D/2]$  size). Beyond that, nothing is visible from the DS rings in the vertical direction. However, calculating the horizontal limits is trickier, the left and right image limits are calculated based on minimum and maximum of the  $2\theta$  and  $\eta$  azimuth angles given on the control panel. The 'min  $2\theta$ ' and 'max  $2\theta$ ' values at  $Z=0$

(along the red dashed lines in Fig.3.26) determines the horizontal limits of the detector image, also considering that the  $[\min \eta, \max \eta]$  range must be visible in the image. DS rings are only calculated in the  $[\min 2\theta, \max 2\theta]$  and  $[\min \eta, \max \eta]$  range in the detector image. In short: the area of the detector image which limited by the  $[\min 2\theta, \max 2\theta]$  range, the  $[\min \eta, \max \eta]$  range, and  $D$ , is always visible. The minimum and maximum azimuthal angle also plays an important role in defining the integration limits of the DS rings (more details later). The allowed  $2\theta$  range:  $[0, 180 \text{ deg}]$ , and the allowed  $\eta$  range:  $[0, 360 \text{ deg}]$  or  $[-180, 180]$  (both can be used, but the angular difference between  $\max \eta$  and  $\min \eta$  cannot be greater than 360 degrees).

DS rings should not be calculated over the whole detector surface because they only have a significant intensity near the ring, away from the ring the intensity is zero. Therefore, it does not make sense to calculate the rings in the full  $2\theta$  range, because this would slow down the program runtime. The  $2\theta$  angular range where the intensity of a specific Debye-Scherrer ring is calculated and plotted can be set by the ' $2\theta^\circ$  range' parameter on the control panel. The ring is calculated in the  $\pm \frac{2\theta^\circ \text{ range}}{2}$  area.

As it was mentioned in the basic diffraction concepts section, infinitely narrow DS rings and peaks (intensity only at the exact  $2\theta_B$  Bragg angle) would not be illustrative, so all the rings and peaks have artificial Gaussian type broadening with the same width (which has nothing to do with anisotropic peak broadening). This parameter can be set by the ' $\Delta 2\theta^\circ$ ' parameter on the control panel and this parameter means the FWHM of the Gaussian function of the broadening. In other words, the intensity in each  $(2\theta_B, \eta)$  point of the DS ring is calculated using Eq.1.7. However, it means only one not zero intensity value along  $2\theta$ , at the  $2\theta_B$  Bragg angle. Therefore, near the DS ring, a Gaussian function is used to achieve non-zero intensity not only at the Bragg angle. Note that this artificial width is no relevant, it is just a visual element and the intensities calculated by Eq.1.7 or Eq.1.8 represent the maximum intensity of a ring or a peak, i.e. the maximum value of the Gaussian function. Set this ' $\Delta 2\theta^\circ$ ' parameter to large if you prefer thick rings or small if you prefer thin rings, this will not affect to the maximum intensities of the rings or the integration in Eq.1.8 along the  $\eta$  azimuth angle.

The 'detector resolution' is the number of pixels alongside horizontal and vertical directions of the image.

The 'int. band' parameter is used to specify azimuthal integration mode and range of the  $hkl$  DS rings, by which you get the  $hkl$  peaks from rings (more details later).

The 'contrast' parameter is just a visual parameter to enhance the visibility of the integrated area in the detector image (more details later).

### 3.4.1.5 *hkl* list

The *hkl* Miller indices need to be specified in the '*hkl* list' for 2D detector image, 1D diffraction pattern and the  $\chi_{hkl}$  values (Fig.3.28). In the '*hkl* list' each line must contain a certain *hkl*. Negative values for the Miller indices are not allowed, because the software calculates all the permutations of *hkl* values including negative values, so you don't have to worry about that, just use the conventional powder diffraction *hkl* notation. In other words, the *hkl* values refer to a crystal plane family and not a specific plane. It also means that always 3-index-notation of Miller indices is used, i.e. there is no need to give the fourth  $i=-(h+k)$  index in the case of hexagonal or trigonal systems. Two-digit indices can be specified by using comma to separate them, e.g. 1,1,12.

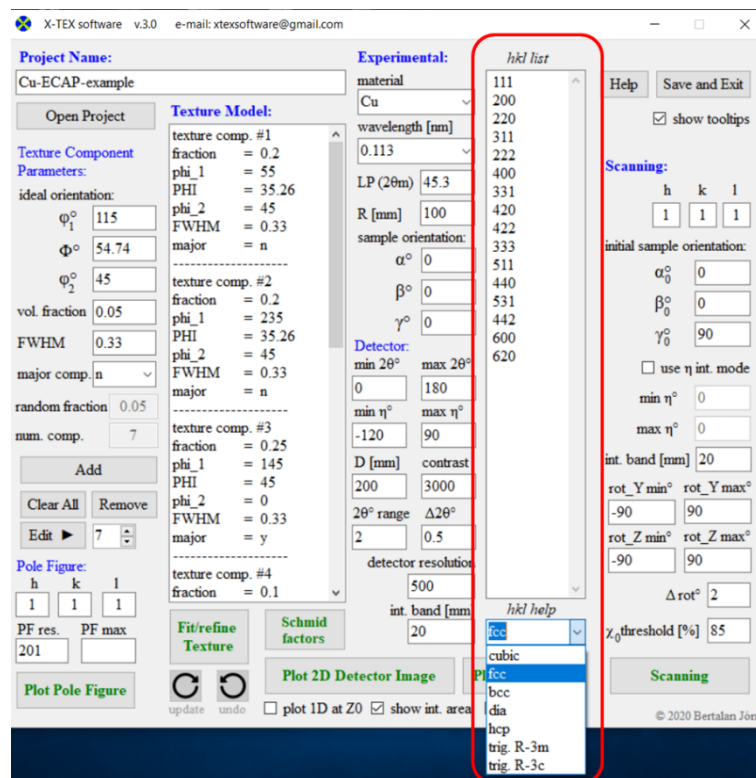


Fig 3.28. The *hkl* list and *hkl* help.

There is a '*hkl* help' drop-down list below the '*hkl* list' that helps you to specify possible *hkl* values for some crystal systems (Fig.3.28). If an item from this drop-down list is selected, the '*hkl* list' will be populated with the corresponding *hkl* indices. Note that it is not the crystal system selected in this drop-down list that determines the crystal

structure of the material, the crystal system should be specified in the 'x\_tex\_crystal\_data.dat' file as mentioned above (in section 2.6.1.2 Crystal data file).

### 3.4.2 Detector images

A detector image (DS rings) can be plotted in order to be able to compare calculated and measured X-ray diffraction data visually. For this, the experimental parameters and settings as well as the *hkl* indices of the peaks to be plotted need to be specified. The intensity in each  $(2\theta_B, \eta)$  point of the DS rings is calculated using Eq.(1.7).

In this section, some examples for calculated 2D detector images according to the texture and the experimental parameters are shown. After specifying all needed parameters, press the 'Plot 2D Detector Image' button and a console application (x\_tex\_detector.exe subroutine) will show up to calculate and plot the detector image with the gnuplot software (Fig.3.29). You can zoom in the 2D image with the right mouse button. Press Enter in the console application to close the image and the console app.

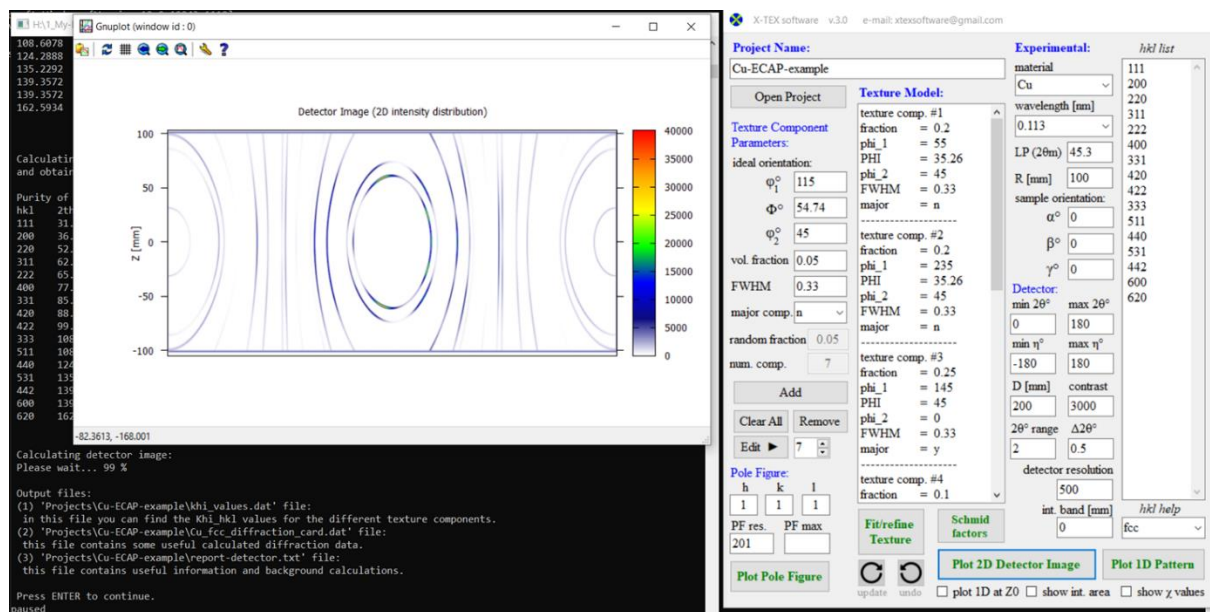
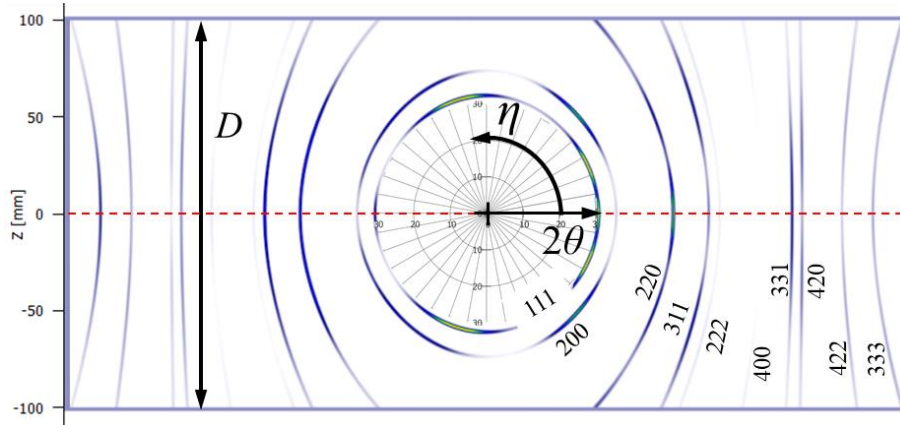


Fig 3.29. After clicking on the 'Plot 2D Detector Image' button, a console application and a gnuplot figure of the 2D detector image will show up.

In Fig.3.29, the control panel, the console application and the detector image are shown for the ECAP deformed Cu from section 3.3.2 with the mentioned seven texture components. The experimental parameters used for the detector image can be seen on the control panel. In Fig.3.30-3.35 the illustrations of some experimental parameters using this Cu specimen are shown.





**Fig 3.30.** The illustration of the detector height,  $D$ , the scattering angle,  $2\theta$ , and the azimuth angle,  $\eta$ , in the 2D detector image for the ECAP deformed Cu specimen. The red dashed line marks the X-Y plane at  $Z=0$ . The  $hkl$  indices of the DS rings are also shown. Note that DS rings are not concentric rings, because of the cylindrical shaped detector.

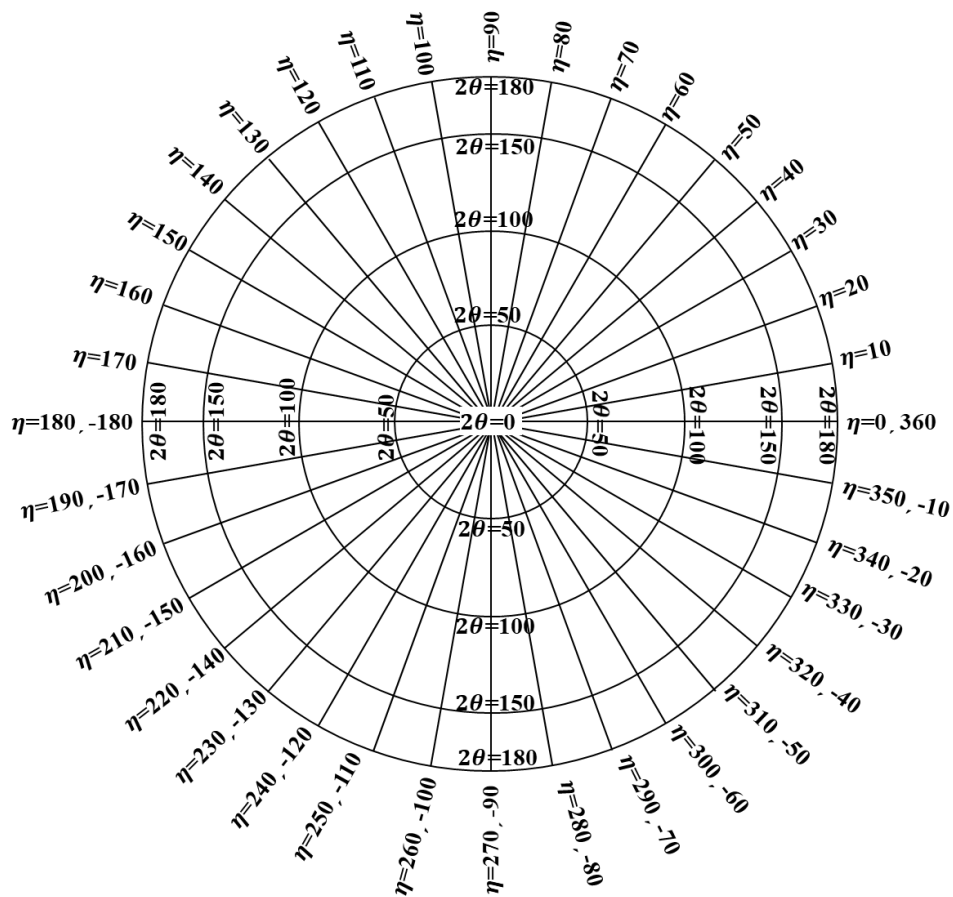


**Fig 3.31.** The schematic figure of the values of the  $2\theta$  and  $\eta$  parameters. The allowed  $2\theta$  range:  $[0,180 \text{ deg}]$ , and the allowed  $\eta$  range:  $[0,360 \text{ deg}]$  or  $[-180,180]$  (both can be used, but the angular difference between max  $\eta$  and min  $\eta$  cannot be greater than 360 degrees).

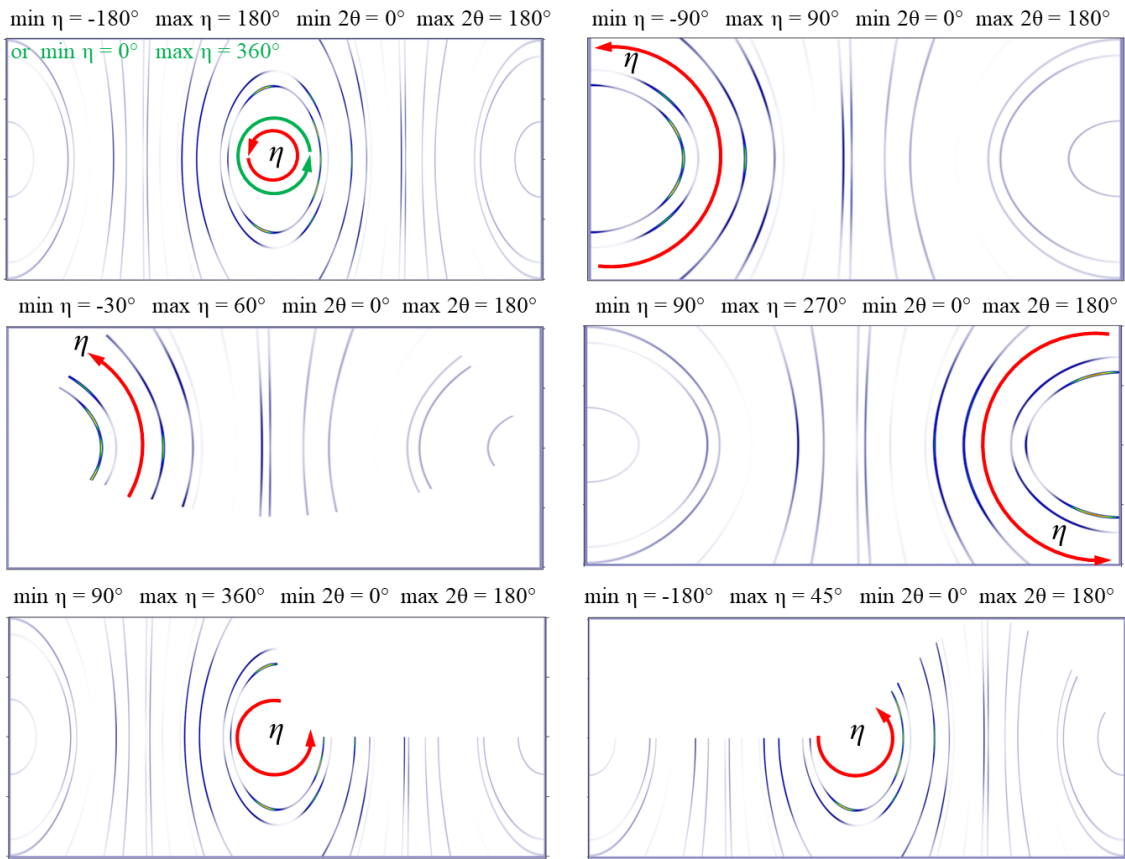


**Fig 3.32.** The illustration of how the 'min  $\eta$ ' and 'max  $\eta$ ' experimental parameters affect to the detector image using different values. The DS rings are only calculated in the  $[\text{min } \eta, \text{max } \eta]$  range. Note that these 'min  $\eta$ ' and 'max  $\eta$ ' parameters have an important role in the integration of the DS rings as well.

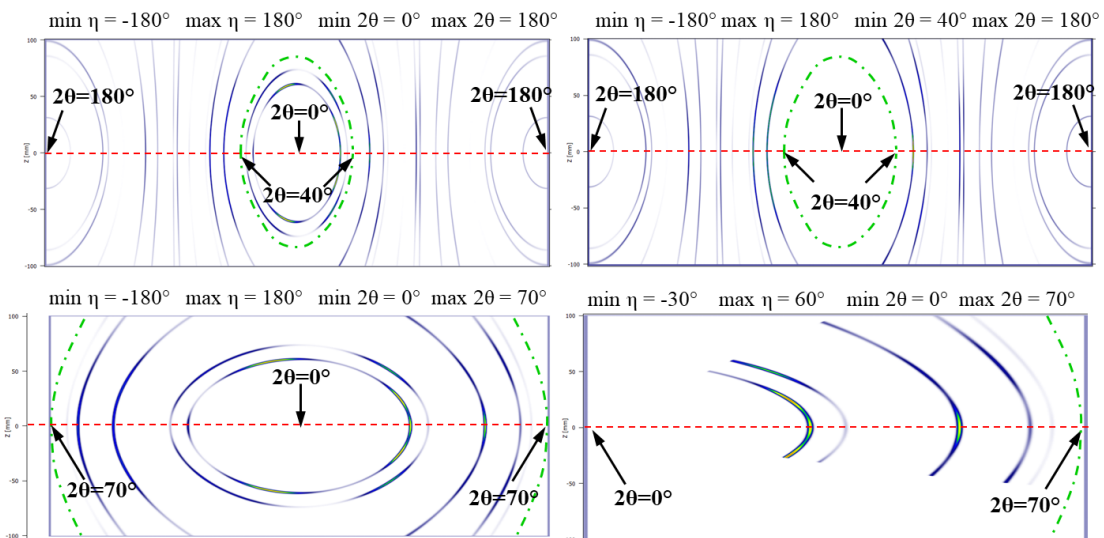


**Fig 3.33.** The illustration of how the 'min  $2\theta$ ' and 'max  $2\theta$ ' parameters affect to the detector image using different values. The 'min  $2\theta$ ' and 'max  $2\theta$ ' values at  $Z=0$  (along the red dashed lines) determines the horizontal limits of the detector image, also considering that the  $[\text{min } \eta, \text{max } \eta]$  range must be visible in the image. Furthermore, the DS rings are only calculated in the  $[\text{min } 2\theta, \text{max } 2\theta]$  range.

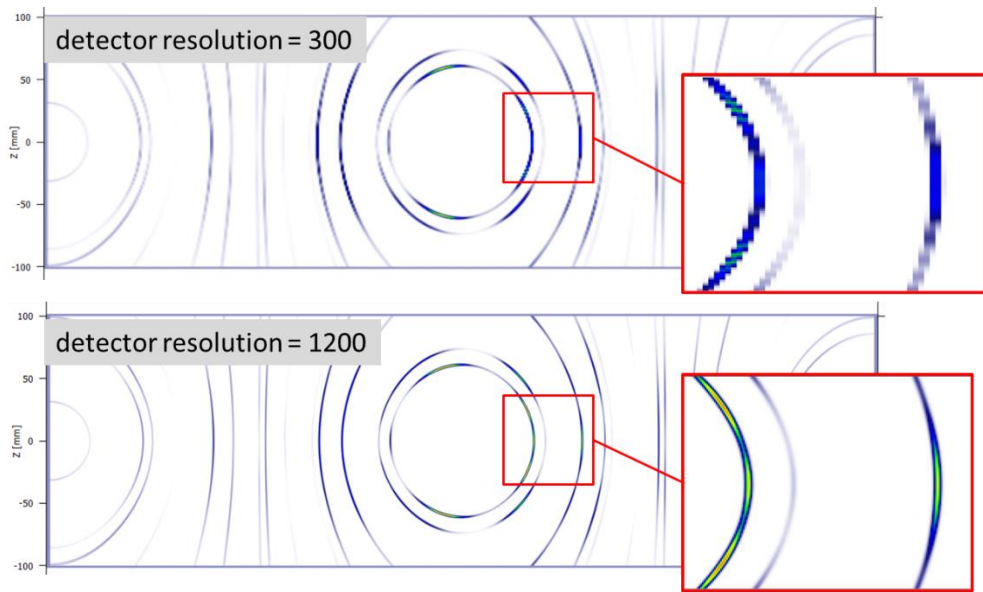


**Fig 3.34.** The illustration of the detector resolution using two different values.

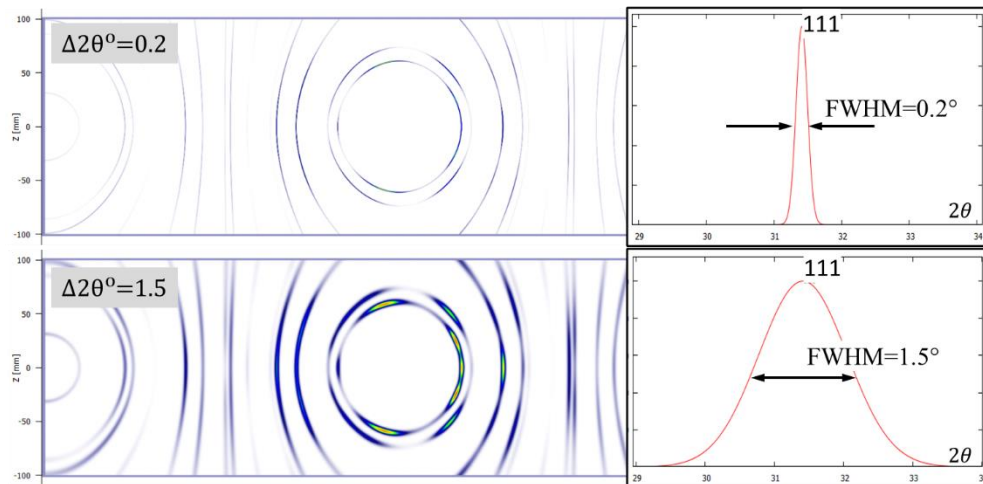


**Fig 3.35.** The illustration of the ' $\Delta 2\theta^\circ$ ' parameter using two different values.

In **Fig.3.36** a detector image of a real diffraction measurement and the calculated detector image are shown for the Cu specimen with  $(\alpha, \beta, \gamma) = (70^\circ, 90^\circ, -55^\circ)$  sample orientation.

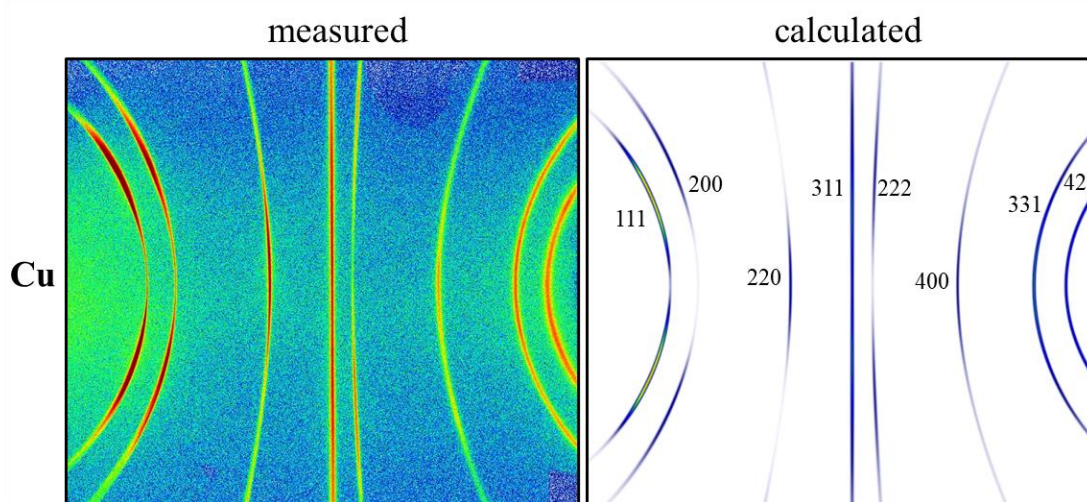
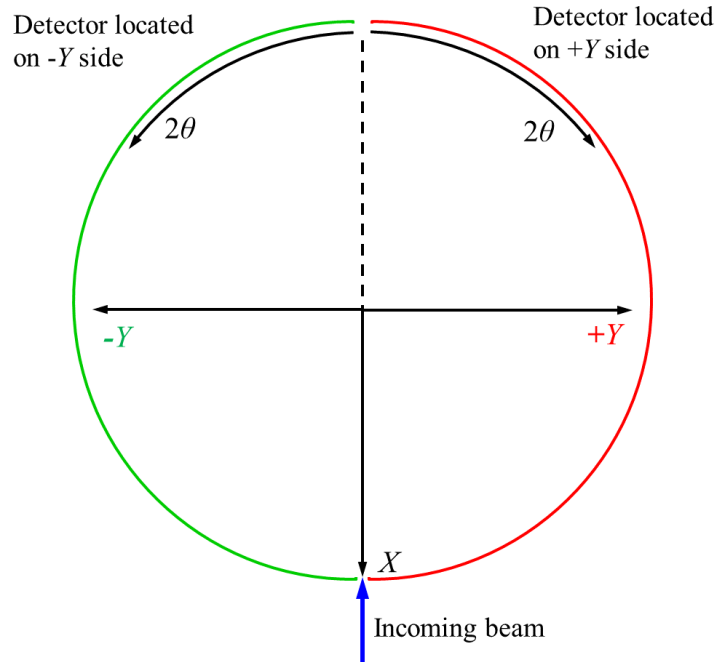


Fig 3.36. Measured and calculated 2D detector image of the ECAP deformed, textured Cu.

### 3.5 Calculating $\chi_{hkl}$ values, plot 1D pattern

#### 3.5.1 Specifying the integrated area

The integration of the  $I_{(2\theta_B, \eta)}$  two-dimensional intensity distribution (Eq.1.7) alongside the  $\eta$  azimuth angle leads to the  $I_{(2\theta_B)}$  one-dimensional (1D) diffraction pattern consisting of  $hkl$  diffraction peaks. The total intensity obtained by integrating the intensity distribution over an  $[\eta_{\min}, \eta_{\max}]$  interval is defined by Eq.1.8. This  $[\eta_{\min}, \eta_{\max}]$  interval can be specified by the 'int. band' parameter on the control panel. The 'int. band' parameter can be zero, positive or negative. If it is zero (or empty field), then 'min  $\eta$ ' and 'max  $\eta$ ' experimental parameters are used as integration limits for all  $hkl$  rings, i.e. the area of the integration is a circular sector. If not zero, then according to the (+) or (-) sign of this parameter, an integration band located on +Y or -Y side determines the  $[\eta_{\min}, \eta_{\max}]$  integration limits for all  $hkl$  rings (Fig.3.37). The full height of the band is the absolute value of the 'int. band' parameter. The former is a common mode of integration in the case of synchrotrons, while the latter in the case of laboratory measurements. Of course, in both cases the  $[\min 2\theta, \max 2\theta]$  range is also taken into account, i.e. there is no integration outside this range.



**Fig 3.37.** Illustration of the detector location when it is positioned on +Y or -Y side.

### 3.5.2 Plot 2D detector image with the integrated area

The integrated area, whether it is a band or a circular sector, can be highlighted in the 2D detector image by checking the 'show int. area' checkbox on the control panel. If 'show int. area' checkbox is checked, the DS rings are calculated on the whole area of the detector image (not just in the  $[\min 2\theta, \max 2\theta]$  and  $[\min \eta, \max \eta]$  range) and the integrated area is highlighted in such a way, that the value of the 'contrast' parameter is added to the intensity distribution. It is therefore advisable to choose a value for this parameter of about 1-10% of the maximum intensity (shown in the color palette). Note that in the 2D detector image over the limits of the detector height the rings are not plotted, however it does not mean that the integration is not executed in there. The integration is carried out in the  $[\min 2\theta, \max 2\theta]$  and  $[\min \eta, \max \eta]$  range, and the  $[\min \eta, \max \eta]$  range can be specified by the 'int. band', 'min  $\eta$ ' and 'max  $\eta$ ' parameters as mentioned above. In **Fig.3.38** and **Fig.3.39** the detector image of the ECAP deformed Cu are shown using band and circular sector, respectively.

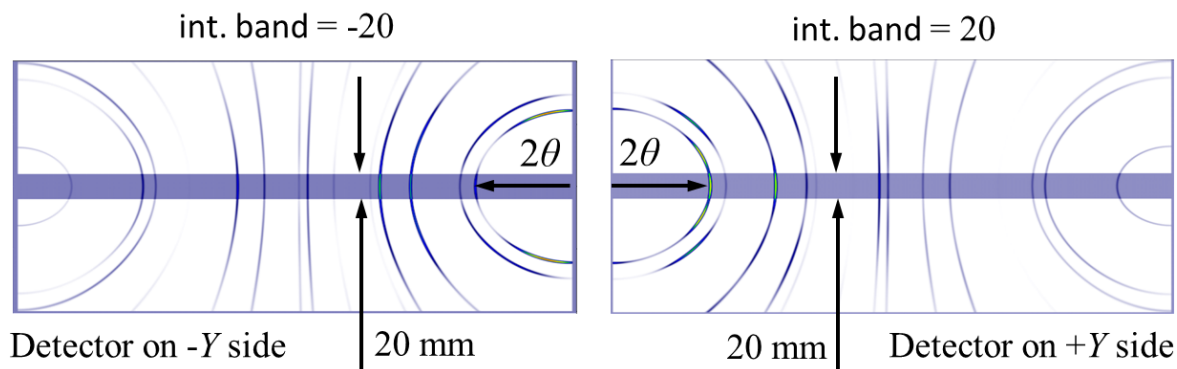


**Fig 3.38.** The 2D detector image when the integrated area is a band positioned on the +Y or -Y side and the height of the band is 20 mm.

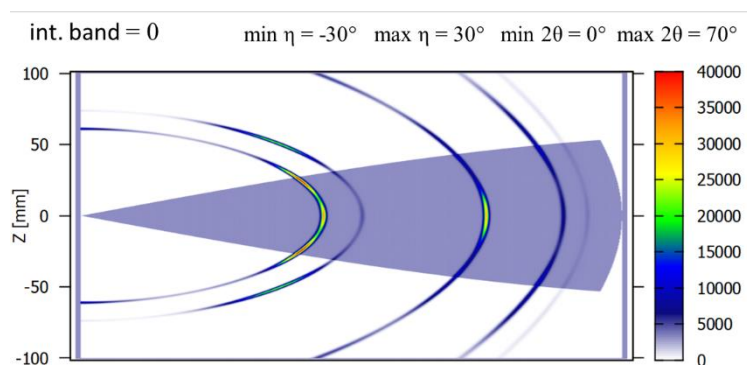


**Fig 3.39.** The 2D detector image when the integrated area is a circular sector, i.e. the 'int. band' parameter is zero and 'min  $\eta$ ' and 'max  $\eta$ ' parameters are used as integration limits for all  $hkl$  rings.

### 3.5.3 Plot 1D pattern

The 1D diffraction pattern,  $I_{(2\theta)}$ , of the 2D intensity distribution integrated on the area specified above can be plotted by pressing the 'Plot 1D Pattern' button on the control panel. If 'show int. area' checkbox is checked, first a schematic figure of the integrated area shows up to check the correctness of the integration. This figure shows a polar coordinate system where  $2\theta$  is the radial coordinate and  $\eta$  is the azimuth (polar angle). In this figure red curves indicates the integrated parts of the DS rings. Press Enter in the console application to close this image, then the 1D pattern shows up (if 'show int. area' is not checked this 1D pattern shows up only). The diffraction patterns corresponding to the **Fig.3.38-39** are shown in **Fig.3.40-41**.

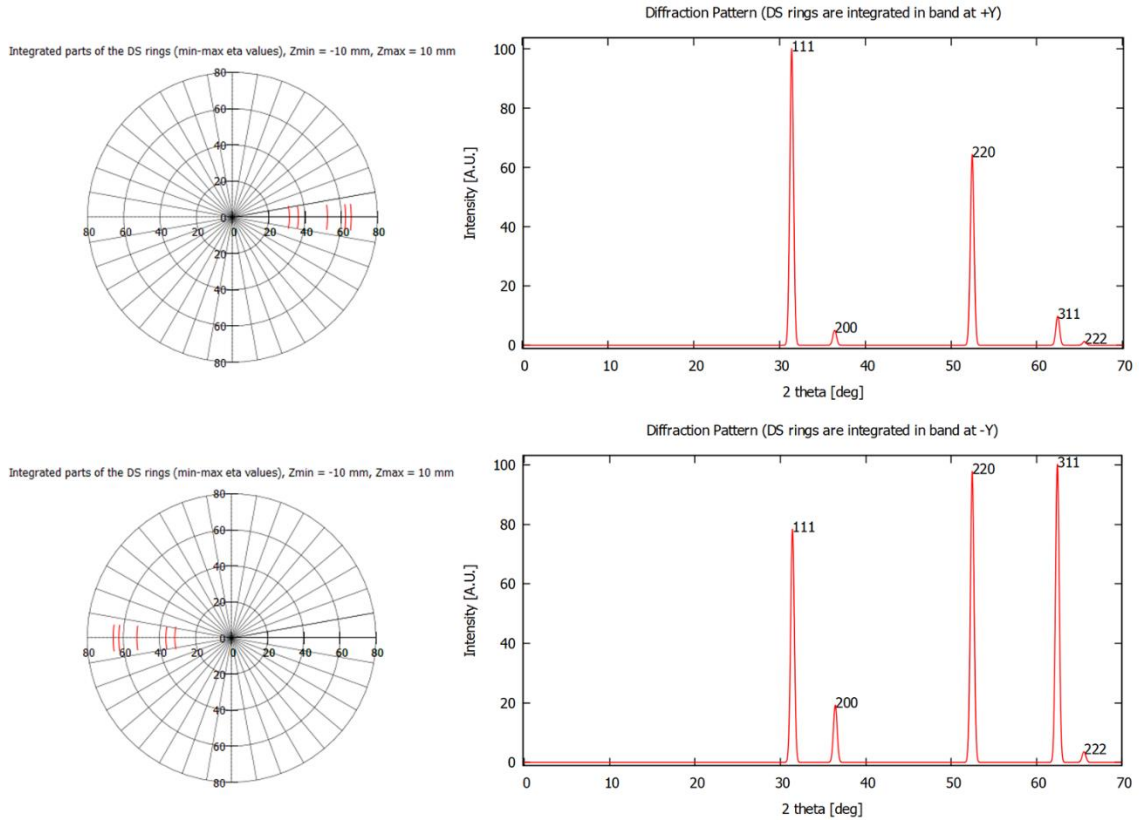


**Fig 3.40.** The 1D diffraction pattern corresponding to the **Fig.3.38**, i.e. the integrated area is a band located on the +Y or -Y side. The schematic figures at left show the integrated parts of the DS rings in polar coordinate system where  $2\theta$  is the radial coordinate and  $\eta$  is the polar angle.

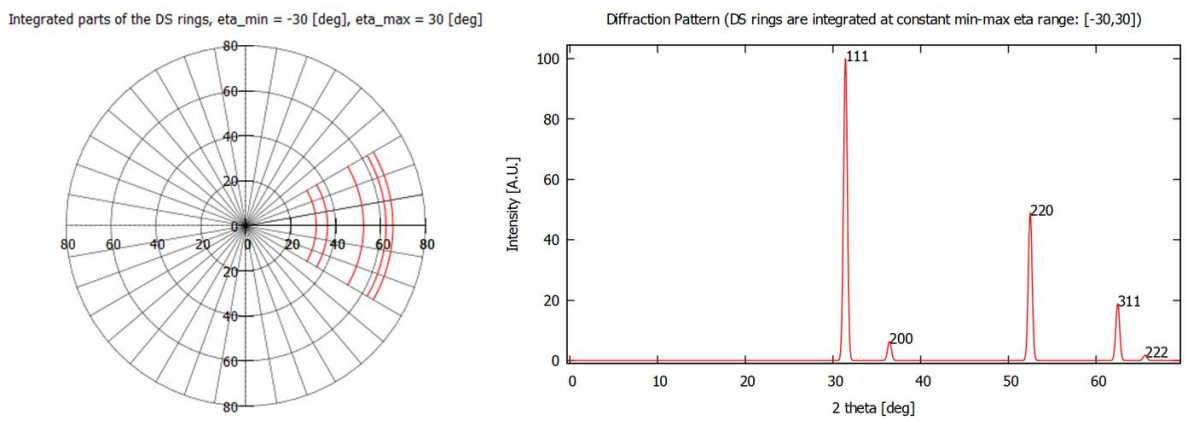


**Fig 3.41.** The 1D diffraction pattern corresponding to the **Fig.3.39**, i.e. the integrated area is a circular sector with  $\min \eta = -30^\circ$  and  $\max \eta = 30^\circ$ .

The intensities in the 1D pattern are relative values, i.e. the peak having the maximum intensity is one hundred.

Note that in the X-TEX method, the calculated intensities of the peaks given by **Eq.1.8**,  $I_{(2\theta_B)}$ , are the functions of the  $2\theta_B$  Bragg angles, not the  $2\theta$  scattering angles, i.e

the natural line broadening is not taken into account in the 1D patterns. This  $I_{(2\theta_B)}$  calculated intensity represents the integrated intensity of a real measured peak (the whole area under the measured peaks). However, for the sake of the better visibility, the peaks in the 1D plots have constant, artificial Gaussian type broadening (this parameter can be set by the  $\Delta 2\theta^\circ$  parameter on the control panel). Therefore, in these 1D patterns, the calculated  $I_{(2\theta_B)}$  values mean the maximum intensities of the peaks (Fig.3.42) and the width of the peaks is not relevant.

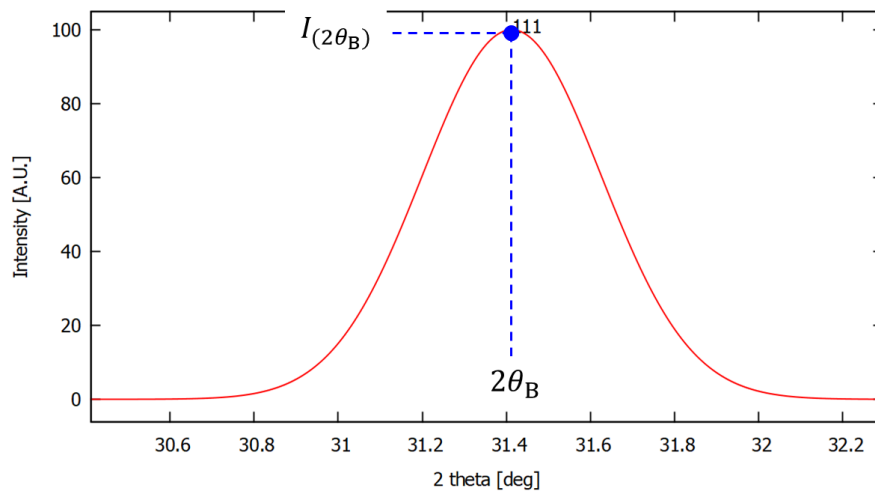


Fig 3.42. The calculated intensities of the peaks given by Eq.1.8,  $I_{(2\theta_B)}$ , are the maximum values of the plotted peaks. The shape of the peaks is given by Gaussian function.

If 'plot 1D at Z=0' checkbox is checked, then 1D 'line' pattern (no integration) of the 2D detector image also appears with intensities exactly at Z=0 (at +Y, -Y or both sides, depends on 'int. band' parameter). These intensities are not relative values, they are the values from the 2D detector image. An example for this line pattern is shown in Fig.3.43.

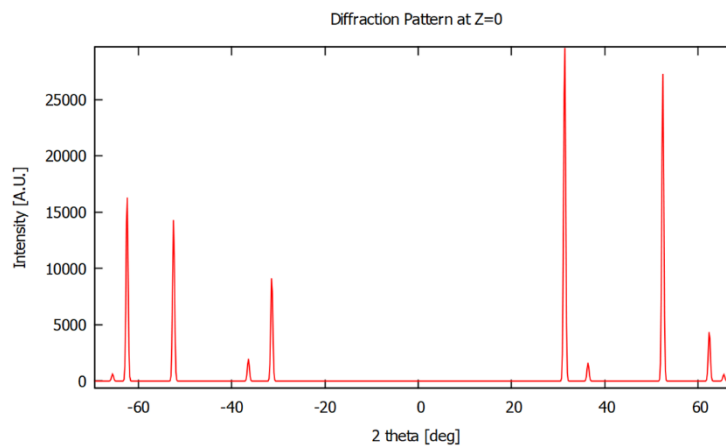


Fig 3.43. The line pattern at Z=0 corresponding to the Fig.3.29.



### 3.5.4 $\chi_{hkl}$ values of the peaks

'Plot 1D Pattern' and 'Plot 2D Detector Image' buttons also generates a 'khi\_values.dat' file in your project directory, which contains the  $\chi_{hkl}$  values (defined by Eq.1.9) of the  $hkl$  peaks for the major, minor (other) and the random texture components. These  $\chi_{hkl}$  values are also printed in the console application. For example, in Fig.3.44 the  $\chi_{hkl}$  values for the  $hkl$  peaks integrated over a 20 mm band on the +Y side in the case of the ECAP deformed Cu are shown. In the X-TEX method the 'major comp.' parameter determines whether a texture component is considered to belong to the major component or to the minor (other) component(s). In Fig.3.44, only the 'C' texture component (i.e. #3) is considered as major texture component. This way the  $\chi_{hkl}$  values of the  $hkl$  diffraction peaks are determined only for 'C' separated from the other components, i.e.  $\chi_{hkl}^{\text{major}} = \chi_{hkl}^{\text{C}}$ ,  $\chi_{hkl}^{\text{other}} = \chi_{hkl}^{\text{A}+\bar{\text{A}}+\text{A}_1^*+\text{A}_2^*+\text{B}+\bar{\text{B}}}$  and  $\chi_{hkl}^{\text{random}}$  for the random texture component is also calculated.

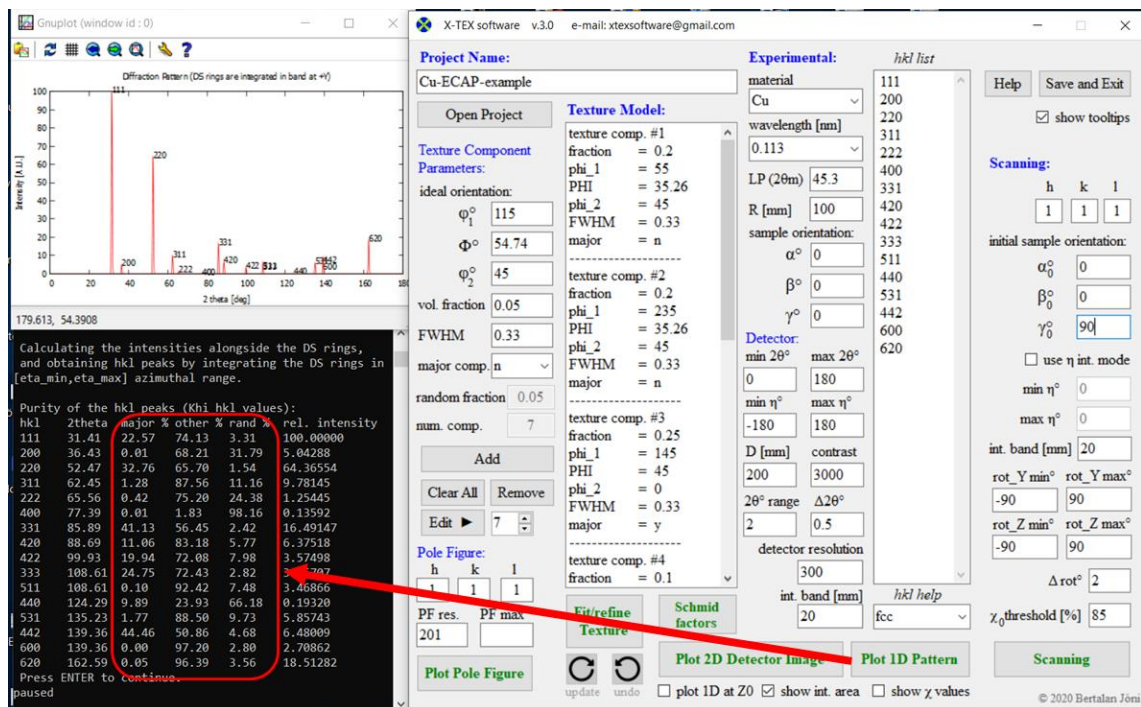


Fig 3.44. After pressing the 'Plot 1D Pattern' or 'Plot 2D Detector Image' buttons, in addition to the 1D pattern or the 2D detector image, the  $\chi_{hkl}$  values of the  $hkl$  peaks for the major, minor (other) and the random texture components are calculated and printed in the console application (see in the red square). In this figure the ECAP deformed, textured Cu sample with 7 texture components is presented, with  $(\alpha, \beta, \gamma) = (0^\circ, 0^\circ, 0^\circ)$  sample orientation and the DS rings are integrated over a band area (with 20 mm height) on the +Y side. In this case only the 'C' texture component (denoted by #3 in the Texture Model listbox) is considered as major texture component.

If 'show  $\chi$  values' checkbox on the control panel is checked, then the  $\chi_{hkl}$  values of the major, minor (other) and the random texture components for each  $hkl$  peak are shown in the 1D pattern with different colors (Fig.3.45).

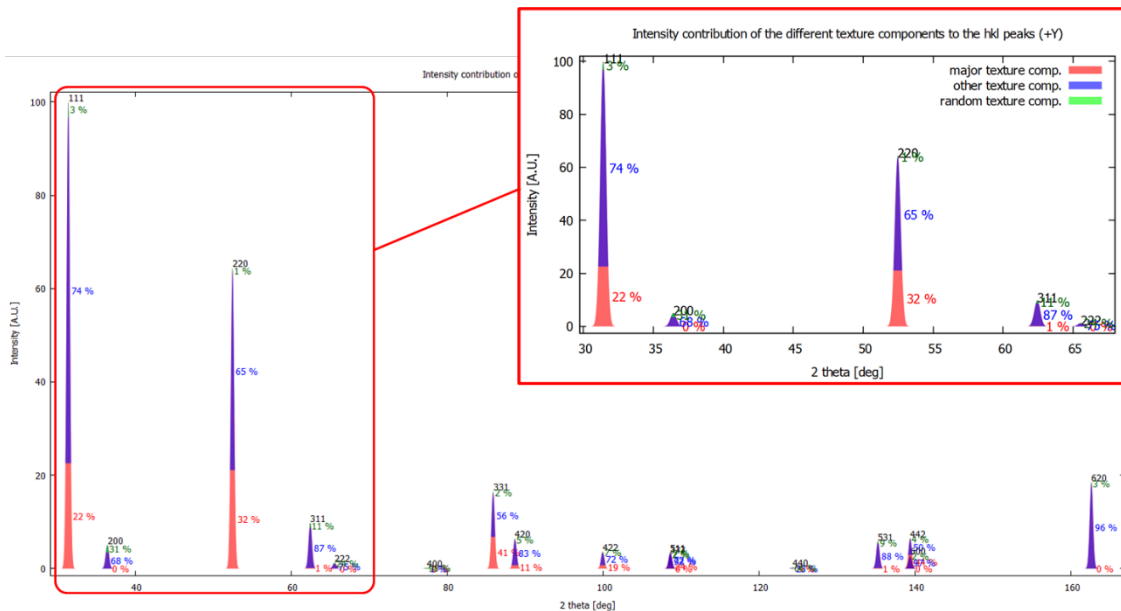


Fig 3.45. 1D pattern with  $\chi_{hkl}$  values for the major, minor (other) and the random texture components.

### 3.6 Scanning function

As it can be seen in Fig.3.44, the  $\chi_{hkl}$  values for the major texture component (the 'C' texture component) vary from 0% to 44%, which are quite low values. However, there is a scanning function in X-TEX, with which the sample orientations can be optimized in order to allow measuring X-ray diffraction peaks corresponding to a chosen texture component with minimal contribution of other components, i.e. the  $\chi_{hkl}$  values can be increased by optimizing the sample orientation. The software calculates a specimen rotation map, where the scattered X-ray intensity of a specific  $hkl$  ring integrated over a  $[\eta_{\min}, \eta_{\max}]$  range is calculated for different sample orientations and plotted as a function of rotation angles. This plot allows the optimal specimen orientation where the intensity of the  $hkl$  diffraction peak is the largest with minimal contribution of other alien texture components to be selected. Note that in addition to the sample orientation, the  $\chi_{hkl}$  values can also be increased by choosing other  $[\eta_{\min}, \eta_{\max}]$  azimuthal integration range. This is usually easy to achieve for synchrotron measurements where a large range of DS rings

can be measured, but this is not usually the case in laboratories and the integration range is limited.

### 3.6.1 Input parameters, initial sample orientation

First the input parameters corresponding to the scanning function need to be specified in the control panel (Fig.3.46). The  $hkl$  Miller index of the peak in question, and the  $\eta$  azimuth interval along which the DS-ring is integrated to obtain the  $hkl$  diffraction peak need to be given. The azimuth interval can be specified using an integration band or direct  $[\eta_{\min}, \eta_{\max}]$  range. If 'use  $\eta$  int. mode' checkbox on the control panel is checked, then 'min  $\eta$ ' and 'max  $\eta$ ' parameters can be used (int. band is inactivated). If it is not checked, then the integration on a band area is used ('min  $\eta$ ' and 'max  $\eta$ ' are inactivated). This 'int. band' can be positive or negative. According to the (+) or (-) sign of this parameter, an integration band located on +Y or -Y side determines the  $[\eta_{\min}, \eta_{\max}]$  integration limits for the  $hkl$  ring.

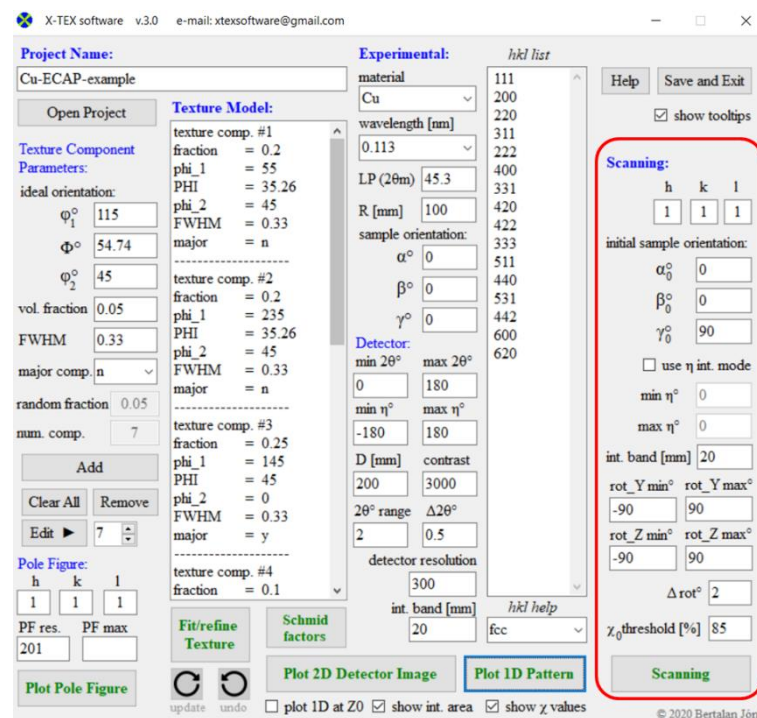
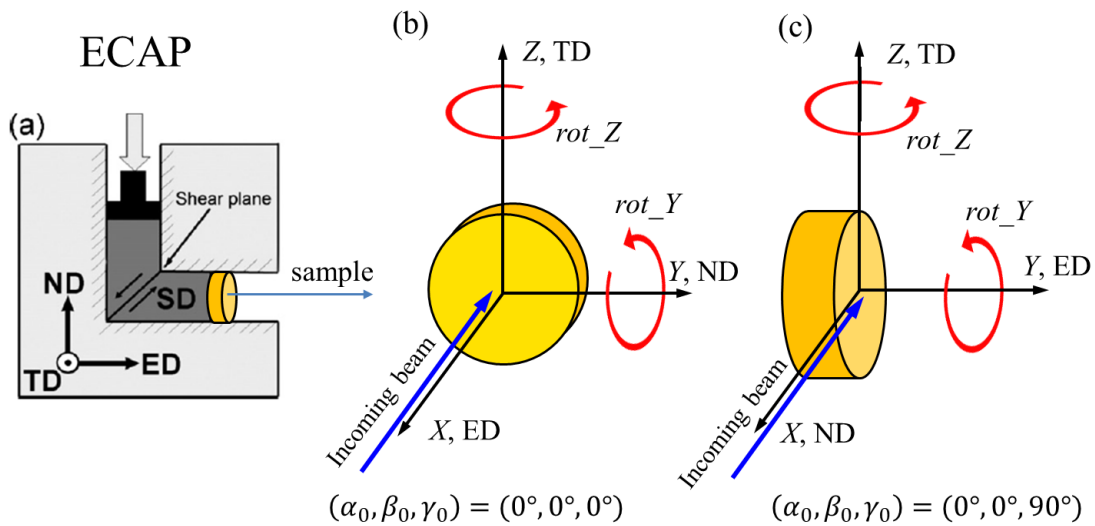


Fig 3.46. The input parameters corresponding to the scanning function on the control panel.

Another important input parameter is the initial sample orientation, the program examines sample rotations around the Y and Z axis relative to this sample orientation. The Eulerian angles of the initial sample orientation is denoted by  $(\alpha_0, \beta_0, \gamma_0)$ . This function is useful mostly for laboratory measurements where the X-ray beam cannot transmit through the sample (reflection mode) and therefore one can talk about measuring one of

the sample surfaces. In this case, several different sample surfaces can be measured after cutting up the sample. The initial sample orientation in the case of measurement with reflection mode should be chosen so that the sample surface to be examined, illuminated by the X-ray beam, is parallel to the X-axis, i.e. the direction of the incoming beam (more details and examples in [1]). In the case of synchrotron measurements, this initial orientation is not very important, use such orientation that allows rotations around the Y and Z axes easy to interpret.

As an example, let's see the ECAP deformed Cu. The Eulerian angles of the ideal orientations in [Table 3.1](#) describe the rotation between the crystallographic and the  $\mathcal{K}_s$  sample coordinate system in such a way that the extrusion direction (ED) of the ECAP deformation is parallel to the x axis of the sample coordinate system and the normal direction (ND) is parallel to the y axis, as it also can be seen in the pole figures of this Cu ([Fig.3.20](#)). Before any sample rotation,  $\mathcal{K}_L = \{X, Y, Z\}$  laboratory coordinate system and  $\mathcal{K}_s = \{x, y, z\}$  the sample coordinate system coincide, i.e.,  $x \parallel X$ ,  $y \parallel Y$  and  $z \parallel Z$  ([Fig.3.27a](#)), and the  $\alpha$ ,  $\beta$  and  $\gamma$  Eulerian angles describe the sample rotation in  $\mathcal{K}_L$ . In [Fig.3.47](#) the illustration of the ECAP, a disc shaped sample cut out from ECAP deformed rod and as examples two different  $(\alpha_0, \beta_0, \gamma_0)$  initial sample orientations are shown.



**Fig 3.47.** (a) Schematic illustration of ECAP and directions designation [6] and (b-c) two different  $(\alpha_0, \beta_0, \gamma_0)$  initial sample orientations. The illustration of rotations around the Z and Y axes are also shown.

If  $(\alpha_0, \beta_0, \gamma_0) = (0^\circ, 0^\circ, 0^\circ)$ , i.e.  $x \parallel X$ ,  $y \parallel Y$  and  $z \parallel Z$  remain, then the rotations around the Z and Y axes are not ideal for measuring the flat surface of the disc in reflection mode ([Fig.3.47b](#)), because the sample itself can block the scattered beam. It is therefore more

worthwhile to apply the other  $(\alpha_0, \beta_0, \gamma_0) = (0^\circ, 0^\circ, 90^\circ)$  initial orientation (Fig.3.47c) for making a rotation map to measure the flat surface in reflection mode.

The limits of the rotations around  $Y$  and  $Z$ ,  $[\text{rot}_Y_{\min}, \text{rot}_Y_{\max}]$  and  $[\text{rot}_Z_{\min}, \text{rot}_Z_{\max}]$ , and the angular steps of the rotations,  $\Delta\text{rot}$ , need to be specified as well.

The software also calculates the  $\chi_{hkl}$  values for each  $\text{rot}_Y$  and  $\text{rot}_Z$  rotation pairs (for the major, minor (other) and the random texture components). On the control panel of the software, a  $\chi_0$  threshold value also need to be specified, which the program will use to display only the intensities corresponding to the  $\chi_{hkl}^{\text{major}} > \chi_0$  values on the rotation map, thus controlling the maximum allowed intensity contribution of unwanted texture components.

### 3.6.2 Rotation map

After pressing the 'Scanning' button, a console application (x\_tex\_scan.exe subroutine) shows up and calculates the rotation map, i.e. the scattered X-ray intensity of the  $hkl$  peak as a function of the  $\text{rot}_Y$  and  $\text{rot}_Z$  rotation angles. The rotations of the normal vectors of the  $hkl$  planes around the  $Y$  and  $Z$  axes are taken into account by applying two additional basic rotation matrices, i.e. rotating the sample by  $\alpha_0, \beta_0$  and  $\gamma_0$  then rotating by  $\text{rot}_Y$  and  $\text{rot}_Z$  angles, the normal vectors of the  $hkl$  planes for an ideal orientation of the  $i^{\text{th}}$  texture component will be

$$\mathbf{e}_{hkl}^i = \hat{R}_Z(\text{rot}_Z) \hat{R}_Y(\text{rot}_Y) \hat{R}_{(\alpha_0, \beta_0, \gamma_0)} \hat{R}_{(\phi_1^i, \phi_2^i)} \mathbf{e}_{hkl}. \quad (3.6)$$

The intensity values of the rotation map are calculated by Eq.1.7-1.8 but with using the Eq.3.6 formula for the normal vectors, instead of Eq.1.6. Note that the Eq.3.6 implies that the rotation around the  $Y$ -axis is done first, and only then the rotation around the  $Z$ -axis, the two rotations are not interchangeable.

On the console application and also on the rotation map the  $(\text{rot}_Y, \text{rot}_Z)$  rotation point belonging to the maximal intensity is printed. These are the recommended rotations around  $Y$  and  $Z$  axes with which the intensity of the  $hkl$  peak is the largest but the  $\chi_0$  threshold value is also taken into account. In practice, this means first orienting the sample according to the  $(\alpha_0, \beta_0, \gamma_0)$  initial orientation and then rotating it around the  $Y$ -axis and then around the  $Z$ -axis according to the recommended values. However, the console application also calculates an equivalent orientation which describes the mentioned rotations with one single three-dimensional rotation matrix:

$$\hat{R}_{(\alpha^{eqv.}, \beta^{eqv.}, \gamma^{eqv.})} = \hat{R}_Z(\text{rot}_Z) \hat{R}_Y(\text{rot}_Y) \hat{R}_{(\alpha_0, \beta_0, \gamma_0)}. \quad (3.7)$$

On the console application this  $(\alpha^{eqv.}, \beta^{eqv.}, \gamma^{eqv.})$  equivalent orientation is also printed. If calculating and plotting the 2D detector image or the 1D diffraction pattern with the sample orientation corresponding to the recommended rotation values of the rotation map is needed, then using this equivalent orientation as sample orientation (on the control panel among the experimental parameters) is recommended.

If 'show int. area' checkbox is checked on the control panel, before the rotation map plotting, a schematic figure of the integrated area shows up to check the correctness of the azimuth integration limits for the scanning procedure. This figure shows a polar coordinate system where  $2\theta$  is the radial coordinate and  $\eta$  is the azimuth (polar angle), similarly to the integration for 1D pattern detailed above.

As an example, let's see the ECAP deformed Cu. Let's say we want to measure the 111 and 220 peaks integrated over a band with the height of 20 mm positioned on the +Y side (i.e. 'int. band' = 20), and we want to measure these  $hkl$  peaks stemming from the 'C' texture component. As it can be seen in Fig.3.44-45, if the sample orientation is  $(\alpha, \beta, \gamma) = (0^\circ, 0^\circ, 0^\circ)$ , the  $\chi_{hkl}$  values are only  $\chi_{111}^{\text{major}} = \chi_{111}^C = 22.57\%$  and  $\chi_{220}^{\text{major}} = \chi_{220}^C = 32.76\%$ , which are low values. Let's say we want to measure these peaks with intensity contribution of the 'C' texture component over 85%, i.e. we apply  $\chi_0 = 85$  threshold value. Let's apply  $(\alpha_0, \beta_0, \gamma_0) = (0^\circ, 0^\circ, 90^\circ)$  initial sample orientation, which is more suitable for measuring the flat surface of the disc, as it was mentioned above. In Fig.3.48 and Fig.3.49 the rotation maps for the 111 and 220 peaks are shown, respectively. The results are the followings. The recommended rotations for the 111 peak are  $(\text{rot}_Y, \text{rot}_Z) = (0^\circ, 75^\circ)$ , which is equivalent with the  $(\alpha^{eqv.}, \beta^{eqv.}, \gamma^{eqv.}) = (180^\circ, 0^\circ, -15^\circ)$  orientation. In this orientation, the 'C' major texture component has  $\chi_{111}^{\text{major}} = \chi_{111}^C = 85.7\%$  value. The recommended rotations for the 220 peak are  $(\text{rot}_Y, \text{rot}_Z) = (-82^\circ, -60^\circ)$ , which is equivalent with the  $(\alpha^{eqv.}, \beta^{eqv.}, \gamma^{eqv.}) = (30^\circ, -82^\circ, 0^\circ)$  orientation. In this orientation, the 'C' major texture component has  $\chi_{220}^{\text{major}} = \chi_{220}^C = 85.1\%$  value. These results seem to be impressive, however with other azimuth interval and initial sample orientation they can be enhanced and even almost 100% is possible for the  $\chi_{hkl}$  values.

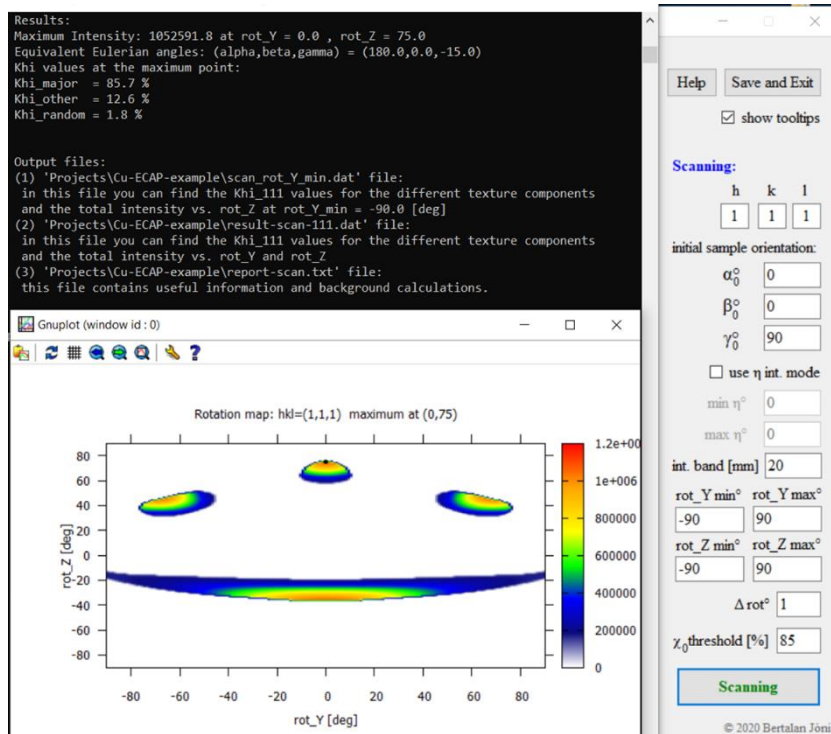


**Fig 3.48.** Rotation map for the 111 diffraction peak. The applied scanning parameters can be seen on the control parameter. The recommended (rot\_Y, rot\_Z) rotations and the equivalent sample orientation can be seen in the console application.

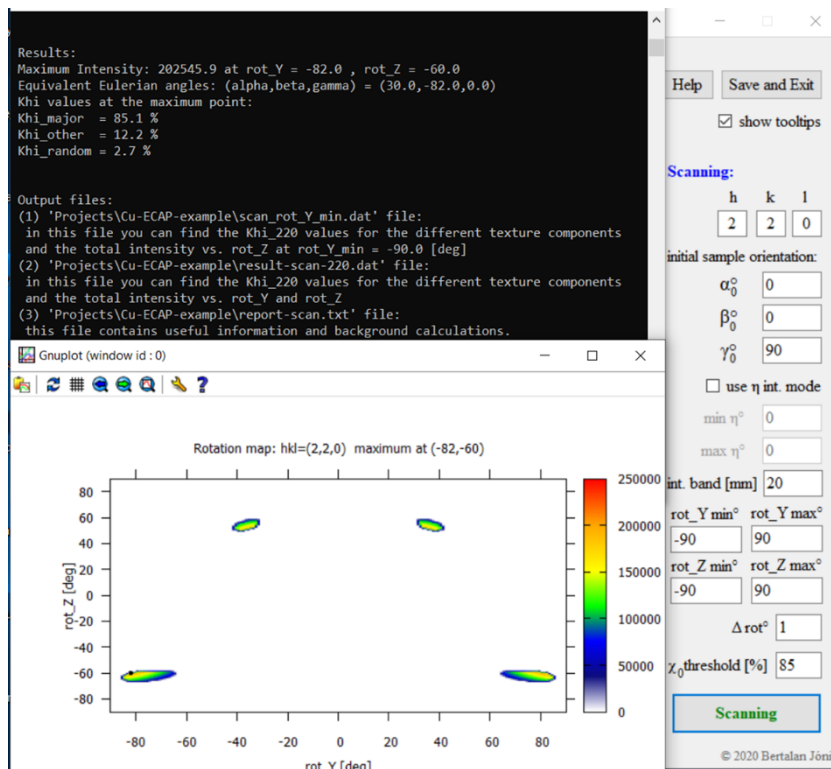


**Fig 3.49.** Rotation map for the 220 diffraction peak. The applied scanning parameters can be seen on the control parameter. The recommended (rot\_Y, rot\_Z) rotations and the equivalent sample orientation can be seen in the console application.

In **Fig.3.50** the 1D diffraction patterns and the 2D detector images according to the scanning results are shown. It can be seen well that the scan-based sample orientations provide diffraction peaks belonging to the 'C' texture component for 111 and 220.

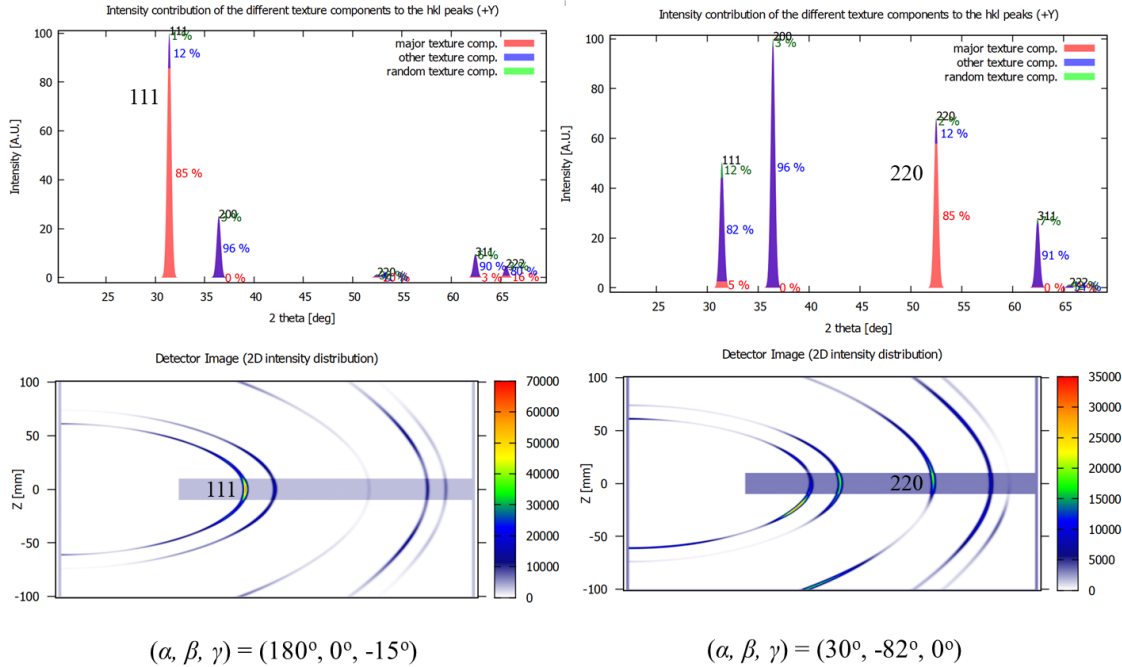


**Fig 3.50.** The 1D diffraction patterns (with  $\chi_{hkl}$  values) and the 2D detector images (with the integrated area) according to the scanning results for the 111 and 220 diffraction peaks and rings.

Let's notice something important thing. Actually, we applied the initial sample orientation for the scanning according to the **Fig.3.47c**. With this sample orientation, the first rotation, i.e. the rotation around  $Y$  axis cannot change the angle between the flat surface of the disc and the incoming beam. Then we rotate the disc around  $Z$  axis with  $rot\_Z$ . All in all, this means that the absolute value of the  $rot\_Z$  gives the angle between the flat surface of the sample and the incoming beam in the case of such initial sample orientations, where the flat surface of the sample is parallel to the incoming beam. However, let's notice that the  $2\theta_B$  Bragg angles of the 111 and 200 is smaller than  $|rot\_Z|$ ,  $2\theta_B^{111} = 31.4^\circ, rot\_Z^{111} = 75^\circ$ , and  $2\theta_B^{220} = 52.5^\circ, rot\_Z^{220} = -60^\circ$ , which means that the scattered beam must transmit through the sample itself to reach the detector. It means that the scanning results works only in the case of transmission mode, where the wavelength of the beam and therefore the energy of the beam is suitable for transmission measurement (a synchrotron measurement is probably this case). For reflection mode (usually it means typical laboratory measurement with X-ray tube), it is recommended to cut out several pieces from the specimen (in our case from the ECAP deformed Cu rod)



differently (under different angles) and carry out the scanning procedure for all of them (an example for differently cut pieces can be found in [1]). As a result, a series of measurements can be planned in order to measure as many peaks as possible belonging to different texture components separately.

### 3.7 Calculating Schmid factors

In X-TEX software it is possible to determine the Schmid factors corresponding to the preferred orientations of the texture components. For this purpose, the loading direction and the slip systems to be investigated (the *hkl* Miller indices of the slip planes and Burgers vectors) need to be specified in an input file. The name of the input file must be 'Slip-systems.dat' and it must be located in the project directory.

```

1 Schmid factor calculation input parameters
2
3 loading direction (in Cartesian coordinates, unit vector not necessary):
4 load_x=0
5 load_y=1
6 load_z=0
7
8 slip systems:
9 <110>{001} BE_a
10 <110>{100} PrE_a
11 <001>{100} PrE2_c
12 <113>{100} PrE3_c+a
13 <110>{101} PyE_a
14 <113>{112} PyE2_c+a
15 <113>{111} PyE3_c+a
16 <113>{101} PyE4_c+a
17
18 ##### NOTES and HELP:
19 You must specify a slip system this way:
20 <Burgers_hkl>{slip_plane_hkl} identifier
21
22 The slip plane and the slip direction (Burgers vector) together define the slip system.
23 brackets for Burgers vector: <>
24 brackets for slip plane: {}
25 h,k,l can be separated by comma: h,k,l
26 identifier is an arbitrary text
27
28 examples:
29
30 for fcc crystal system:
31 <110>{111} fcc
32
33 for bcc crystal system:
34 <1,1,1>{1,1,0}
35
36 for hcp crystal system:
37 <1,1,0>{001} BE_a
38 <110>{100} PrE_a
39 <001>{100} PrE2_c
40 <113>{100} PrE3_c+a
41 <110>{101} PyE_a
42 <113>{112} PyE2_c+a
43 <113>{111} PyE3_c+a
44 <113>{101} PyE4_c+a
45

```

Fig 3.51. The 'Slip-systems.dat' file with the input parameters (in the red square).

In [Fig.3.51](#) an example for this input file with the loading direction and the slip systems is shown. After the '### NOTES AND HELP' text some helpful notes can be read. The loading direction is a vector and its coordinates ( $load\_x$ ,  $load\_y$ ,  $load\_z$ ) are expressed in the  $\mathcal{K}_s$  sample coordinate system.

After clicking on 'Schmid factors' button on the control panel, a console application will show up and calculate the Schmid factors of the ideal orientations for the slip-systems and loading direction given in the input file. The results are also printed into the 'Schmid-results.dat' output file.

### 3.8 Fit/refine texture parameters

The parameters used to describe textures in this method ( $\varphi_1$ ,  $\Phi$ ,  $\varphi_2$ ,  $f$ , FWHM) can be determined by common texture measurements, but X-TEX also has an option of using a Monte-Carlo algorithm to fit/refine these parameters based on X-ray diffraction measurements according to how the intensity varies along the DS rings.

The input parameters of the texture refinement need to be specified in a file named 'x\_tex\_fit.dat' located in the project directory. An example for this file is shown in [Fig.3.52](#). The input parameters in this file can be split into two types: (1) Experimental parameters, (2) Monte-Carlo Fit/Refine Control parameters. Let's take them in turn.

For 'Experimental parameters' ([Fig.3.53](#)), first, you need to specify the number of files that contain the measured X-ray intensities (integrated intensities, i.e. integration alongside  $2\theta$ ) of  $hkl$  peaks. In these files the first column must be the  $hkl$  value, the second column must be the integrated intensity of the  $hkl$  peak. These files must be located somewhere in the 'Projects' directory.

Then you need to specify the azimuthal integration mode (i.e. integration alongside  $\eta$ ) of the DS rings, with which you got the  $hkl$  peaks:

-if it is 'eta', then  $\eta_{min}$  and  $\eta_{max}$  integration limits need to be given,

-if it is 'band\_positive\_Y' or 'band\_negative\_Y' then an integration band located on the +Y or -Y side determines the  $\eta_{min}$  and  $\eta_{max}$  integration limits for all  $hkl$  rings. The height (i.e. the vertical width) of the band is defined by  $Z_{min}$  and  $Z_{max}$  edge values of the band.

Then you need to specify for all files (containing the measured X-ray intensities) in one line: the name of the file (with full path and extension; directories and subdirectories are separated by the '\' backslash symbol), the allowed  $2\theta_{min}$  and  $2\theta_{max}$  values, the  $Z_{min}$  (or  $\eta_{min}$ ) and the  $Z_{max}$  (or  $\eta_{max}$ ) values corresponding to the azimuthal

integration of the measured peaks, and the  $\alpha$ ,  $\beta$ , and  $\gamma$  Eulerian angles of sample orientations, respectively. They need to be separated by Tab or Space from each other and each line contains parameters for one file only. Note that the other necessary experimental parameters (R, LP, wavelength) come from the control panel.

```

1 #Monte-Carlo fitting/refinement of the texture parameters
2
3 # (1) Experimental parameters:
4
5 Number of files = 15
6 integration mode (eta/band_positive_Y/band_negative_Y) = band_positive_Y
7 Projects\Fit\Measured-intensities-for-texture-fit\Ti-23-measured-intensities-RDZ-N002.dat 0 180 36 60 -15 -90 0
8 Projects\Fit\Measured-intensities-for-texture-fit\Ti-23-measured-intensities-RDZ-N003.dat 0 180 12 36 -15 -90 0
9 Projects\Fit\Measured-intensities-for-texture-fit\Ti-23-measured-intensities-RDZ-N004.dat 0 180 -12 12 -15 -90 0
10 Projects\Fit\Measured-intensities-for-texture-fit\Ti-23-measured-intensities-RDZ-N005.dat 0 180 -36 -12 -15 -90 0
11 Projects\Fit\Measured-intensities-for-texture-fit\Ti-23-measured-intensities-RDZ-N006.dat 0 180 -60 -36 -15 -90 0
12 Projects\Fit\Measured-intensities-for-texture-fit\Ti-23-measured-intensities-TDZ-N002.dat 0 180 36 60 -15 -90 -90
13 Projects\Fit\Measured-intensities-for-texture-fit\Ti-23-measured-intensities-TDZ-N003.dat 0 180 12 36 -15 -90 -90
14 Projects\Fit\Measured-intensities-for-texture-fit\Ti-23-measured-intensities-TDZ-N004.dat 0 180 -12 12 -15 -90 -90
15 Projects\Fit\Measured-intensities-for-texture-fit\Ti-23-measured-intensities-TDZ-N005.dat 0 180 -36 -12 -15 -90 -90
16 Projects\Fit\Measured-intensities-for-texture-fit\Ti-23-measured-intensities-TDZ-N006.dat 0 180 -60 -36 -15 -90 -90
17 Projects\Fit\Measured-intensities-for-texture-fit\Ti-23-measured-intensities-45Z-N002.dat 0 180 36 60 -15 -90 -45
18 Projects\Fit\Measured-intensities-for-texture-fit\Ti-23-measured-intensities-45Z-N003.dat 0 180 12 36 -15 -90 -45
19 Projects\Fit\Measured-intensities-for-texture-fit\Ti-23-measured-intensities-45Z-N004.dat 0 180 -12 12 -15 -90 -45
20 Projects\Fit\Measured-intensities-for-texture-fit\Ti-23-measured-intensities-45Z-N005.dat 0 180 -36 -12 -15 -90 -45
21 Projects\Fit\Measured-intensities-for-texture-fit\Ti-23-measured-intensities-45Z-N006.dat 0 180 -60 -36 -15 -90 -45
22
23
24 # (2) Monte-Carlo Fit/Refine Control parameters:
25
26 Number of MC steps = 10000
27
28 minimal and maximal values of texture parameters:
29 fraction 0.0 1.0
30 Phi_1 -180 180
31 PHI 0.0 90.0
32 Phi_2 0.0 60.0
33 FWHM 0.3 0.7
34
35 Number of Texture Components = 8
36
37 constraints for texture parameters:
38 text.comp. #1 #2 #3 #4 #5 #6 #7 #8
39 fraction 1 1 1 1 5 5 5 5
40 Phi_1 1 1 1 1 5 5 5 5
41 PHI 1 2 3 4 -1 -2 -3 -4
42 Phi_2 1 1 1 1 5 5 5 5
43 FWHM 1 1 1 1 5 5 5 5

```

Fig 3.52. The 'x\_tex\_fit.dat' file with the input parameters for texture parameter fitting.

```

1 #Monte-Carlo fitting/refinement of the texture parameters
2
3 # (1) Experimental parameters:
4
5 Number of files = 15
6 integration mode (eta/band_positive_Y/band_negative_Y) = band_positive_Y
7 Projects\Fit\Measured-intensities-for-texture-fit\Ti-23-measured-intensities-RDZ-N002.dat 0 180 36 60 -15 -90 0
8 Projects\Fit\Measured-intensities-for-texture-fit\Ti-23-measured-intensities-RDZ-N003.dat 0 180 12 36 -15 -90 0
9 Projects\Fit\Measured-intensities-for-texture-fit\Ti-23-measured-intensities-RDZ-N004.dat 0 180 -12 12 -15 -90 0
10 Projects\Fit\Measured-intensities-for-texture-fit\Ti-23-measured-intensities-RDZ-N005.dat 0 180 -36 -12 -15 -90 0
11 Projects\Fit\Measured-intensities-for-texture-fit\Ti-23-measured-intensities-RDZ-N006.dat 0 180 -60 -36 -15 -90 0
12 Projects\Fit\Measured-intensities-for-texture-fit\Ti-23-measured-intensities-TDZ-N002.dat 0 180 36 60 -15 -90 -90
13 Projects\Fit\Measured-intensities-for-texture-fit\Ti-23-measured-intensities-TDZ-N003.dat 0 180 12 36 -15 -90 -90
14 Projects\Fit\Measured-intensities-for-texture-fit\Ti-23-measured-intensities-TDZ-N004.dat 0 180 -12 12 -15 -90 -90
15 Projects\Fit\Measured-intensities-for-texture-fit\Ti-23-measured-intensities-TDZ-N005.dat 0 180 -36 -12 -15 -90 -90
16 Projects\Fit\Measured-intensities-for-texture-fit\Ti-23-measured-intensities-TDZ-N006.dat 0 180 -60 -36 -15 -90 -90
17 Projects\Fit\Measured-intensities-for-texture-fit\Ti-23-measured-intensities-45Z-N002.dat 0 180 36 60 -15 -90 -45
18 Projects\Fit\Measured-intensities-for-texture-fit\Ti-23-measured-intensities-45Z-N003.dat 0 180 12 36 -15 -90 -45
19 Projects\Fit\Measured-intensities-for-texture-fit\Ti-23-measured-intensities-45Z-N004.dat 0 180 -12 12 -15 -90 -45
20 Projects\Fit\Measured-intensities-for-texture-fit\Ti-23-measured-intensities-45Z-N005.dat 0 180 -36 -12 -15 -90 -45
21 Projects\Fit\Measured-intensities-for-texture-fit\Ti-23-measured-intensities-45Z-N006.dat 0 180 -60 -36 -15 -90 -45
22

```

Fig 3.53. The 'Experimental parameters' in the 'x\_tex\_fit.dat' file.

An illustration of the measured intensities is shown in Fig.3.54. The measured intensity distribution in Fig.3.54 belongs to a measurement of a textured, 23% tensile deformed Ti sample from [1]. The 2D detector image of the measured intensity distribution is divided into several horizontal stripes which indicate the 'bands' of the integrations. Note that if the integration mode is 'eta', then they are circular sectors instead of stripes. The measured intensity distribution needs to be integrated over the azimuthal range corresponding to the chosen stripes or circular sectors to get  $hkl$  peaks from the  $hkl$  rings. If the integral mode is 'eta', then  $\eta_{\min}$  and  $\eta_{\max}$  are used as azimuthal integration limits, if it is a 'band', then the software calculates the  $\eta_{\min}$  and  $\eta_{\max}$  values corresponding to a particular ring and  $hkl$  from  $Z_{\min}$  and  $Z_{\max}$  values. Let's denote the integral intensity (the whole area under the peak) of the  $hkl$  peaks for the  $N^{\text{th}}$  stripe (or sector) by  $I_{N,hkl}^{\text{meas}}$ . Files with different names need to contain the  $I_{N,hkl}^{\text{meas}}$  values for each stripe (sector). In Fig.3.54 the file corresponding to the  $N=4$  stripe is shown as an example.

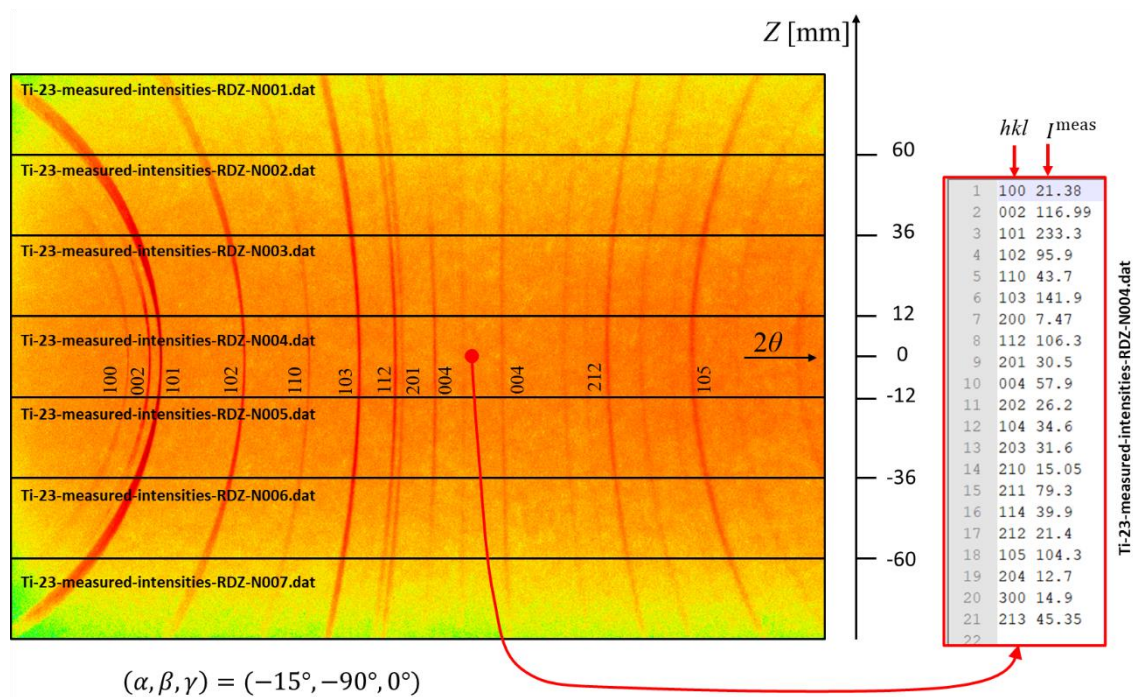


Fig 3.54. Measured 2D intensity distribution for a 23% tensile deformed Ti specimen with  $(\alpha, \beta, \gamma) = (-15^\circ, -90^\circ, 0^\circ)$  sample orientation (in this case RD direction of the sample is parallel to the Z) [1], and the file which contains the  $hkl$  indices and measured intensities for the  $N=4$  stripe. The  $Z_{\min}$  and  $Z_{\max}$  values for the stripes are also shown.

Note that in this texture refinement procedure many measurements with different sample orientations can be used at the same time, which can enhance the accuracy of the method. For example, in Fig.3.53 three measurements with different Eulerian angles of the sample are shown. Note that though the 'Experimental parameters' is the 'x\_tex\_fit.dat'

file can be different for the different measurements, the other experimental parameters from the control panel, such as the radius of the detector (R), the LP parameter, or the wavelength of the beam must be the same for all measurements.

The X-TEX software varies the  $(\varphi_1, \Phi, \varphi_2, f, \text{FWHM})$  texture parameters with a Monte-Carlo algorithm and calculates the intensity of diffraction peaks in each stripe (circular sector) with different texture parameters. The obtained results,  $I_{N,hkl}^{\text{calc}}$  are compared with the measured intensities for all the stripes (sectors). The texture parameters are optimized by minimizing the sum of squared residuals (SSR):

$$\text{SSR} = \sum_{N,hkl} (I_{N,hkl}^{\text{meas}} - I_{N,hkl}^{\text{calc}})^2. \quad (3.8)$$

For 'Monte-Carlo Fit/Refine Control parameters' (Fig.3.55), first, you need to specify the number of Monte-Carlo (MC) steps, then minimal and maximal limits of the texture parameters, then the number of texture components, then constraints for the texture component parameters (fraction, Eulerian angles and FWHM for all components, respectively).

```

24 # (2) Monte-Carlo Fit/Refine Control parameters:
25
26 Number of MC steps = 10000
27
28 minimal and maximal values of texture parameters:
29 fraction      0.0    1.0
30 Phi_1        -180   180
31 PHI          0.0    90.0
32 Phi_2         0.0    60.0
33 FWHM         0.3    0.7
34
35 Number of Texture Components = 8
36
37 constraints for texture parameters:
38 text.comp.  #1 #2 #3 #4 #5 #6 #7 #8
39 fraction    1  1  1  1  5  5  5  5
40 Phi_1       1  1  1  1  5  5  5  5
41 PHI         1  2  3  4 -1 -2 -3 -4
42 Phi_2       1  1  1  1  5  5  5  5
43 FWHM        1  1  1  1  5  5  5  5
44

```

Fig 3.55. The 'Monte-Carlo Fit/Refine Control parameters' in the 'x\_tex\_fit.dat' file.

If one constraint parameter is '0', then this parameter is fixed (will not be refined) during the MC procedure. If one constraint parameter is 'n' (where 'n' is an integer), then this parameter will be either refined, if it is identical with its texture component serial number (the number after the # symbol), or linked with all the other former texture component parameters which also have 'n' value. All of them will change identically during the MC

procedure. If one constraint parameter is '-n', then this will change identically with all n values, but with negative sign (where negative value is allowed). The 'n' cannot be larger than the texture component serial number, i.e. the first 'constraint parameters' (belonging to #1 texture comp.) can only be 0 or 1, the second 'constraint parameters' (belonging to #2 texture comp.) can only be 0, 1 or 2 (and -1), the third 'constraint parameters' (belonging to #3 texture comp.) can only be 0, 1, 2 or 3 (and -1 or -2), and so on.

For example:

```
PHI  1    2    -1    -2    3    6    0
```

This line that consists of 'constraint parameters' for PHI texture parameter means (we have 7 texture components here): PHI(#1) is refining freely, PHI(#2) is refining freely, PHI(#3)=-PHI(#1), PHI(#4)=-PHI(#2), PHI(#5)=PHI(#3)=-PHI(#1), PHI(#6) is refining freely, PHI(#7) is fixed.

The min and max texture parameter values matter only if one parameter is refining freely, i.e. its 'constraint parameters' equals its texture component serial number. When negative constraint parameter (-n) is used, i.e. the parameter is linked with the n-th value with negative sign, then only the absolute value of the parameter has to fulfil the min-max conditions.

For example: if min\_PHI=20 and max\_PHI=40 and the third constraint parameter is -1, then the PHI(#1) value can only be between 20 and 40, however PHI(#3) can be between -20 and -40.

After clicking on 'Fit/refine Texture' button on the control panel, a new windows form shows up (Fig.3.56). After clicking on 'Start fit' button on the form, a console application shows up to starts the Monte-Carlo (MC) fitting procedure if each experimental and control parameter is valid. The MC process takes some time, depending on the MC steps and the number of freely refinable parameters. The process can be aborted by the 'Stop fit' button. After reaching the maximum MC steps ('Number of MC steps' in the 'x\_tex\_fit.dat' file) or clicking on the 'Stop fit' button, the refined parameters are printed on the screen and saved into an output file named 'report-fit.txt'. Apply 'update' button on the control panel to replace the old texture parameter values in the 'Texture Model' listbox with the refined values. Apply 'undo' button to undo the replacement.

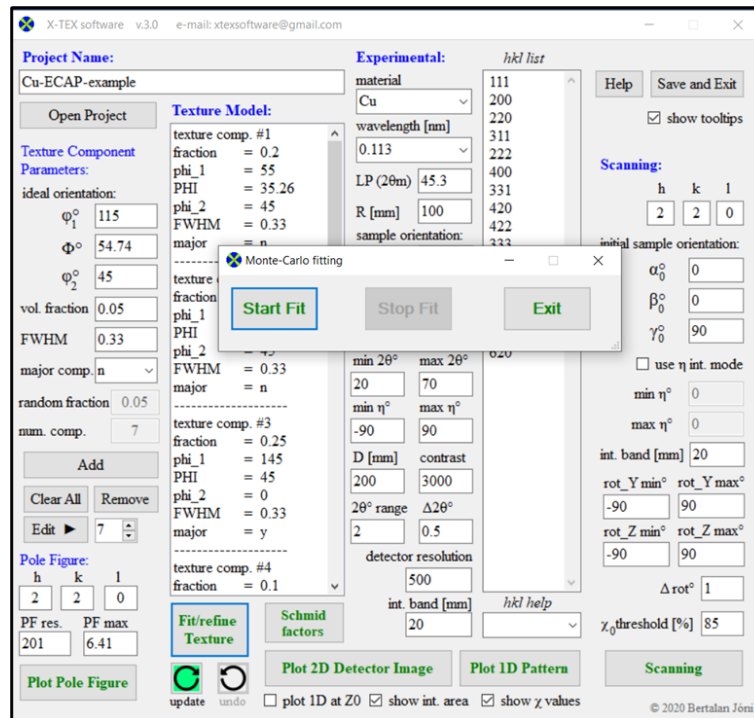


Fig 3.56. The windows form for starting and stopping the texture refinement.

## 4. In the future

### 4.1 Neutron diffraction

Under construction

### 4.2 Texture parameter refinement by measured pole figures

Under construction

# Appendix

## A. Useful links

Atomic positions:

<https://materialsproject.org>

for example, NaCl:

<https://materialsproject.org/materials/mp-22862/>

(Tip: it may be easier to find in google, this way: "materialsproject.org NaCl")

For atomic positions download the \*.cif file with conventional standard

Lattice constants and crystal structures:

<https://www.periodictable.com/Properties/A/LatticeConstants.html>

[https://en.wikipedia.org/wiki/Lattice\\_constant](https://en.wikipedia.org/wiki/Lattice_constant)

## B. Atomic scattering factors

Atomic scattering factors for some elements [3].

Appendix IV  
Atomic Scattering Factors\*

(sin $\theta$ )/ $\lambda(A^{-1})$	0.0	0.1	0.2	0.3	0.4	0.5	0.6	0.7	0.8	0.9	1.0	1.1	1.2	1.3	1.4	1.5
H 1	1.0	0.81	0.48	0.25	0.13	0.07	0.04	0.02	0.02	0.01	0.01					
He 2	2.0	1.83	1.45	1.06	0.74	0.52	0.36	0.25	0.18	0.13	0.10	0.07	0.05	0.04	0.03	0.03
Li 3	3.0	2.22	1.74	1.51	1.27	1.03	0.82	0.65	0.51	0.40	0.32	0.26	0.21	0.16		
Be 4	4.0	3.07	2.07	1.71	1.53	1.37	1.20	1.03	0.88	0.74	0.62	0.52	0.43	0.37		
B 5	5.0	4.07	2.71	1.99	1.69	1.53	1.41	1.28	1.15	1.02	0.90	0.78	0.68	0.60		
C 6	6.0	5.13	3.58	2.50	1.95	1.69	1.54	1.43	1.32	1.22	1.11	1.01	0.91	0.82	0.74	0.66
N 7	7.0	6.20	4.60	3.24	2.40	1.94	1.70	1.55	1.44	1.35	1.26	1.18	1.08	1.01		
O 8	8.0	7.25	5.63	4.09	3.01	2.34	1.94	1.71	1.57	1.46	1.37	1.30	1.22	1.14		
F 9	9.0	8.29	6.69	5.04	3.76	2.88	2.31	1.96	1.74	1.59	1.48	1.40	1.32	1.25		
Ne 10	10.0	9.36	7.82	6.09	4.62	3.54	2.79	2.30	1.98	1.76	1.61	1.50	1.42	1.35	1.28	1.22
Na 11	11.0	9.76	8.34	6.89	5.47	4.29	3.40	2.76	2.31	2.00	1.78	1.63	1.52	1.44	1.37	1.31
Na <sup>+</sup> 11	10.0	9.55	8.39	6.93	5.51	4.33	3.42	2.77	2.31	2.00	1.79	1.63	1.52	1.44	1.37	1.30
Mg 12	12.0	10.50	8.75	7.46	6.20	5.01	4.06	3.30	2.72	2.30	2.01	1.81	1.65	1.54		
Al 13	13.0	11.23	9.16	7.88	6.77	5.69	4.71	3.88	3.21	2.71	2.32	2.05	1.83	1.69	1.57	1.48
Si 14	14.0	12.16	9.67	8.22	7.20	6.24	5.31	4.47	3.75	3.16	2.69	2.35	2.07	1.87	1.71	1.60
P 15	15.0	13.17	10.34	8.59	7.54	6.67	5.83	5.02	4.28	3.64	3.11	2.69	2.35	2.10	1.89	1.75
S 16	16.0	14.33	11.21	8.99	7.83	7.05	6.31	5.56	4.82	4.15	3.56	3.07	2.66	2.34		
Cl 17	17.0	15.33	12.00	9.44	8.07	7.29	6.64	5.96	5.27	4.60	4.00	3.47	3.02	2.65		
Cl <sup>-</sup> 17	18.0	16.02	12.20	9.40	8.03	7.28	6.64	5.97	5.27	4.61	4.00	3.47	3.03	2.65	2.35	2.11
A 18	18.0	16.30	12.93	10.20	8.54	7.56	6.86	6.23	5.61	5.01	4.43	3.90	3.43	3.03		
K 19	19.0	16.73	13.73	10.97	9.05	7.87	7.11	6.51	5.95	5.39	4.84	4.32	3.83	3.40	3.01	2.71
Ca 20	20.0	17.33	14.32	11.71	9.64	8.26	7.38	6.75	6.21	5.70	5.19	4.69	4.21	3.77	3.37	3.03

(cont.)

\* Reprinted from *International Tables for X-Ray Crystallography*, Vol. III, with the permission of the Editorial Commission of the International Tables. The values for elements 1–36 are computed from self-consistent or variational wave functions, while those for elements 37–92 are obtained from the Thomas-Fermi-Dirac statistical model. For values corresponding to ionized states, reference should be made to the International Tables.



Appendix IV (cont.)

$(\sin \theta)/\lambda(A^{-1})$		0.0	0.1	0.2	0.3	0.4	0.5	0.6	0.7	0.8	0.9	1.0	1.1	1.2	1.3	1.4	1.5
370	Sc 21	21.0	18.72	15.39	12.39	10.12	8.60	7.64	6.98	6.45	5.96	5.48	5.00	4.53	4.09	3.68	3.31
	Ti 22	22.0	19.41	16.07	13.20	10.83	9.12	7.98	7.22	6.65	6.19	5.72	5.29	4.84	4.41	4.01	3.64
	V 23	23.0	20.47	17.03	14.03	11.51	9.63	8.34	7.48	6.86	6.39	5.94	5.53	5.10	4.71	4.30	3.93
	Cr 24	24.0	21.93	18.37	15.01	12.22	10.14	8.72	7.75	7.09	6.58	6.14	5.74	5.34	4.94	4.55	4.18
	Mn 25	25.0	22.61	19.06	15.84	13.02	10.80	9.20	8.09	7.32	6.77	6.32	5.93	5.54	5.18	4.80	4.45
	Fe 26	26.0	23.68	20.09	16.77	13.84	11.47	9.71	8.47	7.60	6.99	6.51	6.12	5.74	5.39	5.03	4.69
	Co 27	27.0	24.74	21.13	17.74	14.68	12.17	10.26	8.88	7.91	7.22	6.70	6.29	5.91	5.58	5.23	4.90
	Ni 28	28.0	25.80	22.19	18.73	15.56	12.91	10.85	9.33	8.25	7.48	6.90	6.47	6.08	5.75	5.41	5.09
	Cu 29	29.0	27.19	23.63	19.90	16.48	13.65	11.44	9.80	8.61	7.76	7.13	6.65	6.25	5.90	5.57	5.25
	Zn 30	30.0	27.92	24.33	20.77	17.42	14.51	12.16	10.37	9.04	8.08	7.37	6.84	6.42	6.07	5.73	5.43
	Ga 31	31.0	28.65	24.92	21.47	18.26	15.38	12.95	11.02	9.54	8.46	7.64	7.05	6.58	6.21	5.88	5.58
	Ge 32	32.0	29.52	25.53	22.11	19.02	16.19	13.72	11.68	10.08	8.87	7.96	7.29	6.77	6.37	6.02	5.72
	As 33	33.0	30.47	26.20	22.69	19.69	16.95	14.48	12.37	10.67	9.34	8.32	7.57	6.98	6.54	6.17	5.86
	Se 34	34.0	31.43	26.91	23.24	20.28	17.63	15.20	13.06	11.27	9.83	8.71	7.86	7.21	6.72	6.31	5.99
	Br 35	35.0	32.43	27.70	23.82	20.84	18.27	15.91	13.78	11.93	10.41	9.19	8.24	7.51	6.95	6.51	6.16
	Kr 36	36.0	33.44	28.53	24.40	21.34	18.82	16.54	14.44	12.57	10.97	9.66	8.62	7.81	7.19	6.70	6.31
	Rb 37	37.0	34.11	28.97	24.75	21.29	18.55	16.30	14.47	12.94	11.66	10.58	9.65	8.84	8.14	7.53	6.99
	Sr 38	38.0	35.06	29.83	25.51	21.96	19.15	16.84	14.96	13.39	12.07	10.95	9.99	9.16	8.44	7.80	7.24
	Y 39	39.0	36.01	30.68	26.28	22.64	19.76	17.39	15.46	13.84	12.48	11.32	10.34	9.48	8.73	8.08	7.50
	Zr 40	40.0	36.96	31.54	27.04	23.32	20.37	17.94	15.95	14.29	12.89	11.70	10.68	9.80	9.03	8.36	7.76
	Nb 41	41.0	37.91	32.40	27.81	24.01	20.98	18.49	16.45	14.74	13.31	12.08	11.04	10.13	9.33	8.64	8.02
	Mo 42	42.0	38.86	33.25	28.57	24.69	21.60	19.04	16.95	15.20	13.73	12.46	11.39	10.45	9.64	8.92	8.29
	Tc 43	43.0	39.81	34.12	29.34	25.38	22.21	19.60	17.46	15.65	14.15	12.85	11.74	10.78	9.94	9.21	8.55
	Ru 44	44.0	40.76	34.98	30.12	26.07	22.83	20.16	17.96	16.12	14.57	13.24	12.10	11.11	10.25	9.49	8.82
Rh 45	45.0	41.72	35.84	30.89	26.76	23.46	20.72	18.47	16.58	14.99	13.63	12.46	11.45	10.56	9.78	9.09	
Pd 46	46.0	42.67	36.70	31.67	27.46	24.08	21.28	18.98	17.05	15.42	14.02	12.82	11.78	10.87	10.07	9.37	
Ag 47	47.0	43.63	37.57	32.44	28.16	24.71	21.85	19.50	17.52	15.85	14.42	13.19	12.12	11.19	10.37	9.64	
Cd 48	48.0	44.58	38.44	33.22	28.85	25.34	22.42	20.02	17.99	16.28	14.81	13.56	12.46	11.51	10.66	9.92	
In 49	49.0	45.5	39.3	34.0	29.6	26.0	23.0	20.5	18.5	16.7	15.2	13.9	12.8	11.8	11.0	10.2	
Sn 50	50.0	46.5	40.2	34.8	30.3	26.6	23.6	21.1	18.9	17.2	15.6	14.3	13.2	12.1	11.3	10.5	
Sb 51	51.0	47.5	41.1	35.6	31.0	27.2	24.1	21.6	19.4	17.6	16.0	14.7	13.5	12.5	11.6	10.8	
Te 52	52.0	48.4	41.9	36.4	31.7	27.9	24.7	22.1	19.9	18.0	16.4	15.1	13.8	12.8	11.9	11.0	
I 53	53.0	49.4	42.8	37.1	32.4	28.5	25.3	22.6	20.4	18.5	16.8	15.4	14.2	13.1	12.2	11.3	
Xe 54	54.0	50.3	43.7	37.9	33.1	29.2	25.9	23.2	20.9	18.9	17.2	15.8	14.5	13.4	12.5	11.6	
Cs 55	55.0	51.3	44.5	38.7	33.8	29.8	26.5	23.7	21.3	19.4	17.7	16.2	14.9	13.8	12.8	11.9	
Ba 56	56.0	52.3	45.4	39.5	34.5	30.4	27.0	24.2	21.8	19.8	18.1	16.6	15.3	14.1	13.1	12.2	
Ta 73	73.0	68.6	60.4	53.1	46.9	41.7	37.3	33.6	30.4	27.7	25.4	23.3	21.6	20.0	18.6	17.4	
W 74	74.0	69.5	61.3	54.0	47.6	42.3	37.9	34.1	30.9	28.2	25.8	23.7	21.9	20.3	18.9	17.7	
Re 75	75.0	70.5	62.2	54.8	48.3	43.0	38.5	34.7	31.4	28.7	26.3	24.2	22.3	20.7	19.3	18.0	
Os 76	76.0	71.5	63.1	55.6	49.1	43.7	39.1	35.3	32.0	29.1	26.7	24.6	22.7	21.1	19.6	18.3	
Ir 77	77.0	72.4	64.0	56.4	49.8	44.4	39.7	35.8	32.5	29.6	27.1	25.0	23.1	21.4	19.9	18.6	
Pt 78	78.0	73.4	64.9	57.2	50.6	45.0	40.3	36.4	33.0	30.1	27.6	25.4	23.5	21.8	20.3	18.9	
Au 79	79.0	74.4	65.8	58.0	51.3	45.7	41.0	37.0	33.5	30.6	28.0	25.8	23.9	22.2	20.6	19.3	
Hg 80	80.0	75.3	66.7	58.8	52.1	46.4	41.6	37.5	34.1	31.1	28.5	26.3	24.3	22.5	21.0	19.6	
Tl 81	81.0	76.3	67.6	59.7	52.8	47.1	42.2	38.1	34.6	31.6	29.0	26.7	24.7	22.9	21.3	19.9	
Pb 82	82.0	77.2	68.5	60.5	53.6	47.8	42.9	38.7	35.1	32.1	29.4	27.1	25.1	23.3	21.7	20.3	
Bi 83	83.0	78.2	69.3	61.3	54.3	48.5	43.5	39.3	35.7	32.6	29.9	27.5	25.5	23.6	22.0	20.6	
Th 90	90.0	85.0	75.6	67.1	59.6	53.3	47.9	43.3	39.4	36.1	33.1	30.5	28.3	26.3	24.5	22.9	
U 92	92.0	86.9	77.4	68.7	61.1	54.7	49.2	44.5	40.5	37.1	34.0	31.4	29.1	27.0	25.2	23.6	

## C. Atomic positions/coordinates

Atomic coordinates and structure factor calculations for some materials [5].

Pearson Symbol and Typical Examples	Atom Coordinates	$F^2$
cP1 ( $\alpha$ -Po)	0,0,0	$F^2 = f^2$ for all $hkl$ values
cP2 (CsCl, $\beta$ -CuZn)	Cs: 0,0,0; Cl: $\frac{1}{2}, \frac{1}{2}, \frac{1}{2}$	$F^2 = (f_{\text{Cs}} + f_{\text{Cl}})^2$ for $h + k + l$ even $F^2 = (f_{\text{Cs}} - f_{\text{Cl}})^2$ for $h + k + l$ odd
cP4 ( $\text{Cu}_3\text{Au}$ )	Au: 0,0,0 Cu: $\frac{1}{2}, \frac{1}{2}, 0$ ; $\frac{1}{2}, 0, \frac{1}{2}$ ; $0, \frac{1}{2}, \frac{1}{2}$	$F^2 = (f_{\text{Au}} + 3f_{\text{Cu}})^2$ for $hkl$ unmixed $F^2 = (f_{\text{Au}} - f_{\text{Cu}})^2$ for $hkl$ mixed
cI2 (W, Cr, $\alpha$ -Fe)	0,0,0; $\frac{1}{2}, \frac{1}{2}, \frac{1}{2}$	$F^2 = 4f^2$ for $h + k + l$ even $F^2 = 0$ for $h + k + l$ odd
cF4 (Al, Cu, Ni)	0,0,0; $\frac{1}{2}, \frac{1}{2}, 0$ ; $\frac{1}{2}, 0, \frac{1}{2}$ ; $0, \frac{1}{2}, \frac{1}{2}$	$F^2 = 16f^2$ for $hkl$ unmixed $F^2 = 0$ for $hkl$ mixed
cF8 (Si, Ge)	0,0,0; $\frac{1}{2}, \frac{1}{2}, 0$ ; $\frac{1}{2}, 0, \frac{1}{2}$ ; $0, \frac{1}{2}, \frac{1}{2}$ $\frac{1}{4}, \frac{1}{4}, \frac{3}{4}$ ; $\frac{3}{4}, \frac{1}{4}, \frac{1}{4}$ ; $\frac{3}{4}, \frac{3}{4}, \frac{1}{4}$ ; $\frac{1}{4}, \frac{3}{4}, \frac{3}{4}$	$F^2 = 64f^2$ for $h + k + l = 4N$ $F^2 = 32f^2$ for $h + k + l$ odd $F^2 = 0$ for $hkl$ mixed $F^2 = 0$ for $h + k + l = 4N \pm 2$
cF8 (NaCl, TiN)	Na: 0,0,0; $\frac{1}{2}, \frac{1}{2}, 0$ ; $\frac{1}{2}, 0, \frac{1}{2}$ ; $0, \frac{1}{2}, \frac{1}{2}$ Cl: $\frac{1}{2}, 0, 0$ ; $0, \frac{1}{2}, 0$ ; $0, 0, \frac{1}{2}$ ; $\frac{1}{2}, \frac{1}{2}, \frac{1}{2}$	$F^2 = 16(f_{\text{Na}} + f_{\text{Cl}})^2$ for $hkl$ even $F^2 = 16(f_{\text{Na}} - f_{\text{Cl}})^2$ for $hkl$ odd $F^2 = 0$ for $hkl$ mixed
cF8 (ZnS, GaAs)	S: 0,0,0; $\frac{1}{2}, \frac{1}{2}, 0$ ; $\frac{1}{2}, 0, \frac{1}{2}$ ; $0, \frac{1}{2}, \frac{1}{2}$ Zn: $\frac{1}{4}, \frac{1}{4}, \frac{3}{4}$ ; $\frac{3}{4}, \frac{1}{4}, \frac{1}{4}$ ; $\frac{3}{4}, \frac{3}{4}, \frac{1}{4}$ ; $\frac{1}{4}, \frac{3}{4}, \frac{3}{4}$	$F^2 = 16(f_s + f_{\text{Zn}})^2$ for $h + k + l = 4N$ $F^2 = 16(f_s - f_{\text{Zn}})^2$ for $h + k + l = 2N$ $F^2 = 16(f_s^2 + f_{\text{Zn}}^2)$ for $h + k + l$ odd $F^2 = 0$ for $hkl$ mixed
hP2 (Zn, Mg, Ti)	0,0,0; $\frac{2}{3}, \frac{1}{3}, \frac{1}{2}$	$F^2 = 4f^2$ for $h + 2k = 3N$ and $l$ even $F^2 = 3f^2$ for $h + 2k = 3N \pm 1$ and $l$ odd $F^2 = f^2$ for $h + 2k = 3N \pm 1$ and $l$ even $F^2 = 0$ for $h + 2k = 3N$ and $l$ odd

text

## D. How to add gnuplot to the environmental variables

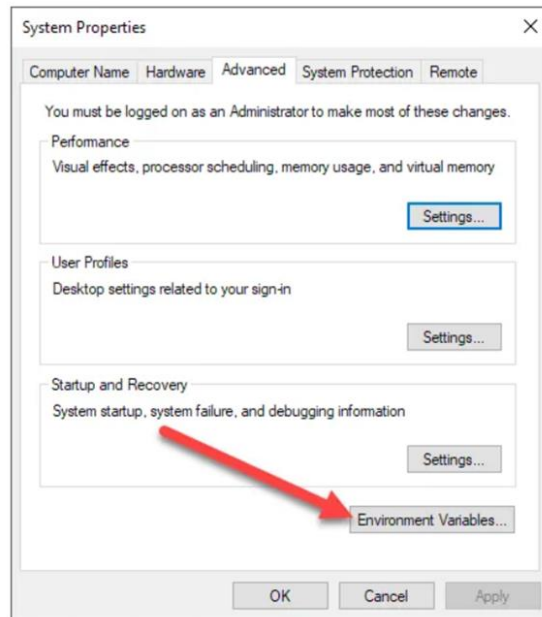
Download and install gnuplot:

<https://sourceforge.net/projects/gnuplot/files/gnuplot/>

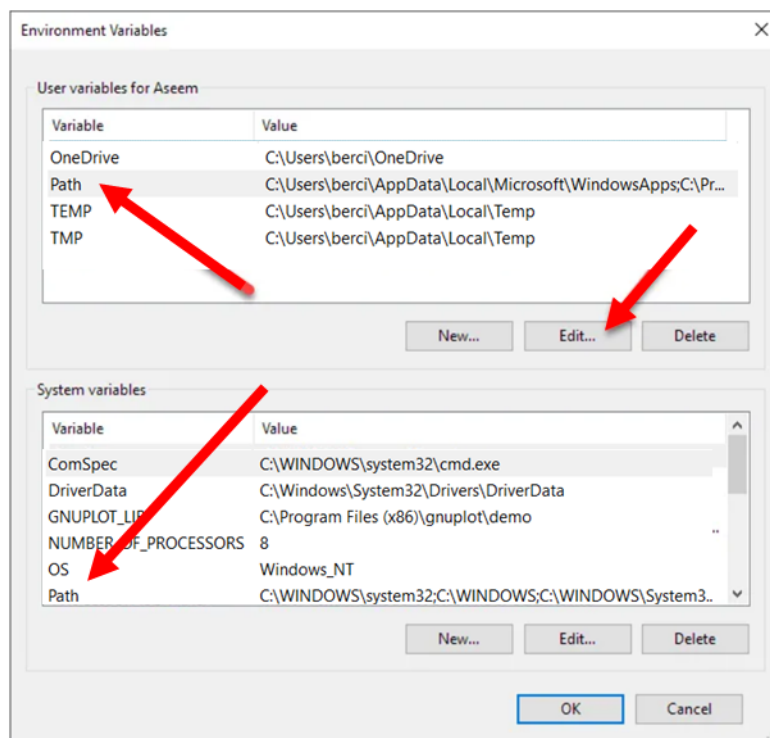
The path of the gnuplot on your computer will be something like this:

C:\Program Files (x86)\gnuplot\bin

Open the Start Search, type in “environment variables” (in your language) and choose “Edit the system environment variables”. Go ahead and click on the **Environment Variables** button at the very bottom.

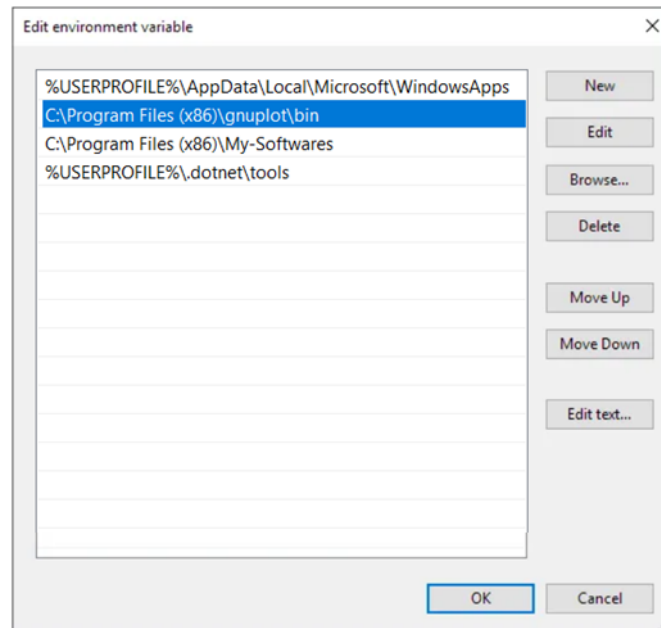


On the **Environment Variables** dialog, you’ll see two sets of variables: one for user variables and the other for system variables. Both lists have the **PATH** variable, so you have to decide which one to edit.



If you only need the commands for your own user account, then edit the user variable. If you need it to work across the computer system regardless of which user is

logged in, then edit the system variable. Click on **Path** and then click on **Edit**. On the **Edit environment variable** dialog, you'll see a list of all the paths that are currently in the PATH variable.



To add a new path, simply click on **New** and it'll add a new line to the bottom of the list. If you know the path (in our case: C:\Program Files (x86)\gnuplot\bin), simply type it in or copy and paste it. If you prefer, you can also click **Browse** and then navigate to the desired path.

## References

- [1] Jóni, B.; Ódor, É.; Maric, M.; Pantleon, W.; Ungár, T. Microstructure Characterization in Individual Texture Components by X-ray Line Profile Analysis: Principles of the X-TEX Method and Practical Application to Tensile-Deformed Textured Ti. *Crystals* 2020, *10*(8), 691. doi:10.3390/cryst10080691
- [2] Jóni, B. Textúrált anyagok vonalprofil analízise. PhD dissertation. doi: 10.15476/ELTE.2021.032
- [3] Warren, B.E. X-ray Diffraction; Dover Publications: New York, NY, USA, 1990; p. 269.
- [4] B.D. Cullity, Elements of X-ray Diffraction, Addison-Wesley, Reading, MA, 1978
- [5] C. Suryanarayana, M. Grant Norton, X-Ray Diffraction: A Practical Approach, 1998.
- [6] Beyerlein, I.J.; Tóth, L.S. Texture evolution in equal-channel angular extrusion. *Prog. Mat. Sci.* 2009, *54*, 427-510.
- [7] Wu, L.; Agnew, S. R.; Ren, Y.; Brown, D. W.; Clausen, B.; Stoica, G. M.; Wenk, H. R. and Liaw, P. K. (2010). The effects of texture and extension twinning on the low-cycle fatigue behavior of a rolled magnesium alloy, AZ31B, *Materials Science and Engineering: A* 527: 7057 - 7067.
- [8] <http://pd.chem.ucl.ac.uk/pdnn/diff2/polar.htm>